INVESTIGATING THE ROLE OF THE N-TERMINUS OF YEAST TELOMERASE REVERSE TRANSCRIPTASE IN TELOMERE MAINTENANCE

By

Hong Ji

Dissertation

Submitted to the Faculty of the

Graduate School of Vanderbilt University

in partial fulfillment of the requirements

for the degree of

DOCTOR OF PHILOSOPHY

in

Biological Sciences

December, 2007

Nashville, Tennessee

Approved:

Professor Ellen Fanning

Professor Katherine L. Friedman

Professor Todd R. Graham

Professor James G. Patton

Professor Christopher F. J. Hardy

ACKNOWLEDGEMENTS

After five and half years in the department of Biological Sciences, I would like to thank a lot of people for their support and assistance. The most important person in the development of my graduate career is my advisor, Katherine Friedman. I am very thankful for all the time and thoughts she put into my research. She has made a lot of efforts in developing my skills as a scientist, discussing research progress and literature on a weekly basis, giving advice on my presentations, helping with everyday research and being very patient in revising my manuscripts.

My committee members, Ellen Fanning, Todd Graham, James Patton and Chris Hardy, have all made valuable suggestions in the progress of my research. I would particularly like to thank Ellen Fanning and her lab members for technical advice in biochemistry. I also want to thank Todd Graham for reading my manuscripts and his lab members for sharing scientific thoughts, techniques and reagents.

I will always remember the Friedman Lab in which I spent the first few years in the United States. The lab members have made the process of achieving a Ph. D. more fun. Margaret Platts, who has been in the lab longer than I have, has made significant contributions to my first paper and she always gives me good advice on research, manuscripts, presentations and everyday life. I also thank Jennifer Osterhage, Jennell Talley, Robin Bairley, Jenifer Ferguson, Jacquelynn Brown, Stan Sonu, Chris Adkins, Bethany Cartwright, Latif Dharamsi, Geoff Todd, and Elliott Kim for their technical assistance and advice. The undergraduates I directly work with (Stan Sonu, Chris Adkins, Bethany Cartwright, Geoff Todd and Elliott Kim) have all contributed to my

own projects and training as a mentor. I would like to especially thank Bethany and Chris for their intelligence and efforts in my second paper.

I also owe my thanks to my friends in Nashville, especially to Xiaohua who has been my classmate and best friend for more than ten years. The two of us share a lot of precious memories. For most of my friends here, we have gone through our graduate school together. We traveled around the country and exposed to a lot of American customs and culture. We are always supportive to each other, in good or bad time. I would like to thank them for their help in many aspects of my life.

Finally, I would like to thank my family for always being by my side. Talking to my parents and brother on the phone every week becomes a routine of my life. Their love and support help me to finish my degree in a foreign country. I wish they are proud of me, and I miss them very much.

TABLE OF CONTENTS

LIST OF TABLES

LIST OF FIGURES

LIST OF ABBREVIATIONS

DNA	Deoxyribonucleic acid
G	Guanine
A	Adenine
C	Cysnosine
T	Thymine
bp	base pairs
RNA	Ribonucleic acid
mRNA	messenger RNA
TERT	Telomerase reverse transcriptase
TR	Telomerase RNA
TPE	Telomere position effect
RNP	Ribonucleoprotein
S	Synthesis phase
G1	Growth phase 1
G2	Growth phase 2
M	Mitosis
ChIP	Chromatin Immunoprecipitation
IP	Immunoprecipitation
HA	Hemagglutinin-A
ProA	Protein A
IgG	Immunoglobulin G

PCR	Polymerase Chain Reaction
RT-PCR	Reverse transcription-PCR
Gal	Galactose
HO	“HO”ming endonuclease
DMSO	dimethyl sulfoxide
OD	Optical density

CHAPTER I

INTRODUCTION

Linear eukaryotic chromosome ends are capped by telomeres, protein-DNA complexes that protect the chromosome from nucleolytic degradation and random fusions[1]. In most eukaryotes, telomeres are composed of repetitive G-rich DNA sequences that are maintained by a ribonucleoprotein complex named telomerase. In *S. cerevisiae*, telomeric repeats are irregular TG_{1-3} repeats while in most higher eukaryotes the repeats are perfect hexanucleotides (for example, TTAGGG in human). Telomere length is regulated at multiple levels, including telomerase assembly, telomerase recruitment and telomere accessibility. Besides telomerase, Rap1p in *S. cerevisiae* and its mammalian orthologues Taz1 and TRF1 are major regulators of telomere length[2-4]. This dissertation describes experiments to investigate the mechanism through which several mutations in the telomerase catalytic subunit (Est2p) cause over-elongated telomeres. In this process, a novel role of Est2p in regulating template usage and telomere length indirectly through Rap1p is uncovered.

End Replication Problem and Telomerase

Because of the nature of DNA polymerase, semiconservative DNA replication results in loss of terminal DNA sequences with cell division, a phenomenon originally proposed by James Watson and Alexey Olovnikov in the early 1970s and known as the "end replication problem." All known DNA polymerases require a polynucleotide primer

(either DNA or RNA) with a 3'-hydroxyl (3'-OH) group to initiate synthesis in the 5'-3' direction. At the end of a linear chromosome, DNA polymerase can synthesize the leading strand until the end of the chromosome. On the lagging strand, however, DNA polymerase's synthesis is based on a series of fragments, called Okazaki, each requiring an RNA primer. Without DNA to serve as template for a new primer, the replication machinery is unable to synthesize the sequence complementary to the final RNA primer. The result is the "end-replication problem" in which sequence is lost at each round of DNA replication (Figure 1; ref. [5, 6]). This phenomenon has been shown to occur *in vitro*, and it is supported by the observation that telomeres shorten over successive cell divisions [7, 8]. Without a solution, DNA sequences continue to shorten and cells enter replicative senescence.

Telomeres and telomerase have been proposed to solve the end replication problem. First discovered in *Tetrahymena* in 1985[9], telomerase, a ribonucleoprotein that contains a reverse transcriptase and RNA template, can synthesize telomere sequences *de novo* at chromosome ends[1]. Telomerase specifically lengthens the 3' strand, and the lagging strand replication machinery can then fill in the opposite strand. This synthesis compensates the loss of sequence due to the "end replication problem." We now recognize that the "end replication problem" is not directly due to the primer removal event on the lagging strand, but rather the processing of the leading strand to generate a 3'overhang substrate for telomerase (Figure 1; ref. [10]). In species that do not contain telomerase, other mechanisms have evolved to solve the problem. For example, in *Drosophila*, retrotransposons insert near chromosome ends, thus maintaining chromosomal integrity[11].

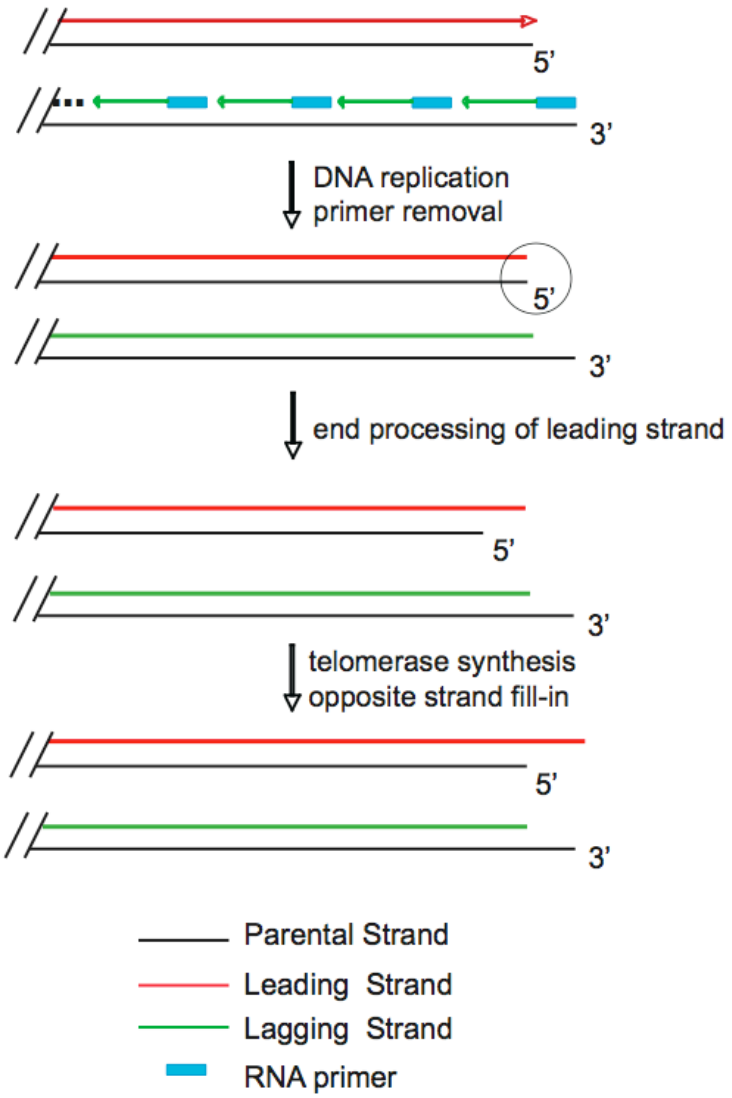

Figure 1. Telomerase helps solve the "end replication problem."
At the end of a linear chromosome, DNA polymerase can synthesize the leading strand until the end of the chromosome. On the lagging strand, however, DNA polymerase's synthesis involves synthesis of series of fragments, called Okazaki fragments, each requiring an RNA primer. Without DNA to serve as template for a new primer, the replication machinery is unable to synthesize the sequence complementary to the final RNA primer. Meanwhile, the leading strand synthesis generates a blunt end, which is processed by nucleolytic activity to generate a 3' overhang. The result is the "end-replication problem" in which sequence is lost during each round of DNA replication. Telomerase acts on the 3'overhang at chromosomal termini and synthesizes telomeric repeats *de novo* to counteract the sequence loss.

In humans, telomerase is active only during embryogenesis, in immature germ cells and in a subset of stem/progenitor cells during postnatal life[12]. Telomere length can be maintained or increased by telomerase, a process that appears to be regulated by a variety of telomere-binding proteins that control telomerase recruitment and activity at the telomeres. During mammalian embryogenesis, telomerase is strongly activated at the morula/blastocyst transition by transcriptional activation of the catalytic subunit. At this transition, telomeres are significantly elongated in murine and bovine embryos. Early embryonic telomere elongation is telomerase-dependent and leads to a rejuvenation of telomeres in somatically cloned bovine embryos. Understanding the molecular mechanisms underlying this early embryonic telomere elongation program is of great interest for medical research in the fields of regeneration, cell therapies and therapeutic cloning.

Many essential components and regulation mechanisms of telomerase are conserved between yeast and mammalian systems. Unlike mammalian cells, *S. cerevisiae* telomerase is active in all dividing cells. Genetic tools have been well developed and make it easier to study the function and regulation of telomerase than in mammalian systems.

Telomeres and Telomere End Structure

In addition to facilitating DNA replication by solving the end replication problem, telomeres have many other functions including protecting chromosome ends from being recognized as broken ends by the DNA repair machinery, protecting chromosomes from

degradation by nucleases, regulating gene expression and serving as a biological clock to control the replicative capacity of a cell[1].

First sequenced in *Tetrahymena thermophila* by Liz Blackburn[9], telomeres are GC-rich repetitive sequences found at eukaryotic chromosomal ends. A given species has a characteristic telomeric repeat sequence and also a characteristic length. Human telomeres contain ~10-15 kb CCCTAA/TTAGGG telomere sequence and mouse telomeres contain ~2-50kb of the same sequence[13]. Other vertebrates, trypanosomes, acellular slime molds, and filamentous fungi contain the same telomeric sequences. In contrast, *S. cerevisiae* telomeres contain 250-350bp of $(TG)_{0\text{-}6}$TGGGTGTG(G) sequences and *S. pombe* telomeres repeats can be loosely abbreviated as $GGTTACAG_{0\text{-}4}$[14].

Telomeres contain both double stranded telomere sequences and a single-stranded 3'overhang (G-tail). These sequences contain binding sites for telomere-associated proteins that cap chromosome ends, regulate telomerase recruitment and telomere length. Human telomeres contain a G-tail of 75-300bp throughout the cell cycle[13]. The single-stranded G-tail invades into the double-stranded region and forms a structure called the T-loop[15]. Formation and stabilization of the T-loop is facilitated by the shelterin/telosome complex, a network of many telomere-associated proteins (Figure 2; ref. [16]). Shelterin contains proteins that bind to the G-tail such as the POT1/TPP1 heterodimer, and proteins that bind to the double-strand repeats. These include the Myb-domain-containing telomere binding factors TRF1 and TRF2 and their associated proteins RAP1, TIN2 and TPP1, proteins that generally have roles in telomere capping and length regulation. TRF1 specifically associates with duplex TTAGGG repeats, and diminished TRF1 loading on telomeres leads to telomere over-extension, but not telomere capping

A.

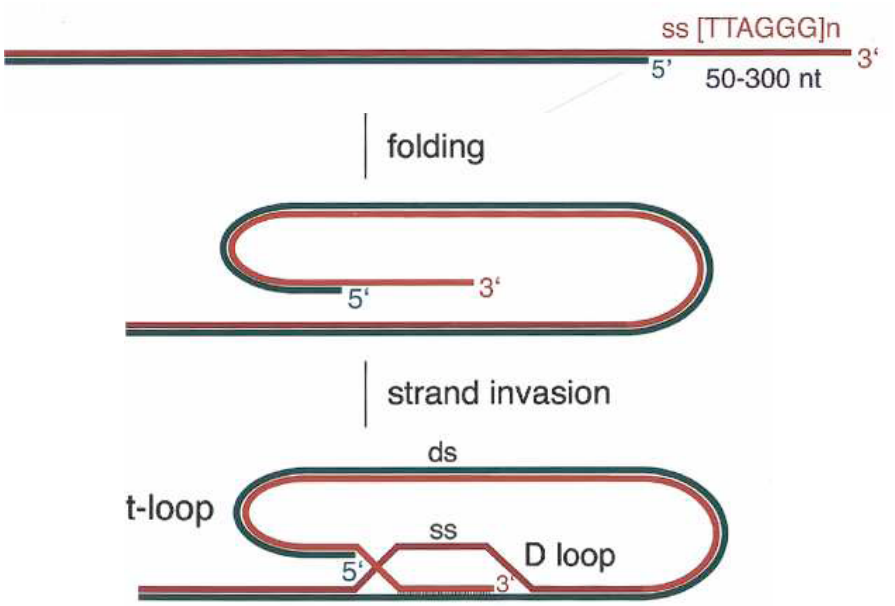

B.

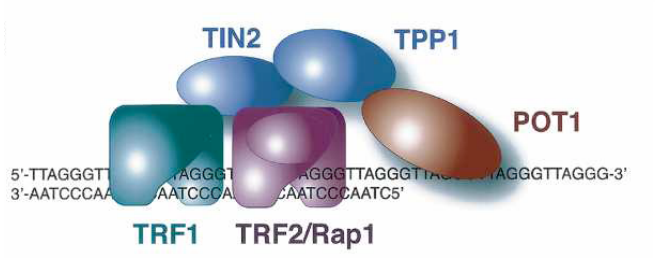

Figure 2. Human Telomeres and Shelterin[16]**.**

A. Schematic of human telomeres in the "open" and "t-loop" state.

B. Schematic of the overall composition of Shelterin. See text for details.

defects. Artificially tethering TRF1 to telomeres results in telomere shortening, suggesting a negative role of TRF1 in regulating telomere length[4]. TRF2 shares homology with TRF1, and overexpression of TRF2 results in the progressive shortening of telomeres, similar to the phenotype observed with TRF1[17]. *In vitro* experiments demonstrated that Trf2p promotes the formation and possibly maintenance of the "t loop"[18]. Trf2p was observed bound to the t loop-tail junction, where the terminal G-tail overhang strand invades the duplex DNA, producing a displacement loop of up to 300 nucleotides. hRap1p interacts with TRF2. Although hRap1p has a role in telomere length regulation and affects telomere length heterogeneity[19, 20], it doesn't bind to telomeric DNA directly[19].

Telomerase function is also regulated by the Protection of Telomeres (POT1) protein. POT1 and TPP1 form a heterodimer, and TPP1 is required to recruit POT1 to telomeres. POT1 interacts with telomeres both through directly interacting with the 3' single stranded G tail and through interaction with TPP1[1]. The POT1-TPP1 telomere complex also serves as a telomerase processivity factor during telomere extension *in vitro*[21], though the significance of this observation *in vivo* is not understood.

Although some components are shared, the telomeres of *S. cerevisiae* have a different set of telomeric proteins and structure than their human counterparts. The length of the G-tail is cell-cycle regulated. The G-tail is normally 12-15 nucleotides long, but in late S phase when telomeres are replicated, it increases to 50-100 nucleotides [22, 23]. There is thought to be no large T-loop formation in *S. cerevisiae* as in humans. However, protein-protein interactions between telomere associated proteins Sir2p, Sir3p and Sir4p and histones H3 and H4 form a heterochromatin structure at telomeres that results in

transcriptional silencing of genes located close to telomeres (termed Telomere Position Effect)[24]. Proteins that associate with telomeres or subtelomeric regions include Cdc13p, Rap1p/Rif1p/Rif2p, Tel1p, and the Mre11p/Rad50p/Xrs2p complex. These proteins all have roles in telomere length regulation that will be discussed in detail below.

Structure and Function of the Telomerase Complex

First identified in ciliated protozoa, telomerase is highly conserved in eukaryotic evolution. As an obligate ribonucleoprotein (RNP), its catalytic function requires two components: the TERT protein (Telomerase Reverse Transcriptase) and the RNA (alternately known as TR, TER or TERC or *TLC1* in *S. cerevisiae*) [25-27]. The telomerase RNA component contains a short stretch of residues complementary to the telomere repeat and serves as the template for reverse transcription by TERT[28].

TERT Structure and Function. The gene encoding the TERT protein was initially cloned from *S. cerevisiae* as *EST2* and subsequently from ciliated protozoa (*Euplotes aediculatus*). Generally, TERTs can be divided into three conserved functional domains, an N terminal region (Figure 3; TEN domain in *S. cerevisiae;* RID1/I-A+N-DAT+I-B in hTERT), an RNA interacting region (RBD in *S. cerevisiae* and RID2 in hTERT) and a C terminal RT domain. The Reverse Transcriptase domain is the most highly conserved part of protein and is shared with viral reverse transcriptases and telomerases from different species[29]. Three absolutely conserved aspartate residues are required for catalytic activity. In addition to reverse transcriptase activity, TERT also has other functions such as interacting with other components of the telomerase complex and with the DNA substrate. Most species also have a C terminal extension region (CTE) that

has been implicated in promoting telomerase processivity and localization but not in catalytic activity *per se*.

Interactions between telomerase and its DNA substrate (the chromosome 3' terminus) are critical to the correct activity and regulation of the enzyme. Specific primer-substrate interactions of telomerase are mediated by hybridization of the DNA substrate to the RNA template and also by interaction of the chromosome terminus with a single-stranded DNA binding site (called the "anchor site") in the telomerase complex. The presence of an "anchor site" has been suggested in many species including *Tetrahymena*, Euplotes, yeast and human[30-33].

In human TERT, anchor-site interactions have been mapped to the N-terminal RID1 domain and the C terminal CTE domain (Figure 3). Several NAAIRS substitutions (a six-amino acid sequence that less likely disrupts protein structure) within the N-DAT domain have been reported to Dissociate the biological and catalytic Activities of Telomerase. These mutants have nearly normal catalytic activities, but do not support telomere replication *in vivo*. This activity is partially or fully rescued by fusing the mutant hTERT to POT1, a protein bound at the chromosome terminus. This result suggests that some DAT sequences may be important for the recruitment and/or activation of telomerase[32]. More recently, it has been suggested that many of these mutants may not truly maintain normal catalytic activity. Some DAT mutants impair telomerase processivity on short telomeric primers in a conventional telomerase assay. Given that this assay is thought to be sensitive to the strength of telomerase-primer interaction, it is possible that DAT sequences are important for the specificity and affinity of telomerase-DNA interactions[34]. Thus these residues would meet the definition of an

anchor site. In a direct primer binding assay, hTERT forms stable and specific contacts with telomeric DNA in the absence of the human telomerase RNA component (hTR)[35]. The first 350 amino acids of hTERT have a critical role in regulating the strength and specificity of these protein-DNA interactions, providing additional evidence that the TERT N terminus contains an anchor site. The same appears true of yeast TERT. *S. cerevisiae* telomerase remains tightly bound to its reaction products in a manner dependent on the 5' end of telomeric primers[36]. Mutational analysis and crosslinking experiments have mapped the anchor-site to the N-terminal Region I of Est2p in *S. cerevisiae*[33]. Further structure modeling and mutational analysis reveal a positive patch on the surface of Region I structure (including residues R151 and N153) that appears to modulate the interaction between Est2p and its primer/substrate[37].

The oligomeric state of the telomerase complex is still unresolved. Both TERT and TR have been shown capable of forming dimers. Evidence for physical and functional dimer formation have been reported for human, yeast and *Euplotes crassus*. Two separate, catalytically inactive hTERT proteins can complement each other *in trans* to reconstitute catalytic activity, suggesting that hTERT multimerizes *in vivo*[38]. This complementation requires the amino terminus of one hTERT and the reverse transcriptase and C-terminal domains of the second hTERT. The telomerase RNA must associate with only the latter hTERT for reconstitution of telomerase activity to occur. RID1 and RID2 in hTERT physically interact with RT-CTE in absence of RNA *in vitro*, suggesting that these regions are important for telomerase dimerization[39]. Est2p has been shown to dimerize *in vivo* in a manner dependent on T motif and RT domain [40]. However, the functional relevance of dimerization is still not understood.

Telomerase RNA. In contrast to TERTs, the RNA subunits are highly divergent among different species, varying in both size and sequence composition from ~150 nt in ciliates and ~450 nt in vertebrates to ~930-1300 nt in the budding yeasts *Kluyveromyces lactis* and *Saccharomyces cerevisiae*[41]. Secondary structures of ciliate and vertebrate RNAs have been proposed by phylogenetic analysis and determined by mutational analysis (Figure 3B). All TERs contain a 5' template boundary element (TBE; a structure that limits reverse transcription), a large loop that includes the template, a potential pseudoknot and a loop-closing helical region[41]. However, the vertebrate and yeast RNAs have acquired additional structures that serve to bind species-specific proteins. *TLC1* RNA in *S. cerevisiae* serves as a flexible scaffold that interacts with other components of telomerase[42]. Its pseudoknot binds Est2p, while a stem loop structure binds to Est1p. Sm proteins stablize *TLC1* RNA and Ku also binds to a 48 nt stem loop structure that is important for telomerase recruitment in G1 and S phase. Deleting much of the RNA that separates these protein-binding elements generates a 500 nt mini-RNA molecule that is functional *in vivo*, although the telomeres are stably shorter than wild-type strains[43]. This results in decrease in hTR levels, and is accompanied by telomere shortening. Indeed, mutations in hTR have also been found to cause autosomal dominant DC[44]. These mutations are found mostly in the pseudoknot and CR4/VR5 domains that are required for telomerase catalytic activity. Mutations in TERT have been identified in DC patients too, further supporting that DC patients with dyskerin, hTR and TERT mutations suffer from defective telomerase function[44].

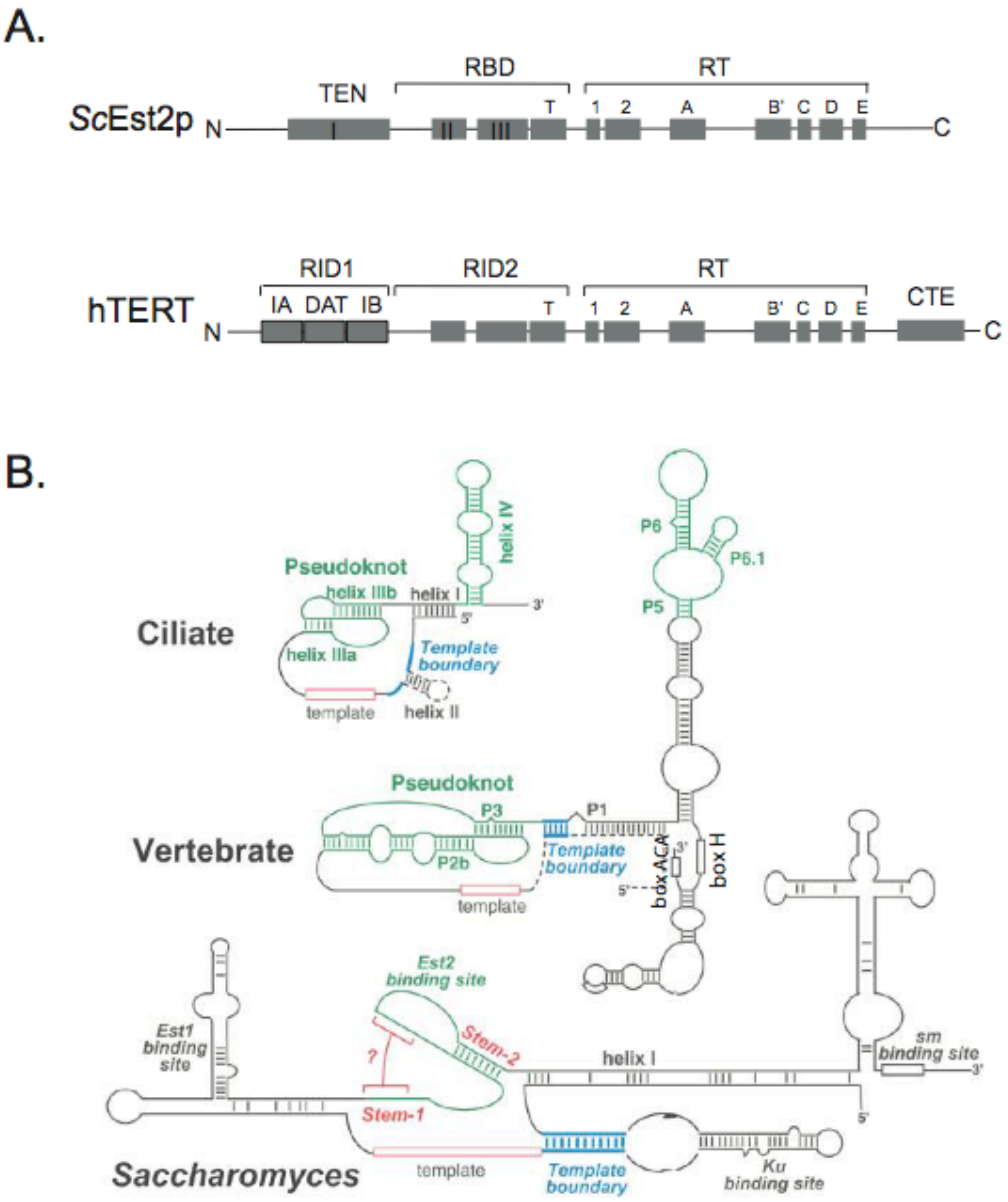

Figure 3. Structures of TERT and TR.

A. Functional Domains in hTERT and ScEst2p. See text for description.

B. Secondary structures of ciliate, vertebrate, and *S. cerevisiae* telomerase RNAs [41]. Structural elements in green represent conserved regions that bind to TERT. The structures that are present in some but not all species within a group are shown by dashed lines. The structures that define template region (red) and the template boundary (blue) are indicated. The RNA structural elements bound by protein components are indicated. In the *Saccharomyces* RNA, a proposed stem-1 that would form a pesudoknot is indicated by red brackets.

Other Components of Yeast Telomerase

Besides TERT (Est2p) and TR (*TLC1* RNA), yeast telomerase also has other components, Est1p and Est3p, that were identified in a screen for genes that when deleted, cause progressive telomere shortening and senescence (referred to as *EST* [ever shorter telomere] phenotype)[45]. These accessory proteins are dispensable for *in vitro* telomere addition but are required for telomerase activity *in vivo*[27].

Est1p binds to *TLC1* RNA via a bulged stem structure (Figure 3B; ref. [46]). It has weak single-strand G-rich DNA binding activity, though the relevance of this activity *in vivo* is unclear. Est1p interacts with Cdc13p, a single-stranded DNA binding protein involved in telomere capping and telomerase length regulation[47]. These two proteins directly interact and collaborate to positively regulate access of telomerase to the telomeres. Fusion of Est1p to the DNA binding domain of Cdc13p over-elongates telomere length, suggesting that their interaction is normally regulated[48]. Est1p also regulates telomerase assembly during the cell cycle. Its level is low in G_1 phase because of proteasome-dependent degradation and this low protein level restricts telomerase assembly in G_1 phase[49].

Like Est1p, Est3p interacts with the telomerase complex, although its role is largely unknown. Interaction of Est3p with *TLC1* is dependent on Est2p, and its assembly into the telomerase complex in G_1 is dependent on Est1p[49]. Overexpression of Est3p rescues the growth of temperature-sensitive mutations in Region I of Est2p, suggesting that Est3p might interact with Est2p through this N-terminal region[50]. Wide-scale mutagenesis analysis and sequence alignment within fungal species shows that Est3p has three functional domains: N-terminal Region, Central region and C-terminal region

(Margaret Platts, unpublished data). Est3p dimerizes *in vitro*, and mutations that disrupt dimerization causes telomere shortening[51]. Est3p also weakly unwinds RNA-DNA duplex *in vitro*[52]. However, the *in vivo* relevance of these activities is unclear.

PinX1 is an essential protein involved in rRNA and snoRNA maturation, and overexpression of PinX1p results in telomere shortening and reduced telomerase activity *in vitro*[40]. PinX1 coimmunoprecipitates with the same region of Est2p that interacts with *TLC1* RNA. As such, Est2p and PinX1 appear to form mutually exclusive complexes with *TLC1* RNA such that the level of one is up-regulated when the other is down-regulated. This observation suggests that PinX1 regulates telomerase activity by sequestering Est2p from complexing with *TLC1* RNA. Human PinX1 also forms a complex with hTR to inhibit telomerase activity, suggesting a conserved role of PinX1 in regulating telomerase[53].

TLC1 RNA also contains a canonical binding site for Sm proteins, which are essential for the assembly of small nuclear RNPs involved in mRNA splicing[54]. Sm proteins bind to the *TLC1* RNA and are retained in the active complex following assembly. Mutations in the Sm binding site of TLC1 severely reduce RNA levels and cause telomere shortening. The Sm proteins may be required for removal of the poly(A) tail from TLC1 precursor and hypermethylation of the 5' 7-methylguanosine cap of TLC1.

Other Components of Human Telomerase

Iterative profile searches have identified three human homologs of the yeast telomerase subunit Est1p, hEST1A, hEST1B and hEST1C[55]. These proteins all contain

weak sequence similarity with yeast Est1p. Both hEST1A and hEST1B proteins specifically associate with telomerase activity in human cell extracts and bind hTERT in rabbit reticulocyte lysates independently of the telomerase RNA[56]. Overproduction of hEST1A cooperates with hTERT to lengthen telomeres, an effect that is specific to cells with detectable telomerase activity. Like Est1p, hEST1A (but not hEST1B) exhibits a single-stranded telomere DNA binding activity. These results suggest that the telomerase-associated factor Est1p is evolutionarily conserved in humans.

The molecular chaperones p23 and Hsp90 associate with hTERT, promoting the *in vitro* assembly of hTR and hTERT in rabbit reticulocyte lysate[57]. The *S. cerevisiae* p23 homolog Sba1p has a role in telomerase-mediated telomere extension by modulating the DNA binding activity of telomerase[58], suggesting that a requirement for chaperone functions is a conserved aspect of the telomerase complex.

Telomere Maintenance Mechanisms

In most species, telomeric DNA is maintained at a particular length by a dynamic process that includes a variety of proteins including telomerase. In *S. cerevisiae*, most strains have a length of $TG_{1\text{-}3}$ repeats that varies between 225~375bp (reviewed in [59]). In contrast to yeast, human cells show telomere attrition with cell division, which results from limiting amount of telomerase activity in the adult organism that cannot compensate for progressive telomere shortening that occurs as cells divide. Cancer cells frequently maintain very short telomeres, but only slightly longer than the length needed to prevent uncapping.

Maintenance by Telomerase

In all organisms studied to date, the single-stranded G-tail is the substrate for telomerase activity. In absence of telomerase, telomeres shorten as cells divide. As a result, processes affecting the expression/stability of telomerase components, and the assembly or localization of telomerase can influence telomere length. For example, mutations that destabilize the RNA template can cause telomere shortening and senescence.

In human cells, the telomerase RNA is ubiquitously expressed and the absence of telomerase activity in somatic cells is due to the lack of expression of the TERT subunit. Introduction of ectopic hTERT is sufficient to allow *in vitro* telomerase activity and life-span extension of some cell types[60, 61]. Also, expression of hTERT correlates very well with telomerase activity (for example, in tumor cells), while expression of hTR does not. Concomitant overexpression of hTERT and hTR is necessary and sufficient to increase telomerase activity and telomere length becomes substantially longer than physiological size in less than 50 passages[62]. These results imply that telomerase is normally limiting for elongation of telomeres in human cells.

Consistent with this idea, cells that have half the level of the telomerase RNA cannot maintain telomere length through multiple cell divisions. As mentioned earlier, people who are heterozygous for mutations in the telomerase RNA have the diseases dyskeratosis congenita and/or aplastic anemia. Symptoms are manifested in highly proliferative tissues and are thought to result from short telomeres that impair tissue renewal capacity. Mice heterozygous for telomerase RNA show haploinsufficiency in telomere length maintenance and also show loss of tissue renewal capacity. Furthermore,

genotypically wild-type mice derived from heterozygous parents with short telomeres display hematopoetic stem cell defects and short telomeres (so called "occult" disease), suggesting that telomere length determines these phenotypes and that normal telomerase level is limiting and can't rescue the short telomere phenotype[63]. In *S. cerevisiae*, a *TLC1/tlc1Δ* heterozygote maintains shorter telomeres and this haploinsufficiency is consequence of the low *TLC1* RNA level[64]. The number of *TLC1* RNA molecules in a haploid yeast cell has been estimated to be ~29, less than the number of chromosome ends (64) in late S-phase. Wild-type diploid cells contain approximately 37 telomerase RNAs, while diploids heterozygous for a null *tlc1* allele have half the wild-type amount, approximately 19 *TLC1* molecules. Based on these observations, telomerase is outnumbered by its substrates in late S phase. In support of this idea, sequencing and analysis of telomere addition events from one cell cycle show that not all telomeres are extended by telomerase in one cell cycle, and that the shorter telomeres are preferentially elongated. The ability of telomerase to preferentially target the shortest telomere is a conserved property of the enzyme and is likely critical for genomic stability in the face of limiting telomerase levels.

Alternative Lengthening of Telomeres

In the absence of telomerase activity, both mammals and yeast are able to maintain or even amplify their telomeric and/or subtelomeric DNA through recombination-dependent mechanisms. This phenomenon was first described in budding yeast strains lacking the *EST1* gene[65]. Telomeres in *S. cerevisiae* are normally a few hundred base pairs in length and shorten at 3-5 bp per cell division in the absence of

telomerase. Telomeres of telomerase-deficient mutants shorten to less than ~100bp before most cells stop dividing and enter replicative senescence[28, 45, 66]. Rarely, survivors arise from Rad52p-dependent recombination pathways. There are two types of survivors, Type I and Type II. Initially described by Lundblad and Blackburn[65], Type I survivors amplify the subtelomeric Y' sequences that exist at more than half of yeast chromosome ends. Telomeres of Type II survivors are more heterogeneous in length, with few alterations in subtelomeric sequences. Recent evidence suggests that a roll-and-spread mechanism is responsible for Type II survivor formation[67]. A small circle of telomeric DNA, possibly resulting from an intratelomeric deletion, is used as the template for rolling-circle replication, resulting in an elongated telomere. Sequence of this first elongated telomere can subsequently be spread to all other telomeres through recombination events. Type II survivors arise less frequently than Type I survivors. However, they grow faster and eventually overgrow Type I survivors in liquid cultures. In absence of Rad52, neither Type I nor Type II survivors can form. The appearance of Type I survivors depends on the "canonical" homologous recombination proteins Rad51, Rad54, Rad55 and Rad57[68, 69].The Type II pathway requires the MRX (Mre11-Rad50-Xrs2) complex and Rad59[68-71].

Telomere Maintenance and Cancer

Reactivation of a telomere maintenance pathway to prevent telomere loss is a critical step in cancer development. Most cancer cells (~90%) maintain telomeres by reactivating telomerase. However some cancer derived mammalian cell lines maintain telomere length by a telomerase-independent mechanism termed ALT (Alternative

Lengthening of Telomeres)[72]. ALT cells have an extremely heterogeneous telomere length. For comparison, telomeres of human somatic cells shorten 40-200bp/cell division until cells senesce at a length of ~5-8kb[8, 73-75]. Human germ line cells maintain their telomere length at ~15kb by telomerase, while human cancer cells and immortal cells with active telomerase have a telomere length of less than 10kb[76-78]. In contrast, ALT cell lines have a very broad telomere length distribution ranging from <3kb to >50kb, with an average of ~20kb[72, 79-82]. ALT cells have specific nuclear structures, referred to as ALT-associated PML Bodies (APBs), that contain telomeric DNA, TRF1 and TRF2, and also proteins involved in telomere binding, DNA replication, repair and recombination processes[83]. These structures might facilitate the ALT mechanism or sequester extrachromosomal telomeric DNA generated by ALT. Telomere lengthening in ALT cells is dependent on recombination, but the exact substrates are unclear. These events could be inter-telomeric or intra-telomeric recombination in the context of a T-loop, extrachromosomal recombination with a circular molecule, or recombination between linear chromosomes. These changes are highly reminiscent of Type II survivors in yeast.

Telomere Length Regulation

Telomere length is maintained through a balance of activities that shorten telomeres (by negative regulators) and activities that lengthen telomeres (such as telomerase). Proteins that influence the activity or access of telomerase at the telomere terminus are therefore important players in telomere length regulation. There are two major classes of such proteins: proteins that are involved in telomeric chromatin

formation/modification, and proteins that influence lagging-strand replication and may help coordinate telomerase synthesis with C-strand replication.

Negative Regulators of Telomere Activity/Access

Rap1p. Rap1p negatively regulates telomere length through its cofactors Rif1-Rif2 (Rap1-interacting factor 1 and 2) [2, 84, 85]. Artificially targeting Rap1p or Rif1p/Rif2p to an individual telomere proportionally shortens telomere length. Rif1p and Rif2p restrict the accessibility of telomeres to telomerase based on the observation that in *rif1Δ* and *rif2Δ* strains the frequency of telomere addition is increased while the preferential lengthening of short telomeres persists[86].

Pif1p. Pif1p is a helicase that belongs to the SFI helicase superfamily and is conserved from yeast to humans. Yeast Pif1p is involved in the maintenance of mitochondrial, ribosomal and telomeric DNA and may also have a general role in chromosomal replication by affecting Okazaki fragment maturation[87]. Pif1p prefers an RNA-DNA hybrid substrate *in vitro*[88]. *In vivo*, overexpression of Pif1p reduces telomerase association with telomeres, whereas depleting cells of Pif1p increases the levels of telomere-bound Est1p, suggesting that Pif1p limits telomerase function by removing telomerase from telomeres[89]. Negative regulation of telomerase may be mediated via the interaction of Pif1p with the finger subdomain of the RT domain in Est2p[90].

Lagging Strand Replication Machinery. Many proteins that are involved in lagging-strand replication also negatively influence telomere length. During DNA replication, it is widely accepted that removal of the RNA primer on the end of the

lagging strand or processing of the leading strand leaves a 3' overhang that serves as the substrate for telomerase. Replication of the complementary C-rich strand is accomplished by the conventional lagging-strand replication machinery. Mounting evidence suggests that telomere synthesis by telomerase is tightly co-regulated with the synthesis of the opposite C-strand. Such coordination may prevent telomerase from generating excessively long single-stranded tails, which may be deleterious to chromosome stability in *S. cerevisiae*.

Several lines of evidence link DNA replication to telomere length regulation. In *S. cerevisiae*, Polα, Polδ and DNA primase are required for telomerase-mediated telomere addition *in vivo*[91]. Co-immunoprecipitation (CoIP) experiments in *S. pombe* showed that Polα interacts with TERT, indicating that these proteins may form a complex *in vivo*[92]. Aphidicolin, an inhibitor of Polα and Polδ, causes abnormal lengthening of the G-strand and concomitant increased C-strand heterogeneity of telomeres in the ciliate *Euplotes*[93], and *Euplotes* telomerase physically associates with primase, a component of the lagging-strand machinery[94]. In agreement with the role for lagging-strand replication in telomere homeostasis, mutations in many components of the lagging-strand replication machinery (such as Polα, RFC, Elg1p, Dna2p and Rad27p) cause telomere over-elongation[95-98].

How lagging strand replication and telomere elongation are coordinated is currently unclear. Cdc13p, a single-stranded telomeric DNA binding protein, may play a role in this coordination. Cdc13p is involved both in telomere capping through interaction with Stn1p [99] and in telomerase recruitment to the telomeres [48]. Cdc13p is proposed to regulate telomere length in two steps-first positive and then negative. In its positive role,

Cdc13p activates telomerase through its interaction with Est1p [48, 100]. Remarkably, direct fusion of the DNA-binding domain of Cdc13p to the catalytic subunit of telomerase, Est2p, eliminates the requirement for Est1p in telomere maintenance [48]. However, telomeres in this strain are significantly over-elongated, suggesting that these interactions must be regulated. Cdc13p then binds Stn1p, which prevents telomerase recruitment to telomeres, subsequently limiting G-strand synthesis by telomerase in response to C-strand replication [101]. Cdc13p physically interacts with the catalytic subunit of DNA polymeraseα, a component of the lagging-strand machinery, suggesting a link between telomere addition and DNA lagging- strand replication [47]. Intriguingly, mutations that weaken the Cdc13-Pol1p interaction result in telomere over-elongation. However because apparent complete loss of this interaction only slightly increases telomere length, additional mechanisms may contribute to the coordination of telomerase activity with lagging-strand replication.

Positive Regulators of Telomerase Activity/Access

Tel1p and Tel2p. Tel1p and Tel2p are positive regulators of telomere length [102], with loss of these proteins leading to short but stable telomere length. In a *tel1Δ* strain, the addition of synthetic Rap1p-binding sites at a telomere fails to cause telomere shortening as observed in wild-type or *yku70Δ* strains [103]. Importantly, *rap1 tel1* double mutants exhibit the shorter than normal telomeres characteristic of *tel1* mutants [104]. These results have led to the proposal that Rap1p negatively regulates the telomerase-recruitment activity of Tel1p so that loss of Rap1p function is inconsequential in the absence of Tel1p[104]. Recent research suggests that Tel1p preferentially binds to shorter

telomeres and stimulates their elongation via telomerase, consistent with the role of Tel1p downstream of the Rap1p/Rif1p/Rif2p complex[86].

Ku70/80 heterodimer. A heterodimer of the yKu70 and yKu80 proteins interacts with a 48nt stem-loop in *TLC1* RNA and is essential for recruitment of telomerase to telomeres in G1. In S phase, recruitment of telomerase to telomeres through Cdc13p-Est1p interaction plays a major role. Ku also protects against resection of the C-strand, thereby contributing to protection of chromosome termini[105]. Deletion of *YKU70* or *YKU80* results in short but stable telomeres with a long single-stranded G-tail throughout cell cycle[106, 107]. A *tel1 yku70* double mutant has a telomere length shorter than either single mutant, suggesting that *TEL1* and *YKU70* are in separate telomere regulatory pathways[106].

Mec1p. Mec1p is the homolog of the human ATR checkpoint protein and negatively regulates telomere length. Deletion of Mec1p results in modest telomere shortening. The functions of Mec1p and Tel1p are redundant in recruitment of telomerase and *tel1Δ mec1Δ* strain has an *est* phenotype[71]. They are present at telomeres at different times in the cell cycle in a mutually exclusive manner[108]. In particular, Mec1p is associated with telomeres in late S phase. However, since the telomere shortening experienced in a *mec1Δ* strain is very slight, Tel1p appears largely redundant for Mec1p function at telomeres.

MRX complex. Mre11p is a subunit of the MRX (Mre11-Rad52-Xrs2p) complex, which is required for efficient homologous and non-homologous repair of double-stranded DNA breaks and for activation of the S phase checkpoint[109, 110]. Deletion of any one protein or all three results in short but stable telomeres, and this phenotype is

not exacerbated by *tel1Δ*, suggesting that the MRX complex and Tel1p function in the same pathway[102]. The defect of *tel1Δ mec1Δ* can be bypassed by eliminating the Rif proteins[111]. Taken together, these data suggest that Tel1p, the MRX complex and Mec1p function in a partially redundant manner to promote the access of telomerase to telomeres. In *tel1Δ* and *mre11Δ* strains, the association of Est2p and Est1p with telomeres are severely reduced while *mec1Δ* has a nearly wild-type level, suggesting that Mre11p and Tel1p affect telomere length by promoting telomerase recruitment to telomeres, whereas Mec1p has only a minor role in telomerase recruitment when Tel1p is present[112].

In a genome-wide screen for telomere length regulators in *S. cerevisiae*[113], proteins with very diverse functions were identified. Besides proteins mentioned above, proteins were identified that function in vacuolar trafficking (for example, components of the Endosomal Trafficking complex), in DNA and RNA metabolism (for example, RNA polymerase II subunits), and in DNA modifications (for example, Rpd3 histone deacetylase complex, Mediator, and Nup60). For most of these genes, their roles in telomere length regulation (either direct or indirect) are not understood.

Telomere Position Effect

Proteins that comprise the telomeric heterochromatin also influence telomere length. Chromatin at telomeres has several characteristics that are similar to those of heterochromatin at pericentromeric regions, such as ability to silence nearby genes, which is termed “telomeric silencing” or “Telomere Position Effect” (TPE). Both mammalian and yeast cells demonstrate TPE.

In budding yeast, Rap1p and the Sir proteins are involved in establishing TPE[114, 115]. At telomeres, Sir proteins are recruited through their interactions with C-terminal residues of the telomere binding protein Rap1p, which also binds to Rif1p and Rif2p. This initial interaction promotes additional Sir binding which can spread to subtelomeric regions and interact with the N-terminal tails of histones H3 and H4, promoting their hypoacetylation and leading to transcriptional repression. Rap1p binds directly to double-stranded telomeric DNA and interacts directly with Sir4p[116]. Sir4p in turn recruits Sir2p and Sir3p. The NAD-dependent histone deacetylase Sir2p can deacetylate histone H4 followed by the binding of Sir3p and Sir4p to histone tails at subtelomeric regions, promoting the formation of heterochromatin and spreading of telomeric silencing[117]. These protein-protein interactions are thought to "fold back" the telomeres and form a higher-order structure that further promotes and stabilizes protein-protein interactions. Mutations in Sir proteins disrupt telomeric silencing and cause telomere shortening, though the mechanism through which Sir proteins normally positively regulate telomere length is not understood[118].

The relationship between telomere length and gene silencing is complex. A gene adjacent to a long telomere shows higher and more stable repression than a gene next to a shorter telomere[119]. However, there is no absolute positive link between TPE and telomere length. For example, *rif1Δ rif2Δ* has abnormally long telomeres and increased TPE, and the increased TPE result from more Rap1 binding sites within the long telomeres and reduced competition for Sir binding[85]. In contrast, *rap1^{ts}* has similar elongated telomeres but no TPE because of the elimination of Sir proteins binding by

rap1^{ts}[119]. Likewise, *tel1Δ* has shorter telomere and normal TPE, while *ku70Δ* has shorter telomere and reduced TPE[120, 121].

Importance of Telomere Length Regulation (Cancer and Aging)

The role of telomerase in cancer has been implicated for three decades. Over 90% of tumor cells show up-regulated telomerase activity. A large body of research on the dynamics of telomerase activity and telomere regulation has led to the following model of tumor progression. Since most somatic cells have little or no telomerase activity, telomeres shorten as a cell divides. These cells eventually enter senescence when telomeres are critically short (M1; Mortality Stage 1). However, a small portion of cells can bypass senescence if checkpoint proteins such as p53 and pRb are non-functional. Telomeres in such cells continue to shorten until the cells enter crisis, a predominantly lethal condition in which loss of telomere capping leads to chromosomal instability and accumulation of mutations (M2). At this point, if cells reactivate telomerase or the ALT pathway to maintain critically short telomeres, chromosomes are stabilized and immortal growth can be achieved. Progression to a tumorigenic state requires additional mutations in genes that regulate cell proliferation, the occurrence of which might be increased during the severe genomic instability encountered during crisis. In this model, although short telomeres serves as a tumor suppressing function initially (M1), after the bypass of this checkpoint, short telomeres drive chromosomal instability and increase the possibility of tumor formation. In support of this model, ectopic expression of hTERT is sufficient to maintain telomere length and immortalize telomerase negative human cells[122, 123]. Ectopic expression of TERT, SV40 Large T-antigen (to inactivate p53 and

pRb) and oncogenic Ras are sufficient to convert human epithelial and fibroblast cells to a tumorigenic state[124]. Most telomerase-positive cancer cells have short telomeres compared with their adjacent cells[76], supporting the idea that cells experience severe telomere shortening as part of the tumorigenic process.

Because of the role of telomerase in cancer, it has been a hot target for anti-cancer development. Oncolytic viruses that have the hTERT promoter driving critical adenoviral genes can selectively kill telomerase-positive cells. Direct enzyme inhibitors (including dominant-negative alleles, antisense oligonucleotides directed against the RNA subunit and RNAi) and cancer immunotherapy (hTERT peptide as antigen) are being explored with different levels of success. It is hypothesized that there are cancer stem cell that have self-renewal capacity and are telomerase positive, so that anti-telomerase drugs might be more specifically targeted to these cells than are normal anti-cancer agents.

As described earlier, the link between telomere dynamics and aging can be observed in a human disease Dyskeratosis Congenita (DC), which is a disorder that associates with abnormal pigmentation, nail dystrophy and bone failure. Mutations in hTR itself or genes governing hTR stability have been identified in DC patients. The onset of this disease occurs at progressively younger ages in subsequent generations (a phenomenon termed anticipation), most likely because of the inheritance of progressively shorter telomeres. *mTerc*-/*mTerc*- mouse models also show premature aging. Although to date a definitive connection between telomere dynamics and normal ageing in humans has not yet been established, accumulating evidence strengthens the idea that accelerated telomere attrition contributes directly to inherited degenerative conditions and several premature aging syndromes.

Significance of This Study

Considering the roles of telomerase in cancer and age-related diseases, many aspects of telomerase activity and regulation will present potential targets of therapy. Yeast is an attractive model for the study of telomerase because many aspects of telomerase assembly and at least some aspects of regulation appear well conserved. Many pathways have been identified in this model system that regulate telomere length. Most previous studies have focused on the role of *Sc*TERT (Est2p) in the positive regulation of telomere length. Here, I present data supporting a novel role of the N-terminal region of Est2p in the negative regulation of telomere length through an effect on Rap1p association with telomeres. I also describe a unique alteration in telomere sequences that occurs in several strains in which telomeres are overelongated, perhaps suggesting an altered mode of telomerase synthesis under these conditions.

Chapter II describes the identification of several mutations (*est2-LT*) that cause telomere overelongation (the LT, or long telomere phenotype). I also identify the genetic pathway through which these mutations interact. In Chapter III, I describe an effect on Rap1p binding to telomeres in *est2-LT* strains and the dependence of the LT phenotype on the Rap1p counting mechanism. These mutations also alter telomere sequences. Possible mechanisms for these sequence changes have been explored. Chapter IV describes the materials and methods used to obtain these results. Chapter V summarizes these studies and proposes future directions to investigate the mechanisms underlying the LT phenotype of *est2-LT*. In the Appendix, I describe the investigation of possible interactions between Est2p and lagging strand replication components that regulate telomere length.

CHAPTER II

IDENTIFICATION AND PHENOTYPIC CHARACTERIZATION OF *est2-LT*

Work described in this chapter is included in the following manuscript:
Hong Ji, Margaret H. Platts, Latif Dharamasi, and Katherine L. Friedman**.** Regulation of Telomere Length by an N-terminal Region of the Yeast Telomerase Reverse Transcriptase. Mol Cell Biol. 2005 Oct;25(20):9103-9114.

Abstract

Telomerase is a reverse transcriptase that maintains chromosome integrity through synthesis of repetitive telomeric sequences on the ends of eukaryotic chromosomes. In the yeast *Saccharomyces cerevisiae*, telomere length homeostasis is achieved through negative regulation of telomerase access to the chromosome terminus by telomere-bound Rap1 protein and its binding partners, Rif1p and Rif2p, and positive regulation by factors such as Ku70/80, Tel1p, and Cdc13p. Here we report the identification of mutations within an N-terminal region (Region I) of the yeast telomerase catalytic subunit (Est2p) that cause telomere lengthening without altering measurable catalytic properties of the enzyme *in vitro*. These telomerase mutations affect telomere length through a Ku-independent mechanism, and do not alter chromosome end structure. While Tel1p is required for expression of the telomere-lengthening phenotype, Rif1p and Rif2p are not, suggesting that telomere overextension is independent of Rap1p. Taken together, these data suggest that specific amino acids within Region I of the catalytic subunit of yeast telomerase play a previously unanticipated role in the response to Tel1p regulation at the telomere.

Introduction

Telomeres are nucleoprotein structures that cap the ends of linear eukaryotic chromosomes. In most species, these termini are composed of tandem, short G-rich repeats and associated protein complexes [reviewed in [125]]. Telomeres play an essential role in genome stability by preventing recognition of the normal chromosome terminus as a DNA double-strand break. However, the inability of the conventional DNA polymerase machinery to fully replicate terminal sequences results in gradual erosion of telomeric repeats, leading to checkpoint activation and cellular senescence. In cells that maintain proliferative potential, this end replication problem is counteracted by telomerase, a reverse transcriptase capable of synthesizing telomeric repeats onto chromosome ends using an intrinsic RNA template [126, 127]. In budding yeast, *TLC1* and *EST2* encode the template RNA and reverse transcriptase subunit, respectively, of the catalytic core of the telomerase holoenzyme [28, 45, 128]. As predicted, strains lacking these genes undergo progressive telomere shortening and senescence [referred to as the EST (Ever Shorter Telomere) phenotype]. Mutations of three additional genes [*EST1*, *EST3*, and *EST4* (*CDC13*)] result in the same phenotype [45, 66, 129]. However, unlike strains lacking *EST2* or *TLC1*, strains bearing these mutations retain telomerase catalytic activity, suggesting that these proteins are essential regulators of telomere replication *in vivo* [27, 129].

Est2p belongs to a family of proteins (TERT; TElomerase Reverse Transcriptase) that contains a domain characteristic of reverse transcriptases (RTs) in its C-terminal half [128]. Sequence alignment among numerous TERT proteins as well as functional analysis in ciliates, yeast and human TERT [32, 50, 130-134] have identified three additional essential

regions [I, II, and III [134]; also called GQ, CP, and QFP [132] or RID1 and RID2 [133]] within the N-terminal half of the protein. Mutations within Regions II and III of Est2p result in loss of coimmunoprecipitation with *TLC1* RNA [40, 134], suggesting that these regions participate in RNA binding. Similar sequences are required for association of ciliate and human TERT with their respective telomerase RNAs [133, 135-137].

TERT Region I contributes several functions to the telomerase holoenzyme, many of which are incompletely understood. The RID1 domain of human telomerase (corresponding to *S. cerevisiae* Region I) interacts with the telomerase RNA and contributes to repeat addition processivity and multimerization [39]. Mutations within a subset of these N-terminal residues of both yeast and human TERT (hTERT) abrogate telomere replication *in vivo*, while the catalytic activity of the enzyme is retained [32, 134]. These residues define an N-terminal region of hTERT that Dissociates Activities of Telomerase (N-DAT domain). A subset of N-DAT mutations are rescued by direct protein fusion of hTERT to telomere-binding proteins, suggesting that these residues contribute to the recruitment of telomerase to the telomere *in vivo* [138, 139].

Additional residues in the N-DAT domain have been implicated in primer association because substitution of these residues (amino acids 92-97) influences primer preference of the holoenzyme *in vitro* [140]. The existence of such a primer binding or anchor site in the telomerase enzyme has been inferred from a number of observations [31, 141, 142] including the propensity of yeast telomerase to remain tightly bound to its *in vitro* reaction products in a manner dependent on the 5' end of telomeric primers [36]. Because these 5' nucleotides lie outside of sequences predicted to base pair with the telomerase RNA, this observation implies an interaction between the primer and protein

component(s) of the complex. Indeed, a telomeric primer can be crosslinked to Est2p, supporting the hypothesis that the anchor site lies in Region I of Est2p [33]. Finally, overexpression of yeast *EST3* specifically suppresses temperature-sensitive mutations in *EST2* Region I, suggesting that N-terminal residues of the yeast catalytic subunit may also play a role in recruiting the Est3 protein to the complex [50].

In most species, telomeric DNA is maintained at a constant average length by a dynamic process that involves a number of regulatory proteins in addition to telomerase. In *S. cerevisiae*, telomere length varies between 225 and 375 base pairs [bp; reviewed in [59]]. This average telomere length is maintained by a balance between the telomere-lengthening activity of telomerase and negative regulation of telomerase by the double-stranded telomeric DNA binding protein Rap1p and its associated factors [84, 85, 143-145]. Rap1p binds to the double-stranded telomeric repeats in yeast where it is thought to nucleate binding of a number of additional proteins to the telomere. As the number of bound Rap1 molecules increases, the accessibility or activity of telomerase at the telomere decreases, thereby allowing Rap1p to effectively "measure" telomere length [reviewed in [17]]. Recent results suggest that telomeres switch between telomerase accessible and inaccessible states and that Rap1p and its binding partners Rif1p and Rif2p are critical determinants of those states [86]. Mutations in *RIF1* and *RIF2*, or C-terminal mutations in *RAP1* that prevent association of Rif1p and Rif2p with the telomere, result in telomere overelongation [84, 85, 143]. Although the precise mechanism through which the binding of Rap1p affects telomerase activity is not understood, this negative regulation is dependent on activity of the Tel1p kinase. Deletion of *TEL1* results in significant telomere shortening [146]. Furthermore, deletion of *TEL1* in *rif1Δ* or

rif2Δ strains or in a strain lacking the C-terminus of Rap1p reduces telomere length to the same degree as *tel1Δ* alone [103, 147]. Therefore, *TEL1* acts downstream of *RAP1*, *RIF1*, and *RIF2*.

In this chapter, I describe the identification of several mutations clustered within Region I of Est2p that result in overelongated telomeres (*est2-LT* alleles). Although the *est2-LT* alleles lie in a region of Est2p that corresponds to residues implicated in primer binding, there is no evidence of defects either in primer binding or catalysis by telomerase immunopurified from *est2-LT* strains. Genetic epistasis analysis suggests that these mutations lengthen telomeres by a Tel1p-dependent mechanism, but are independent of Rif1p and Rif2p. I propose that these mutations in Est2p Region I influence a previously unrecognized regulatory function of the catalytic subunit, the nature of which is addressed in Chapter III.

Results

Identification of mutations in S. cerevisiae EST2 *that increase telomere length*

In the course of analyzing telomere length in a large number of strains containing mutations within the N-terminal half of Est2p, we fortuitously identified three mutations [glycine 75 to alanine (G75A) and asparagine 95 to alanine or aspartic acid (N95A, N95D); Figure 1A] that resulted in telomere overelongation (Figure 4B, compare lanes 2, 3, lanes 5, 6, and lanes 11, 12 with lanes 1, 4, 7, 10). Of the 800 bp telomeric fragment derived from *Pst*I digestion in the subtelomeric Y' element (Figure 4B, line), approximately 250-350 bp comprises telomeric repeat sequences. In this strain

background, G75A increased the average length of the terminal *Pst*I fragment by approximately 30 bp, while N95A and N95D caused a 50 bp increase (20%). 25 other mutations in conserved and non-conserved residues of the N-terminal half of *EST2* caused telomeres to be maintained at normal or shorter-than-normal length [data not shown;[50]].

Because of the clustering of the *est2-LT* alleles in the primary amino acid sequence of Est2p, we screened within a 60 amino acid region encompassing *EST2* amino acids 59 to 119 for additional mutations resulting in this phenotype. Briefly, a plasmid encoding Protein-A tagged *EST2* (*ProA-EST2*) was cleaved with *Pfl*MI and *Afl*II (Figure 4A) and the resulting gapped vector DNA was cotransformed into an *est2::HIS3* yeast strain with an overlapping PCR product generated under mutagenic conditions (see Chapter IV). Transformants recovered on media lacking uracil were restreaked three times (eliminating any senescent colonies bearing non-functional *EST2*) and the resulting healthy strains were screened for increased telomere length by Southern blot. Of ~700 colonies screened, four caused increased telomere length upon plasmid isolation and reintroduction. All four plasmids contained a mutation of glutamic acid 76 to lysine (E76K). Although several of these plasmids contained mutations in addition to E76K, subcloning revealed that the long-telomere phenotype was exclusively due in each case to the E76K mutation (data not shown). In this strain, the E76K mutation increased average telomere length by about 100 bp (40%; Figure 4B, lanes 8 and 9). A mutation within Motif E of the reverse transcriptase motif of *EST2* (*est2-motifE*; Figure 4A) was previously reported to cause telomere lengthening, equivalent to that described here [148].

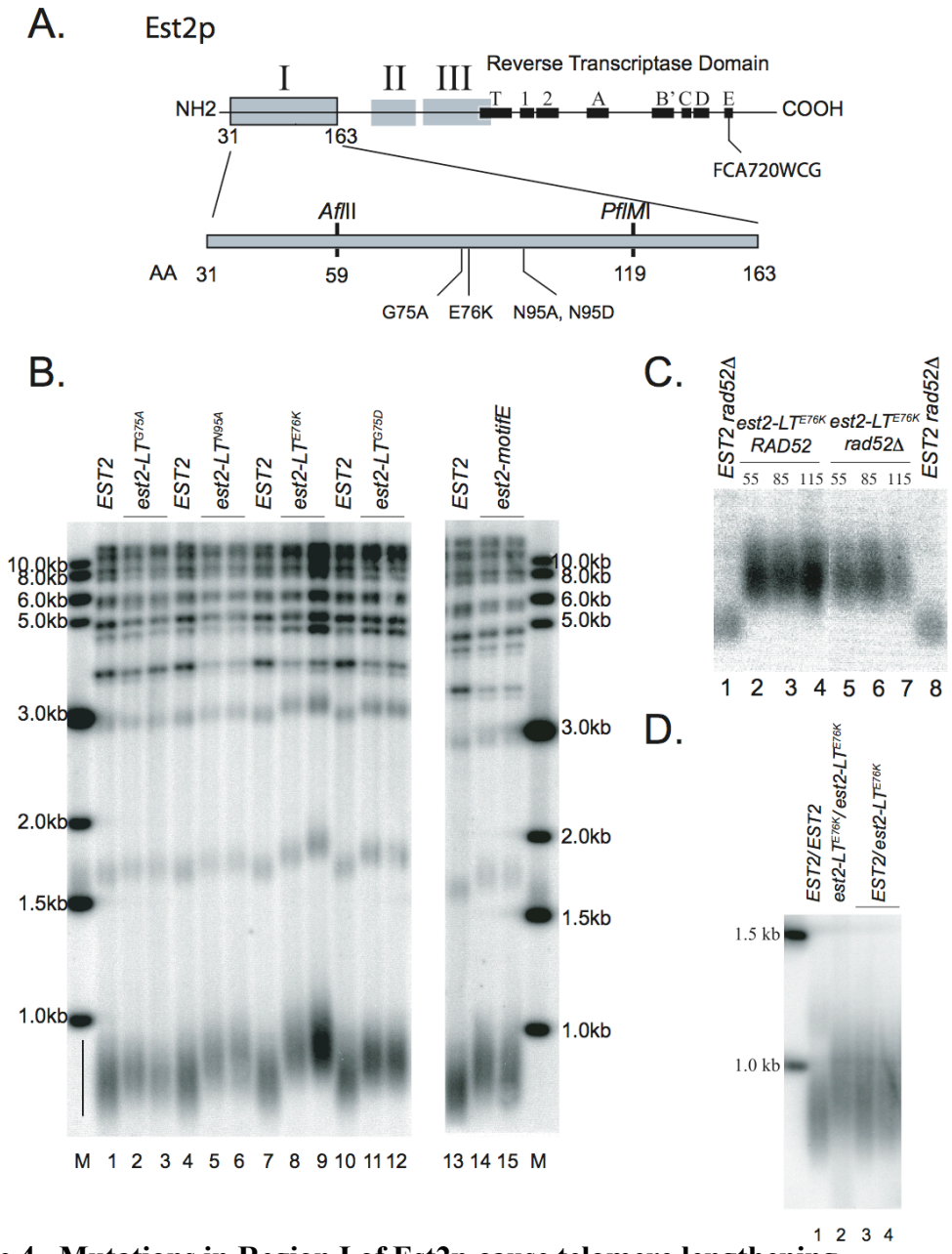

Figure 4. Mutations in Region I of Est2p cause telomere lengthening.

A. Map of functional regions of Est2p. Top: Map of Est2p primary sequence indicating the locations of the reverse transcriptase domain and three N-terminal regions that are essential for telomere maintenance in yeast. The location of the *est2-motifE* mutation is indicated [148]. Bottom: Detailed map of Region I of Est2p. The locations of mutations that result in telomere lengthening are indicated (G75A, glycine 75 to alanine; E76K, glutamic acid 76 to lysine; N95A, asparagine 95 to alanine; N95D, asparagine 95 to aspartic acid). Unique *Afl*II and *Pfl*MI restriction sites were used in a gap-repair strategy to identify additional alleles of *est2-LT* with the long telomere phenotype (see text).

B. Telomere length is increased in strains expressing plasmid-borne *est2-LT* alleles. All strains are derived from YKF120 (*est2::HIS3*) and carry plasmids expressing wild-type or mutant Protein A-tagged *EST2*. Genomic DNA from strains expressing *ProA-EST2* (Lanes 1, 4, 7, 10 and 13), *ProA-est2-LT*^{G75A} (lanes 2 and 3), *ProA-est2-LT*^{N95A} (lanes 5 and 6), *ProA-est2-LT*^{E76K} (lanes 8 and 9), *ProA-est2-LT*^{N95D} (lanes 11 and 12) or *ProA-est2-motifE* (lanes 14 and 15) was digested with *Pst*I, separated in a 1.2% agarose gel, blotted and probed with telomeric DNA. The black bar indicates a smear of fragments derived from the 2/3 of yeast chromosomes that contain a subtelomeric Y' element. Upper bands derive from non-Y' telomeres and tandemly repeated Y' elements. The sizes of maker bands (M) are indicated.

C. Telomere lengthening caused by *est2-LT*^{E76K} is stable and independent of Rad52p. Strains YKF120 (*est2::HIS3 RAD52*; lanes 2-4) and YKF114 (*est2::HIS3 rad52::LEU2*; lanes 5-7) were transformed with pKF410-*est2-LT*^{E76K}, a low-copy number vector expressing the ProA-tagged *est2-LT*^{E76K} allele. Transformants were restreaked once on –ura media and a single colony was grown to saturation in 5 milliliters liquid media lacking uracil. Liquid cultures were serially diluted 1000-fold and allowed to regrow to saturation a total of 10 times. Genomic DNA was harvested from samples corresponding to approximately 55 (lanes 2 and 5), 85 (lanes 3 and 6), and 115 generations (lanes 4 and 7) after transformation of the mutant allele, digested with *Pst*I, separated by gel electrophoresis and probed with a telomeric probe. Control lane contains DNA harvested from YKF120 (*est2::HIS3 RAD52*; lane 1) transformed with a plasmid expressing Protein-A tagged wild-type *EST2* (pKF410) and grown for a minimum of 115 generations. Only the telomeric smear corresponding to Y' chromosomes is shown.

D. The *est2-LT*^{E76K} allele is semi-dominant to wild type. DNA from diploid strains *EST2*/*EST2* (DKF206; lane 1), *est2-LT*^{E76K}/*est2-LT*^{E76K} (DKF207; lane 2), and *EST2*/*est2-LT*^{E76K} (DKF208; lanes 3 and 4) was digested with *Pst*I and subjected to Southern blot as described above. The sizes of marker bands are indicated (M).

Indeed, when this mutation was incorporated into a plasmid-borne, Protein A-tagged allele of *EST2* and transformed into our *est2::HIS3* strain, the extent of telomere lengthening was similar to that caused by the *est2-LT*^{N95A} and *est2-LT*^{G75A} mutations (Figure 4B, lanes 14 and 15).

Because the *ProA-EST2* allele causes slightly decreased telomere length (~50 bp), we were concerned that the effect of telomere lengthening by the *est2-LT* alleles might result from stabilization specific to the Protein-A tagged protein. To address this possibility, *est2-LT*^{E76K} was introduced into the chromosome at the endogenous locus (in the absence of the Protein-A tag) and telomere length was assayed by Southern blot. Under these conditions, the increase in telomere length was comparable to that seen with the plasmid-borne, tagged allele (data not shown; see also Figure 10A, lanes 1 and 2), confirming that the mutation does not simply counteract the negative effect of the epitope tag.

In the absence of functional telomerase, most cells die after ~75 generations. However survivors arise that maintain heterogeneous telomeres through Rad52p-mediated recombination [65]. To assess the role of recombination in telomere lengthening, a plasmid bearing the *est2-LT*^{E76K} allele was introduced into an *est2Δ rad52Δ* strain and the resulting transformants were grown for ~115 generations in liquid culture. Telomere lengthening was identical to that seen in an *est2Δ RAD52* background (Figure 4C, compare lanes 2- 4 with lanes 5- 7). Therefore, recombination does not contribute to the long telomere phenotype. This result also demonstrates that the mutants reach a new, stable telomere length equilibrium and do not undergo continuous elongation.

We considered the possibility that the *est2-LT*^{E76K} allele alters the interaction of Est2p with one or more components of the telomerase complex. Coimmunoprecipitation experiments demonstrated that the ability of the ProA-Est2-LT^{E76K} protein to bind HA-Est1p, HA-Est3p, and Myc-PinXIp was equivalent to wild type (Figure 5), arguing that alteration of the relative stoichiometry of these components in the telomerase complex does not contribute to the telomere lengthening phenotype.

To address whether the telomere lengthening phenotype conferred by *est2-LT*^{E76K} is dominant or recessive to wild type, we created a heterozygous diploid strain. As shown in Figure 4D, two independent *EST2/est2-LT*^{E76K} diploid strains (lanes 3 and 4) had telomere length intermediate between that of an *EST2*/*EST2* diploid (lane 1) and an *est2-LT*^{E76K}/*est2-LT*^{E76K} diploid (lane 2). Telomere length of the heterozygous diploid strain was more heterogeneous than either homozygous diploid strain. We conclude that the *est2-LT*^{E76K} allele is semi-dominant.

Nucleotide-addition processivity of est2-LT *alleles is normal*

The similarity in telomere phenotype between the *est2-LT* Region I mutants and the *est2-motifE* mutant (Figure 4B) suggested that these alleles might be mechanistically related. Increased nucleotide-addition (Type I) processivity demonstrated by the *est2-motifE* allele *in vitro* has been hypothesized to account for increased telomere length *in vivo* [148]. To address whether the *est2-LT* mutations also increase Type I processivity, telomerase was partially purified from yeast cells expressing Protein-A tagged Est2p by adsorption to IgG beads. Bead-bound telomerase was incubated in the presence of ^{32}P-dGTP, cold dTTP, and a 14 nucleotide telomeric primer. This oligonucleotide primer

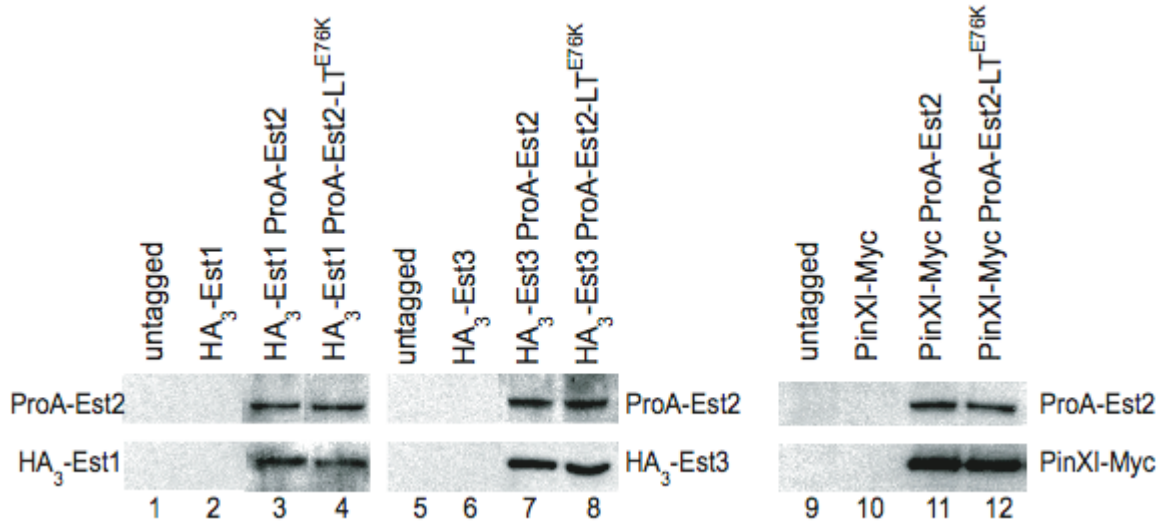

Figure 5. The *est2-LT^{E76K}* allele does not alter interactions with Est1p, Est3p, or PinXIp.

Strains pVL288 (*HA$_3$-EST1*), YKF110 (*EST3-HA$_3$*) and YKF209 (*PINXI-Myc*) were transformed with pKF404 (untagged *EST2*; lanes 2, 6, and 10), pKF410 (*ProA-EST2*; lanes 3, 7, and 11), or pKF410-E76K (*ProA-est2-LT^{E76K}*; lanes 4, 8, and 12). The parental untagged strain (AVL78; *MATa leu2 trp1 ura3-52 prb- pre- pep4-3*) was transformed with pKF404 as an untagged control (lanes 1, 5, and 9). ProA-Est2p was immunoprecipitated on IgG beads as described in Chapter IV and detected with mouse monoclonal anti-Protein A (Sigma). HA$_3$-tagged proteins were detected with monoclonal HA.11 antibody (Covance). PinXI-Myc was detected with monoclonal c-Myc antibody (EMD Biosciences). Secondary was peroxidase-conjugated goat anti-mouse antibody (Chemicon International).

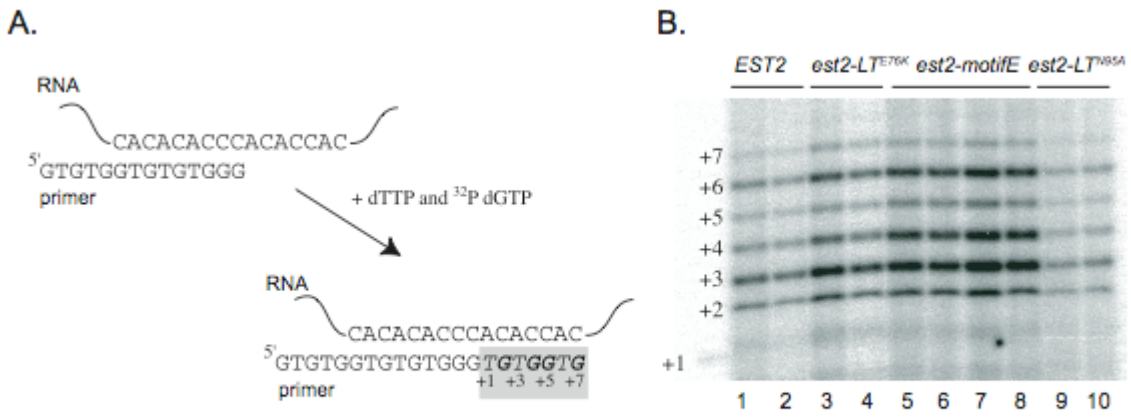

Figure 6. Processivity of telomerase is increased by a mutation in Motif E, but not by mutations in the N-terminal region.

A. Schematic diagram of the *in vitro* telomerase assay. Extension of a 14 nucleotide telomeric primer by immunopurified telomerase in the presence of dTTP and radiolabeled dGTP results in the addition of up to 7 nucleotides.

B. Primer extension of the 14 nucleotide primer by wild-type or mutant telomerase. Extract was isolated from strain YKF120 (*est2::HIS3*) bearing plasmids expressing the indicated alleles (*ProA-EST2*, lanes 1 and 2; *ProA-est2-LT*^{E76K}, lanes 3 and 4; *ProA-est2-motifE*, lanes 5-8; *ProA-est2-LT*^{N95A}, lanes 9 and 10) and telomerase was immunopurified on IgG beads. Telomerase assays were performed as described in Chapter IV. The positions of each consecutive nucleotide added to the 14 nucleotide primer are indicated. +1 marks the position of a 14+1 marker created by incubation of the 14 nucleotide primer with ^{32}P labeled ddTTP and terminal transferase. Processivity of the wild-type and mutant telomerase was calculated from this and other similar experiments (data not shown) as summarized in Table 1.

Note: This experiment was performed by Katherine Friedman.

Table 1. Processivity values of *est2-LT* alleles

Strain	Processivity$^{(+3)}$* (n)	Percent Change$^{\#}$	Significance**
EST2	0.228 +/- 0.009 (6)		
est2-motifE	0.298 +/- 0.007 (4)	+ 31	p≤0.002
est2-LT^{N95A}	0.229 +/- 0.005 (4)	+ 0.4	p≤0.91
est2-LT^{E76K}	0.216 +/- 0.030 (4)	- 5.0	p≤0.38

* Processivity$^{(+3)}$ refers to the frequency with which telomerase synthesizes past the third position. See Chapter IV for details of calculation. Standard deviation (+/-) is indicated as well as the number of independent samples (in parentheses).

$^{\#}$ Percent change of processivity$^{(+3)}$ from wild type is calculated using the average values shown in the second column.

** Significance values were determined relative to wild type using a Student T-test.

aligns with the telomerase RNA to allow addition of up to 7 nucleotides in a single round of polymerization (Figure 6A). Because yeast telomerase remains bound to its reaction products under these conditions [36], the enzyme does not demonstrate repeat-addition (Type II) processivity -- the ability to add multiple repeats to a single primer. Indeed, because most primers fail to become extended to the end of the template, a ladder of products (+2 to +7) is visualized even after prolonged incubation (Figure 6B). Because the largest effect on processivity was previously shown to occur at the third template position [148], nucleotide-addition processivity was expressed as a processivity$^{(+3)}$ value [probability that the enzyme extends past the n+3 position; [148]] by summing the intensity of the last four template positions (n+4 to n+7) and dividing by the total intensity at all 7 template positions (corrected for specific activity; Chapter IV). As expected, the *est2-motifE* allele showed a significant increase in Type I processivity at the third template position (Figure 6B; Table 1). The percent change in processivity compared to wild type (31% increase) was comparable to that previously reported [148], although the absolute processivity value for wild-type telomerase was lower in our experiments. In contrast to *est2-motifE*, the *est2-LT*^{N95A} and *est2-LT*^{E76K} alleles had processivity$^{(+3)}$ values indistinguishable from wild type (Figure 6B; Table 1). We conclude that the telomere length increase caused by mutations in the N-terminal domain of *EST2* differs mechanistically from that resulting from mutation in Motif E of the reverse transcriptase domain.

Primer binding of est2-LT *alleles is unaffected*

Recent results suggest that the yeast anchor site lies within Region I of Est2p [33]. Because altered primer binding might cause telomere lengthening, we addressed the ability of the *est2-LT* alleles to bind telomeric primer using two independent assays. The first was a primer competition experiment described by Prescott and Blackburn[36]. Because yeast telomerase displays single turn-over kinetics *in vitro*, a challenge primer added several minutes after the initiation of primer extension is not utilized. This property is hypothesized to arise from persistent interactions between the telomerase holoenzyme and its reaction products, perhaps mediated by the anchor site. Indeed, a primer with non-telomeric sequence at its 5' end (5' NT primer) is extended normally by telomerase *in vitro*, but fails to block use of the challenge primer [36]. We reasoned that a mutation in the telomerase enzyme itself (perhaps in Est2p) that reduces primer interaction might similarly increase extension of the challenge primer in this assay. Both wild-type and mutant telomerase were immunopurified from whole cell yeast extract and subjected to incubation with one binding as measured in this assay. Furthermore, because these assays were conducted in the presence of all four nucleotides, the failure to detect products longer than +7 (Figure 6) indicated that the *est2-LT* alleles do not cause extension past the template boundary.

We were concerned that increased primer binding would not be detected in the primer competition assay. Therefore, we also examined the response of wild-type and mutant enzyme to decreasing primer concentration. Telomerase immunopurified from *EST2* and *est2-LT*^{E76K} strains was incubated with 5X serial dilutions of a telomeric 14-mer primer and ^{32}P-dTTP. In the absence of dGTP, telomerase adds only a single nucleotide to

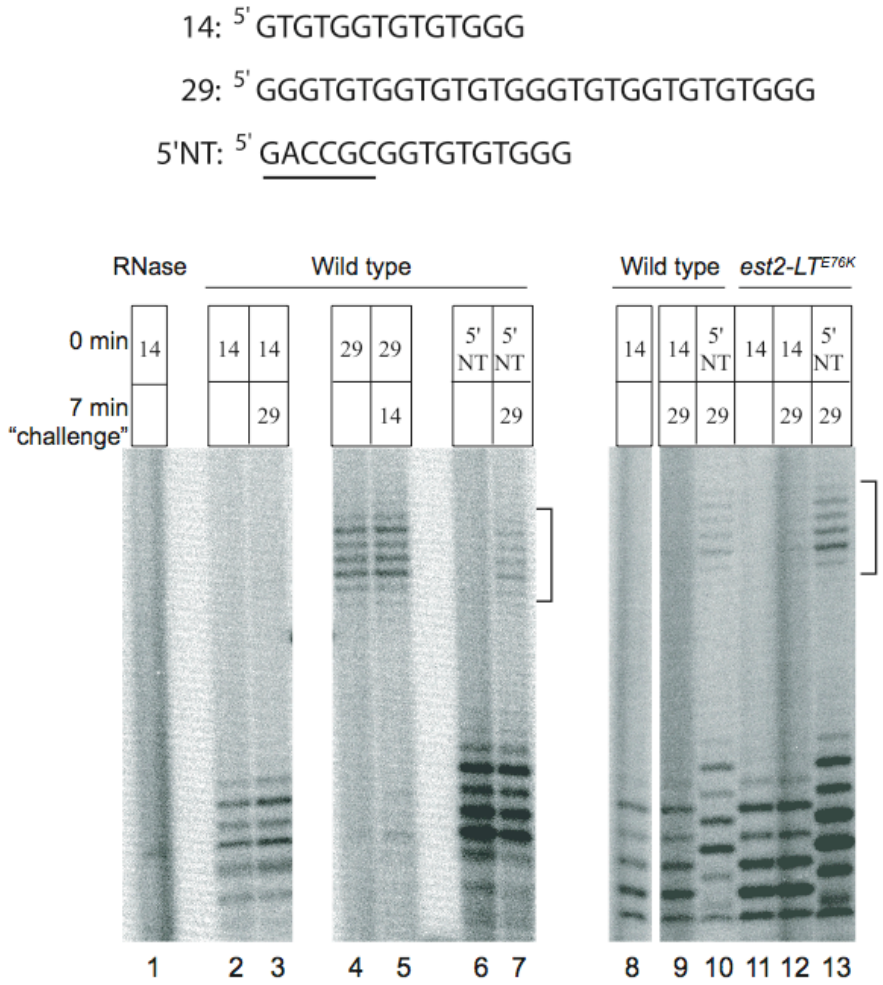

Figure 7. Yeast telomerase containing a mutation at Est2p residue E76 does not exhibit a detectable decrease in product association in a primer-competition assay.
Extract was isolated from strain YKF120 (*est2::HIS3*) containing plasmids expressing either wild-type, Protein-A tagged *EST2* (*ProA-EST2*, lanes 1-10) or Protein-A tagged *est2-LT*^{E76K} (*ProA-est2-LT*^{E76K}, lanes 11-13) and telomerase was immunopurified on IgG beads. Primer sequences are shown (Top). Primers 14 and 29 contain the canonical telomeric sequence, while primer 5'NT contains non-telomeric sequence at its 5' end (underlined). Telomerase assays were performed using the indicated combinations of primers (see boxes). The top primer was added at the beginning of the reaction, while the bottom primer (or buffer alone; empty box) was added after the reaction had proceeded for seven minutes. Products resulting from extension of the 29 nucleotide primer are indicated with brackets. Lane 1 contains a sample that was pretreated with RNase A to eliminate telomerase activity.
Note: This experiment was performed by Katherine Friedman.

the telomeric primer (Figure 8A). The amount of primer-extension product formed at each time point was quantified and normalized using a labeled, 28 nt precipitation and loading control. Wild-type and *est2-LT*^{E76K} telomerase were indistinguishable in this assay (Figure 8B and C), showing that the apparent Km for primer in the reaction is not affected by the *est2-LT*^{E76K} allele.

We consistently observed a slight (less than two-fold) increase in activity in Est2p immunoprecipitates from the *est2-LT*^{E76K} strain (e.g. Figure 5, compare lanes 1 and 2 with lanes 3 and 4). This increased activity can be attributed to a modest increase in the amount of Est2p immunoprecipitated from the mutant strain (Figure 9A). However, when ProA-Est2p was detected in extract, expression of the wild-type and Est2-LT^{E76K} proteins was equivalent (Figure 9B). We conclude that the slightly elevated *in vitro* activity of the mutant protein reflects an increased efficiency of immunoprecipitation, rather than increased enzyme activity *per se*. Although we cannot rule out the contribution of subtle changes in enzyme activity, the results presented here suggest that the *est2-LT* alleles do not alter the intrinsic catalytic properties of yeast telomerase.

The est2-LT *alleles do not affect the single-stranded character of the telomere*

To explore the possibility that the *est2-LT* alleles alter telomerase function in vivo, we used non-denaturing gel electrophoresis to probe the chromosomal end-structure in wild-type and mutant strains. In wild-type cells, yeast chromosomes acquire a long $TG_{1\text{-}3}$ tail (more than 30 bp) late in S phase while the 3' single-strand overhang is <15 bp during the remainder of the cell cycle [22]. As a result, DNA isolated from asynchronous wild-type cells results in very little telomeric signal when cleaved with XhoI to release a

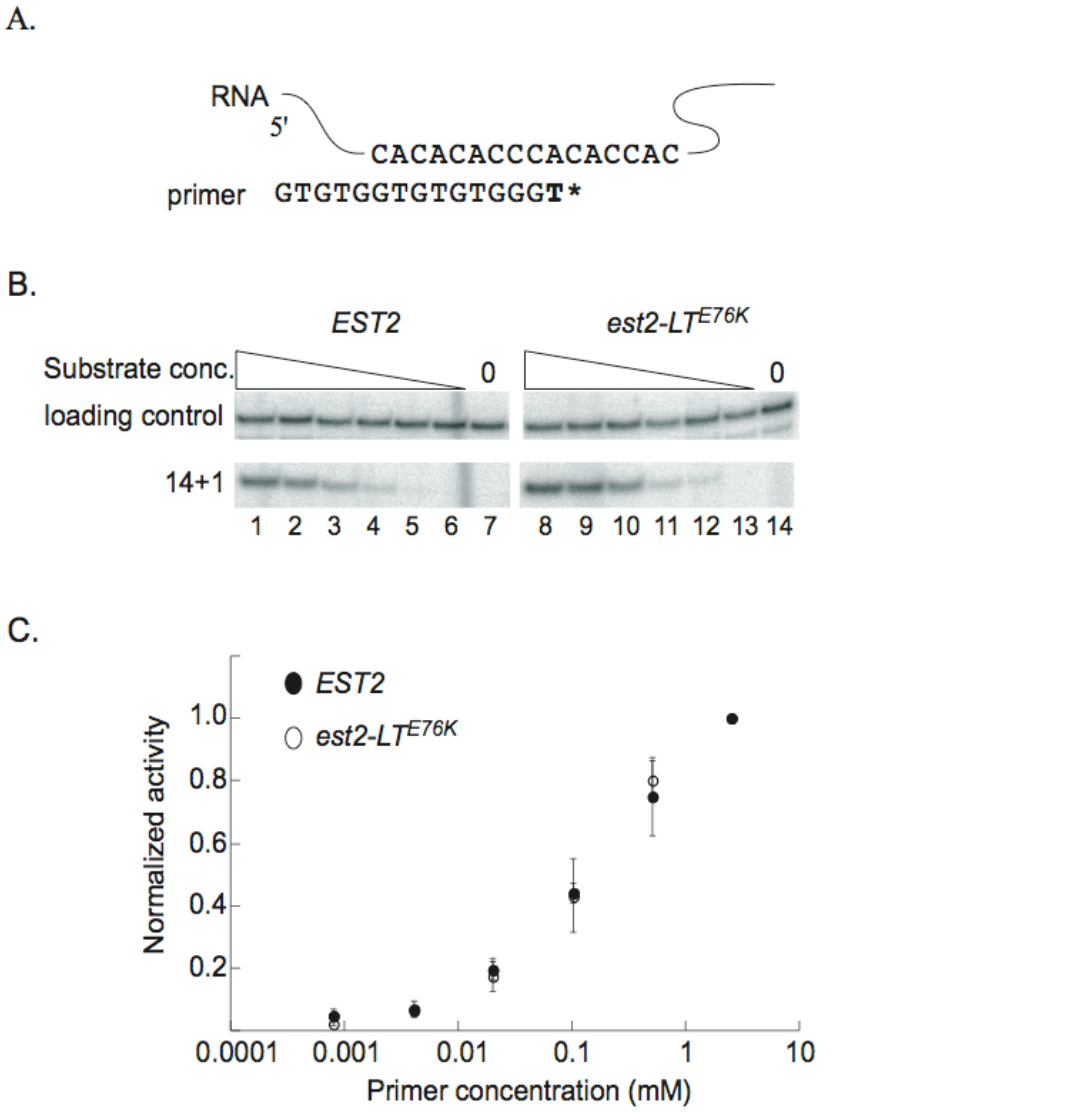

Figure 8. The ability of telomerase to bind primer is unchanged by mutation of Est2p residue E76.

A. Schematic diagram of the *in vitro* telomerase assay. Extension of a 14 nucleotide telomeric primer by immunopurified telomerase in the presence of radiolabeled TTP alone results in the addition of a single nucleotide.

B. Change in activity of wild-type and mutant telomerase with decreasing primer concentration. Telomerase was partially purified from strain YKF120 (*est2::HIS3*) containing plasmids expressing either wild-type, Protein-A tagged *EST2* (*ProA-EST2*, lanes 1-7) or Protein-A tagged *est2-LT*^{E76K} (*ProA-est2-LT*^{E76K}, lanes 8-14) by incubation with IgG conjugated beads. Standard telomerase assays were conducted (see Chapter IV) at decreasing primer concentrations. Production of the 14+1 product and recovery of a labeled 29 nucleotide precipitation and loading control is shown. Primer concentrations are 2.5 μM (lanes 1 and 8), 0.50 μM (lanes 2 and 9), 0.10 μM (lanes 3 and 10), 0.02 μM (lanes 4 and 11), 0.004 μM (lanes 5 and 12), and 0.0008 μM (lanes 6 and 13). Lanes 7 and 14 are assays done in the absence of primer.

C. Quantification of telomerase activity in response to decreasing primer concentration. Band intensities in the experiment shown in Figure 8B and others (data not shown) were determined by phosphorimager. After adjustment for loading and precipitation efficiency, values were normalized to activity obtained at the highest primer concentration (see Chapter IV for detail). Primer concentration (log axis) is graphed versus average, normalized activity level. Closed circles, *EST2*; open circles, *est2-LT*^{E76K}. Error bars represent standard deviation calculated from three independent experiments for wild type and two independent experiments for *est2-LT*^{E76K}.

Note: This experiment was performed by Katherine Friedman.

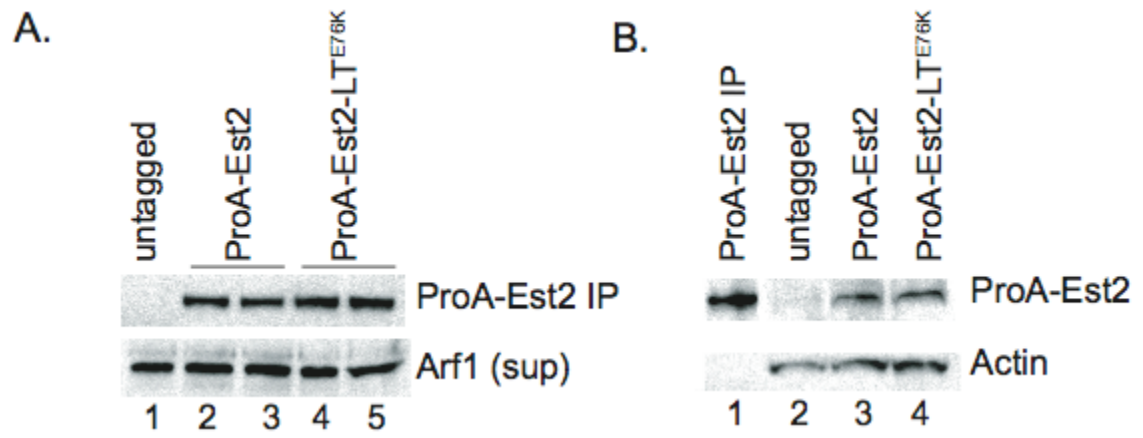

Figure 9. Protein expression of wild-type and mutant Est2p is equivalent.

A. Immunoprecipitation of ProA-Est2p from extract. ProA-Est2p was immunoprecipitated on IgG conjugated beads from strain YKF120 (*est2::HIS3*) containing plasmids expressing either untagged *EST2* (pKF404, lane 1), Protein-A tagged *EST2* (pKF410, lanes 2 and 3) or Protein-A tagged *est2-LT^{E76K}* (pKF410-Est2-LT^{E76K}, lanes 3 and 4) and detected by Western blotting using an anti-protein A primary antibody. (top band). Duplicate lanes (2 and 3; 4 and 5) represent two independent immunoprecipitations from the same extract preparation to show reproducibility. Supernatants from the immunoprecipitations were Western blotted for the presence of Arf1p to verify equivalent extract concentrations (bottom band).

B. Detection of ProA-Est2p in extract. Extracts from strain YKF120 (*est2::HIS3*) containing plasmids expressing either untagged *EST2* (pKF404, lane 2), Protein-A tagged *EST2* (pKF410, lane 3) or Protein-A tagged *est2-LT^{E76K}* (pKF410-Est2-LT^{E76K}, lane 4) were Western blotted and probed with an anti-protein A primary antibody (top band). Lane 1 contains immunoprecipitated Pro-Est2p (identical to Figure 9A, lane 2) as a size marker. Actin was detected as a loading control (bottom band).

terminal fragment of 1.3 kb and hybridized under non-denaturing conditions to an oligonucleotide that specifically recognizes the G-rich, telomeric 3' overhang (Figure 10A, lane 1). In contrast, a *ku70Δ* strain has long single-stranded telomeric overhangs that persist throughout the cell cycle and are therefore easily detected in asynchronous cells [Figure 10A, lane 3; reference [107]]. Hybridization in the native gel was specific to single-stranded DNA because treatment of the DNA with exonuclease I (ExoI) prior to hybridization eliminated the signal (Figure 10A, even numbered lanes).

Strains expressing the *est2-LT*^{N95A}, *est2-LT*^{E76K}, and *est2-motifE* alleles lacked telomeric signal in the native gel (Figure 10A, lanes 5, 7, 9, respectively), indicating no increase in single-stranded character compared to the wild-type strain (Figure 10A, lane 1). The identical gel shown in Figure 10A was denatured and rehybridized with the telomeric oligonucleotide to confirm equivalent loading of the samples (Figure 10B). We conclude that the *est2-LT* alleles (and *est2-motifE*) do not significantly compromise replication or processing of the C-rich strand of the telomere.

The est2-LT *alleles increase telomere length by a* TEL1*-dependent mechanism, but are independent of* YKU70*,* RIF1*, and* RIF2

To determine the genetic pathway through which the *est2-LT* alleles cause telomere lengthening, we used epistasis analysis to examine the involvement of several genes known to influence telomere length. The Ku70/80 complex and Tel1p act in different pathways to positively regulate telomere length [106]. Therefore, we examined the effect of creating double mutations of these genes with the *est2-LT*^{E76K} allele.

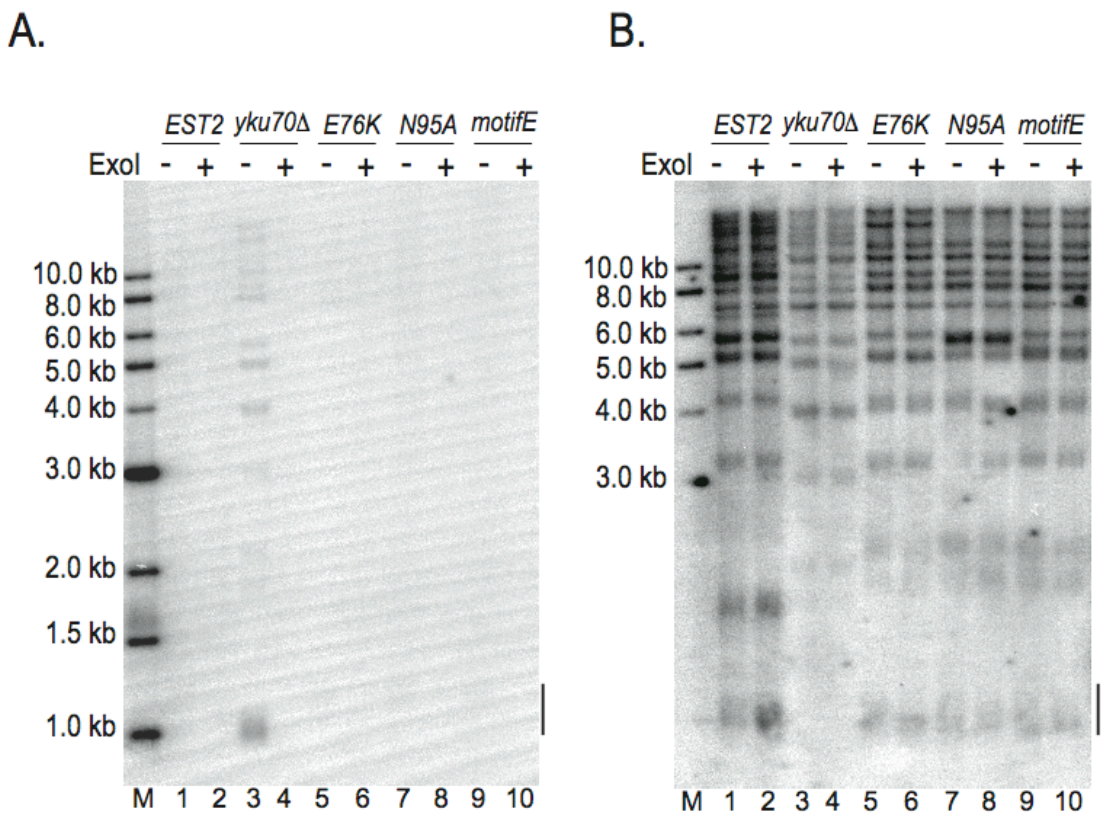

Figure 10. The 3' single-stranded overhang of *est2-LT* mutants is normal.

A. Single-stranded telomeric DNA detected by non-denaturing gel electrophoresis. All strains are derived from YKF120 (*est2::HIS3*) and carry plasmids expressing wild-type or mutant Protein A-tagged *EST2*. Genomic DNA from strains expressing *ProA-EST2* (lanes 1 and 2), *ProA-est2-LT*^{E76K} (lanes 6 and 6), *ProA-est2-LT*^{N95A} (lanes 7 and 8) or *ProA-est2-motifE* (lanes 9 and 10) was digested with *Xho*I, incubated with a labeled 22 nucleotide telomeric probe, and subjected to non-denaturing gel electrophoresis. DNA from a *ku70* deletion strain previously demonstrated to increase the 3' telomeric overhang [107] was used as a positive control (lanes 3 and 4). Samples in lanes 2, 4, 6, 8, and 10 were treated with exonuclease I prior to *Xho*I cleavage to remove the 3' single-stranded overhang. The bar indicates the approximate position of the terminal *Xho*I fragment generated from chromosomes that contain a subtelomeric Y' element. Additional bands detected in lanes 3 and 4 correspond to individual telomeres lacking the Y' element. Lane M, end-labeled DNA size standards.

B. Total telomeric DNA detected by hybridization after denaturation. The same gel shown in A was denatured by treatment with 0.5M NaOH and hybridized with the telomeric probe described in A. The bar indicates the approximate position of the terminal XhoI fragment generated from chromosomes that contain a subtelomeric Y' element. Although fragments corresponding to the shortest telomeres of the *yku70Δ* strain were preferentially lost during the wash steps, relative loading can be assessed by comparison of the higher molecular weight bands.

A deletion of *yku70* was introduced into strains expressing *EST2* or *est2-LT*^{E76K}. Telomere length was assayed by Southern blot after cleavage with *Pst*I. As shown in Figure 11A (lanes 3 and 4), the double mutant strain had telomere length intermediate between that of the *yku70* deletion alone (lane 5) and the *est2-LT*^{E76K} single mutant (lane 2). Restreaking of the double mutant strain nine times did not result in any further change in telomere length (Figure 11A, compare lanes 3 and 4). Because the telomere lengthening phenotype of the *est2-LT*^{E76K} allele was expressed in the absence of Ku70p, we conclude that positive regulation by the Ku70/80 complex contributes little, if at all, to the *est2-LT* phenotype.

To test the requirement for Tel1p, a *tel1::kanMX* disruption was introduced into strains expressing *EST2* or *est2-LT*^{E76K}. Two independent *est2-LT*^{E76K} *tel1Δ* strains had telomeres intermediate in length compared with either single mutant when telomere length was assayed immediately after *TEL1* disruption (Figure 11B, lanes 3 and 11, restreak 1). However, further propagation of the double mutant strains (to restreak 5) resulted in gradual telomere erosion until the double mutant strain attained a telomere length nearly as short as that of the *tel1Δ* strain (Figure 11B, compare lanes 5 and 13 with lanes 9 and 17). Strikingly, both transformants displayed increased heterogeneity of telomere length after further restreaking (Figure 11B, lanes 6-8 and 14-16). In this strain background, the *est2-LT*^{E76K} mutation caused telomere length to increase by nearly 200 bp compared to wild-type. In comparison, the *tel1Δ est2-LT*^{E76K} strain displayed a telomere length at restreak 5 that was only 30 bp longer than the *tel1Δ* strain. We obtained identical results in a *tel1Δ est2-LT*^{N95A} strain (data not shown). We conclude

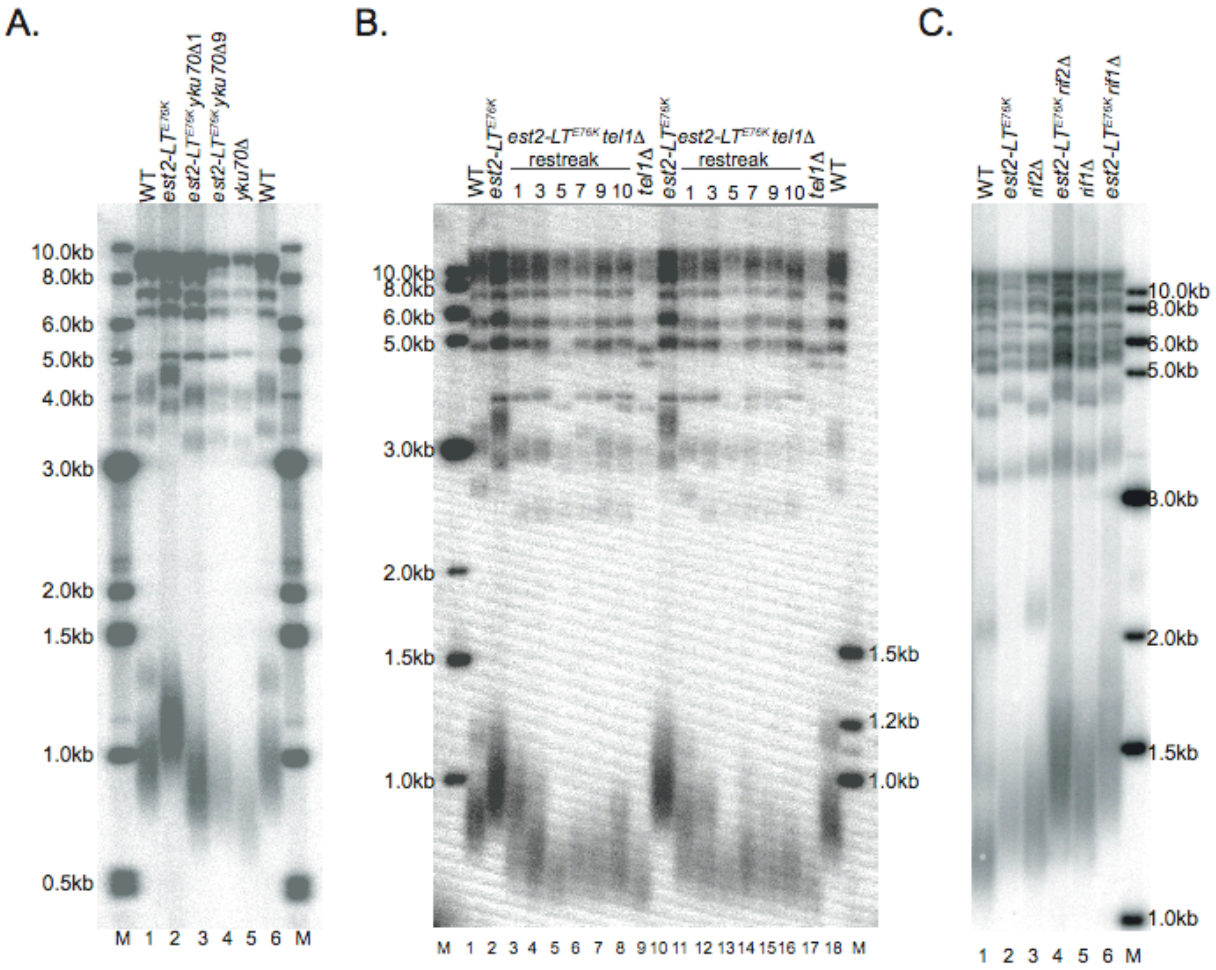

Figure 11. Increased telomere length of the *est2-LT* alleles is dependent on *TEL1*, but independent of *YKU70, RIF1, and RIF2*.

A. Epistasis analysis of *yku70Δ* and *est2-LT*^{E76K}. Gene replacement was used to generate strains deleted for *YKU70* (*yku70::KAN*) and expressing either wild-type *EST2* (YKF203; lane 5) or *est2-LT*^{E76K} (YKF203-E76K; lanes 3 and 4) from the endogenous, chromosomal locus. After isolation of the appropriate *yku70* disruption, the *est2-LT*^{E76K} *yku70::KAN* strain was restreaked 9 times to confirm that telomere length had stabilized. DNA isolated after restreak 1 (lane 3) and restreak 9 (lane 4) is shown. Telomere length was visualized by Southern blotting of *Pst*I digested genomic DNA with a telomeric probe. DNA isolated from isogenic *YKU70* strains expressing wild-type *EST2* (YKF201, lanes 1 and 6) or *est2-LT*^{E76K} (YKF201-E76K, lane 2) was included for comparison. The positions of molecular weight markers are indicated (M).

B. Epistasis analysis of *tel1Δ* and *est2-LT*^{E76K}. Gene replacement was used to generate strains deleted for *tel1* (*tel1::KAN*) and expressing either wild-type *EST2*(YKF202; lanes 9 and 17) or *est2-LT*^{E76K} (YKF202-E76K; lanes 3-8 and lanes 11-16) from the endogenous, chromosomal locus. Because the telomere length phenotype of the *tel1Δ* takes many generations to reach maximum expression, newly transformed strains were sequentially restreaked on plates. For the double mutant, two independent transformants were restreaked and DNA was prepared from restreaks 1, 3, 5, 7, 9, and 10 as indicated. Only restreak 10 of the *tel1Δ* strain is shown. Genomic DNA was

digested with *Pst*I, and telomere length was measured by Southern blotting. DNA isolated from isogenic *TEL1* strains expressing wild-type *EST2* (YKF201, lanes 1 and 18) or *est2-LT*^{E76K} (YKF201-E76K, lanes 3 and 10) was included for comparison. The positions of molecular weight markers are indicated (M).

C. Epistasis analysis of *rif1Δ* and *rif2Δ* with *est2-LT*^{E76K}. Gene replacement was used to generate strains deleted for *rif2* (*rif2::KAN*) and expressing either wild-type *EST2* (YKF205; lane 3) or *est2-LT*^{E76K} (YKF205-E76K; lane 4) from the endogenous, chromosomal locus. Strains deleted for *rif1* (*rif1::KAN*) and expressing wild-type *EST2* (YKF204; lane 5) or *est2-LT*^{E76K} (YKF204-E76K; lane 6) from the chromosomal locus were also created. Genomic DNA was digested with *Xho*I, and telomere length was measured by Southern blotting. DNA isolated from isogenic *RIF1* and *RIF2* strains expressing wild-type *EST2* (YKF201, lane 1) or *est2-LT*^{E76K} (YKF201-E76K, lane 2) was included for comparison. The positions of molecular weight markers are indicated (M).

that telomere lengthening caused by the *est2-LT*^{E76K} allele is nearly completely dependent on Tel1p, though there may be a minor contribution by a Tel1p-independent pathway. Tel1p acts downstream of Rap1p in the regulation of telomere length [147]. Therefore, it was possible that telomere lengthening in the *est2-LT* strains occurred through the same genetic pathway as *RAP1*. Rif1p and Rif2p interact with the C-terminus of Rap1 and negatively regulate telomere length [84, 85]. As shown in Figure 11C, *rif1Δ* and *rif2Δ* strains exhibit increased telomere length compared to a wild-type strain (compare lanes 3 and 5 with lane 1). When the *est2-LT*^{E76K} mutation is combined with a *rif1* or *rif2* deletion, telomere length undergoes an additional increase in each case (Figure 11C, lanes 4 and 6). We obtained identical results when double mutants were constructed using the *est2-LT*^{N95A} allele (data not shown). We conclude that the telomere lengthening phenotype of the *est2-LT* alleles is independent of *RIF1* and *RIF2*.

Discussion

Telomere length homeostasis is critical to the maintenance of stable chromosomes. Previous work has suggested that telomere length is negatively regulated by protein factors that bind to telomeric chromatin [reviewed in reference [17]]. Specifically, Rap1p and its associated proteins bind to the telomeric repeat and regulate a molecular switch between telomerase-extendible and non-extendible states [86]. This mechanism of telomere length regulation is highly dependent on the chromatin context of the telomere, with telomerase presumably acting as a passive downstream target of the regulatory pathway. Here we show that mutations in a small region of the catalytic subunit of telomerase also cause telomere lengthening. Within the limits of our

biochemical assays, the catalytic activity of the mutant enzyme is unaffected, indicating that the catalytic subunit of telomerase may play a previously unanticipated role in the regulation of telomerase activity at the telomere *in vivo*.

Catalytic activity of the mutant telomerase complex

The observation that telomeres become overelongated in the *est2-LT* strains initially suggested that telomerase in these strains may have increased or modified catalytic activity. Several observations argue against this possibility. Processivity of the enzyme is not altered, a phenotype that has previously been associated with telomere lengthening [148]. Telomere lengthening by a defective telomerase enzyme might occur through infidelity of the enzyme resulting in abnormal repeat sequences. Such sequences might disrupt the ability of Rap1p to bind the telomere, increasing telomere accessibility. Although we did not extensively analyze nucleotide usage by the mutant complex, there is no detectable synthesis past the +7 position in our primer-extension analyses, even in the presence of all 4 nucleotides, and no change in the electrophoretic mobility of the products, a characteristic that is sensitive to base sequence [149]. Furthermore, addition of labeled dTTP alone to the telomerase assay results in the addition of a single nucleotide by both mutant and wild-type telomerase, suggesting that fidelity at the second template position remains high. Consistent with these observations, *est2-LT*^{E76K} causes additional telomere lengthening in *rif1Δ* and *rif2Δ* strains, implying that telomere overelongation is independent of the *RAP1* genetic pathway.

Est2p can be physically crosslinked to oligonucleotide primer and some mutations and deletions within the N-terminus alter primer usage in a manner consistent with loss of the telomerase anchor site [33]. Unlike the *est2-LT* alleles, these mutations cause telomere

shortening, suggesting that the *est2-LT* phenotype does not result from loss of anchor site function. Consistent with this assertion, a primer challenge assay shows no evidence of decreased primer association by telomerase in an *est2-LT* strain. Telomere lengthening might occur if the enzyme-DNA interaction were increased, a possibility consistent with the semi-dominant nature of the *est2-LT*^{E76K} allele. However, the amount of activity displayed by wild-type and *est2-LT*^{E76K} telomerase on decreasing concentrations of primer is indistinguishable, indicating that the Km for primer is not significantly altered by the E76K mutation. We conclude that increased anchor site interaction is unlikely to account for the long-telomere phenotype, although we cannot rule out the possibility that slight differences in primer association translate into measurable changes in telomere length *in vivo*.

Our experiments show a slight (<2 fold) but reproducible increase in the amount of *est2-LT*^{E76K} mutant protein that can be immunoprecipitated from cells (Figure 9A). Interestingly, detection of wild-type and mutant ProA-Est2p in extract demonstrates equivalent expression, suggesting that the accessibility of the Protein A epitope tag may be altered by the E76K mutation in Est2p. Because expression of the ProA-Est2-LT^{E76K} protein appears unchanged, it is unlikely that differences in protein expression account for the telomere lengthening phenotype.

PinXIp has been shown to compete with the telomerase RNA for Est2p binding [40]. Therefore, decreased interaction with PinXI might increase telomere length by increasing the amount of assembled holoenzyme *in vivo*. Consistent with the observation that Region I is not required for interaction with PinXIp [40], the ability of PinXIp to bind Est2p is not altered by the E76K mutation (Figure 5). Indeed, although co-overexpression of Est2p and *TLC1* RNA greatly increases the amount of telomerase activity in cell extract, such overexpression

does not cause telomere lengthening, presumably because other critical components of the complex or telomeric chromatin are limiting [150]. Together with the observation that the interaction of Est2p with Est1p and Est3p is not altered by the E76K mutation (Figure 5), these data argue that the long telomere phenotype is not due to alterations in the amount or stoichiometry of the telomerase complex.

Genetic pathway of telomere lengthening by* est2-LT *alleles

Given the lack of evidence for altered catalytic activity of the *est2-LT*^{E76K} enzyme, we favor the hypothesis that these particular mutations in the N-terminus of Est2p impact a regulatory pathway *in vivo*. This possibility is supported by the observation that deletion of the yeast ATM homolog *TEL1* is epistatic to the *est2-LT* mutants. Deletion of *TEL1* in the *est2-LT*^{E76K} background almost completely abrogates the telomere lengthening phenotype. This effect takes 5 restreaks (approximately 125 generations) for full expression and suggests that telomerase requires function of the Tel1 protein in order to manifest the *est2-LT* phenotype. This genetic result distinguishes the *est2-LT* alleles from mutations in *ELG1* [98] and *POL12* [151] that also cause telomere lengthening, but are independent of *TEL1*.

Tel1p is hypothesized to facilitate the recruitment of telomerase to the telomere *in vivo* by facilitating the interaction between telomerase and its substrate, perhaps through modulating activity of the Mre11/Rad50/Xrs2 (MRX) complex [71, 102, 111]. The *est2-LT* alleles may increase the sensitivity of telomerase to this recruitment function. Because we do not detect changes in the interaction between partially purified mutant telomerase and an oligonucleotide primer *in vitro*, we favor the hypothesis that such increased recruitment occurs through changes in the interaction between telomerase and components of telomeric

chromatin. Although *RIF1* and *RIF2* function upstream of *TEL1*, these genes do not appear to play a role in telomere lengthening mediated by the *est2-LT* alleles since telomere lengthening is still apparent in strains completely lacking either *RIF1* or *RIF2*. However, due to the redundancy of Rif1p and Rif2p in telomere length regulation, deleting both genes would better address whether Rap1p/Rif1p/Rif2p complex is involved in generating the LT phenotype, which is discussed in Chapter III.

Interestingly, in two independent *est2-LT*^{E76K} *tel1Δ* transformants (and in *est2-LT*^{N95A} *tel1Δ* strains, data not shown), we observed increased heterogeneity of the telomeric repeats at long generation times, though the minimal telomere length remained approximately the same. This phenomenon suggests that the *est2-LT* alleles can cause telomere lengthening through an alternative pathway that is either selected after long-term growth or becomes activated when telomere length is sufficiently short. This alternate pathway may account for the slight (~30 bp) *TEL1*-independent increase in telomere length seen at moderate generation times.

Because only a small fraction of yeast telomeres are subject to the activity of telomerase in a given cell cycle [86], we suggest that the *est2-LT* alleles alter either the frequency with which telomerase engages the telomere, or the extent of polymerization once a telomere has been "chosen" for elongation. The increased telomere length heterogeneity of a diploid strain expressing both wild-type and mutant telomerase presumably reflects competition for telomere access between telomerase complexes that are correctly regulated, and those that are at least partially refractory to that regulation. Future experiments to distinguish these possibilities may clarify the mechanism through which the *est2-LT* alleles

cause telomere lengthening and uncover a novel role of the telomerase enzyme in telomere length regulation.

CHAPTER III

IDENTIFICATION OF PHENOTYPIC CONSEQUENCES OF *est2-LT IN VIVO*

Work described in this chapter is mostly included in the following manuscript:
Hong Ji, Christopher J. Adkins, Bethany R. Cartwright, and Katherine L. Friedman
Yeast Est2p affects telomere length by influencing association of Rap1p with telomeric chromatin.

Abstract

In *Saccharomyces cerevisiae*, sequence-specific binding of the negative-regulator Rap1p provides a mechanism to "measure" telomere length: as telomere length increases, binding of additional Rap1p inhibits telomerase activity in *cis*. We provide evidence that the association of Rap1p with telomeric DNA *in vivo* occurs in part by sequence-independent mechanisms. Specific mutations in *EST2* (*est2-LT*) reduce the association of Rap1p with telomeric DNA *in vivo*. As a result, telomeres are abnormally long, yet bind an amount of Rap1p equivalent to that observed at wild-type telomeres. This behavior contrasts with a second mutation in *EST2* (*est2-up34*) that increases bound Rap1p as expected for a strain with long telomeres. Telomere sequences are subtly altered in *est2-LT* strains, but similar changes in *est2-up34* telomeres suggest that sequence abnormalities are a consequence, not a cause, of over-elongation. Indeed, *est2-LT* telomeres bind Rap1p indistinguishably from wild type *in vitro*. Taken together, these results suggest that Est2p can directly or indirectly influence the binding of Rap1p to telomeric DNA, implicating telomerase in roles both upstream and downstream of Rap1p in telomere length homeostasis.

Introduction

Telomeres are nucleoprotein structures that protect chromosome ends from nucleolytic digestion and preclude recognition of normal ends as double strand breaks (DSB; [1]). In most eukaryotes, telomeres are maintained by telomerase, a ribonucleoprotein that uses a short region of its RNA subunit as a template for reverse transcription. In *Saccharomyces cerevisiae*, a reverse transcriptase (*EST2*) and RNA subunit (*TLC1*) form the catalytic core of telomerase [28, 45, 128]. Est2p contains at least three functional domains: an N-terminal "TEN" domain that anchors Est2p on its DNA substrate [33, 37] and may interact with other protein components [50], an RBD region that binds *TLC1* RNA and contributes to dimerization [40], and a reverse transcriptase (RT) domain conserved among other telomerases and viral RTs [128].

While many organisms synthesize perfect TG-rich telomeric repeats, several protozoa, fungi, slime molds and plants have heterogeneous telomere sequences [125]. Among these, *Sacchromyces cerevisiae* and *Schizosaccharomyces pombe* have the most profound degeneracy, with telomeric consensus sequences of 5'-$[(TG)_{0\text{-}6}TGGGTGTG(G)]_n$ [14] and 5'-$[GGTTACAG_{0\text{-}4}]_n$ [152], respectively. Several models have been proposed to explain this heterogeneity. Analysis of wild-type (WT) telomeres and telomeres generated in the presence of template mutations suggests that registration of the telomere terminus occurs preferentially at the 3' end of the template, with processive synthesis through a central "core" region and decreasing processivity at the 5' end of the template [14, 153]. In contrast, telomere junction fragments generated during chromosome healing events are more consistent with non-processive synthesis and patterning driven by substrate/template alignment [154]. In "humanized" yeast cells in which the yeast RNA

template is substituted with that of human, Est2p generates perfect hexanucleotide repeats, suggesting that template sequence can influence template usage [155].

In *S. cerevisiae*, normal telomere length varies between 225 and 375bp [156]. The primary negative regulator of telomere length is Rap1p, a protein that associates directly with duplex telomeric DNA on average every 18bp [157]. Artificially targeting Rap1p to an individual telomere proportionately shortens the $TG_{1\text{-}3}$ tract in *cis* [2]. This negative regulation requires Rif1p and Rif2p, proteins that bind to the C-terminus of Rap1p and play overlapping, but not fully redundant, roles in telomere length homeostasis [84, 85, 145]. Deletion of *RIF1* or *RIF2* increases the frequency of telomere elongation during a single cell cycle, suggesting that the Rap1p/Rif1p/Rif2p complex modulates telomerase access in a manner responsive to telomere length [86]. Rap1p also mediates silencing of genes near telomeres and has been implicated in the repression of non-homologous end joining and telomere resection near a DSB [115, 158, 159].

We previously reported mutations (*est2-LT* alleles) in the Est2p TEN domain that cause telomere over-lengthening by an unknown mechanism [160]. Here, we demonstrate that *est2-LT* strains do not increase telomeric Rap1p association or gene silencing as observed upon telomere over-elongation in other genetic backgrounds. The *est2-LT* phenotype is suppressed when Rap1p length regulation is compromised, indicating that the decreased binding of Rap1p per nucleotide within *est2-LT* telomeres causes telomere over-elongation. Although telomere sequences are altered in *est2-LT* strains, the association of Rap1p with these sequences is not detectably changed *in vitro*. Indeed, the same sequence alterations occur in *est2-LT* strains that increase telomere length by other mechanisms. Taken together, these data provide evidence that a subset of residues in the

catalytic subunit of *S. cerevisiae* telomerase modulate the association of Rap1p with telomeric DNA *in vivo* in a sequence-independent manner, thereby affecting the extent of telomere elongation.

Results

Rap1p association with est2-LT *telomeres does not correlate with telomere length*

The *est2-up* alleles were identified in a screen for mutations of *EST2* that improve transcriptional silencing of a telomere-proximal gene [90]. Increased telomere length is thought to mediate this phenotype by increasing Rap1p association and subsequent recruitment of the histone deacetylase Sir2p [115]. Given that the entire *EST2* open-reading frame was subjected to mutagenesis, we were surprised that this screen failed to identify mutations in the *EST2* TEN domain. We speculated that *est2-LT* strains, despite containing longer-than-normal telomeres, might not increase telomeric silencing. Two representative *est2-LT* alleles were chosen for analysis: *est2-LT*^{E76K} (glutamic acid 76 to lysine) and *est2-LT*^{N95A} (asparagine 95 to alanine). *est2-LT*^{E76K} causes telomere length to increase by ~100 bp, while *est2-LT*^{N95A} has a slightly smaller, but reproducible effect (Figure 12B, lanes 2 and 3, respectively).

To assay telomeric gene silencing, plasmid-borne *EST2* alleles were introduced to an *est2Δade2Δ* strain with *ADE2* inserted near the right telomere of chromosome V (Figure 12C). Cells expressing WT *EST2* grow well on plates lacking adenine and are predominantly white, with small red sectors indicative of moderate *ADE2* silencing (Figure 12C). Consistent with the previous report, *est2-up34* [the strongest *est2–up* allele (D460N)] increases telomeric silencing, as indicated by the formation of red colonies

with reduced growth in the absence of adenine. In contrast, telomeric silencing in cells expressing *est2-LT*^{E76K}, *est2-LT*^{N95A}, or *est2-motifE* is indistinguishable from WT (Figure 12C). The difference in silencing behavior of the mutant strains cannot be attributed to differences in telomere length, since all over-lengthen telomeres to a similar extent (Figure 12B). We conclude that telomere over-lengthening in *est2-LT* and *est2-motifE* strains is not accompanied by increased telomeric silencing.

Given that the *est2-up* and *est2-LT* mutations differentially affect telomeric silencing and are located in distinct regions of the Est2 protein, we hypothesized that these alleles increase telomere length through distinct mechanisms. To test this hypothesis, we monitored a genetic interaction previously reported for the *est2-up* alleles. In a strain lacking the Pif1 helicase, a negative-regulator of telomere length, *est2-up34* does not cause any additional telomere lengthening [90]. This result, combined with biochemical evidence, suggests that mutations in the finger subdomain (including *est2-up34*) render telomerase at least partially resistant to negative regulation by Pif1p [90]. To test if other *est2* alleles behave similarly, we created a *pif1Δest2Δ* strain expressing plasmid-borne WT or mutant alleles of *EST2*. As shown in Figure 12D, only *est2-up34* fails to cause additional telomere lengthening in this background. We conclude that *est2-LT* and *est2-motifE* lengthen telomeres by a mechanism distinct from that of *est2-up34*. Since Rap1p is required for telomeric silencing, our observation that increased telomere length is not always accompanied by increased gene silencing suggested that the longer telomeres of the *est2-LT* and *est2-motifE* strains might not undergo the expected increase in total Rap1p association. Chromatin immunoprecipitation (ChIP) was used to address

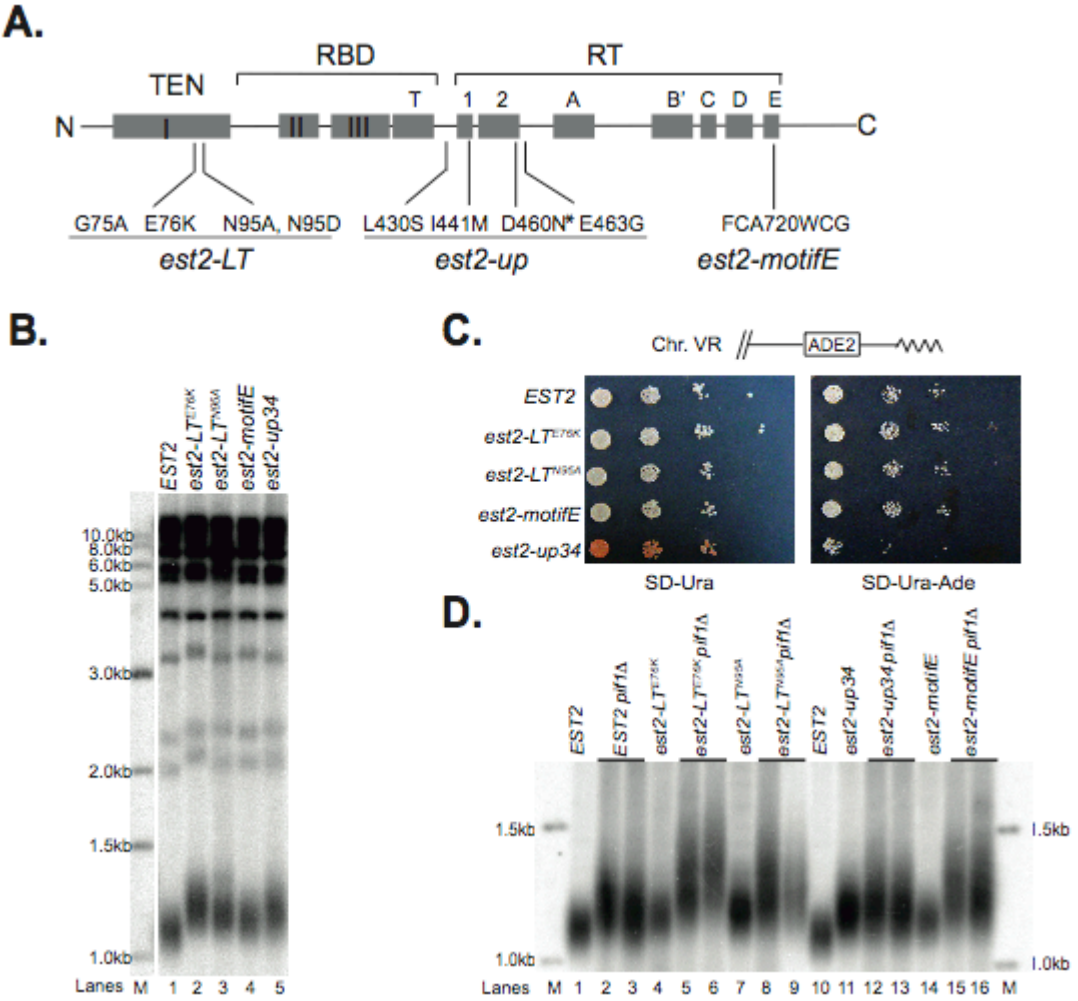

Figure 12. Strains expressing different telomere-lengthening alleles of *EST2* have distinguishable phenotypes.

A. Locations of long-telomere mutations within *EST2*. Domain structure of Est2p is shown [161]. Mutations in three distinct regions cause longer-than-normal telomeres: *est2-LT* in the TEN domain, *est2-up* in motifs 1 and 2, and *est2-MotifE* in the RT domain [90, 148, 160]. The *est2-up34* allele utilized in this study (D460N) is indicated with an asterisk.

B. Telomere length in *est2* strains. Genomic DNA from the indicated strains was cleaved with *Xho*I, separated in a 1.2% agarose gel, Southern blotted, and probed with a telomeric DNA fragment. Strains shown are identical to those used for the silencing (Fig. 12C) and ChIP assays (Figure 13). M=DNA size marker.

C. Expression of a telomere-proximal *ADE2* gene in *est2* strains. Telomeric silencing was tested in an *est2Δade2Δ* strain containing an ectopic copy of *ADE2* inserted near the right telomere of chromosome V (diagram, top). This strain (YKF501) was transformed with a *URA3* plasmid expressing the indicated *EST2* allele. Shown are 10X serial dilutions of cells grown on media lacking uracil or lacking uracil and adenine, ~75 generations after introduction of the complementing plasmids.

D. Dependency of *est2*-mediated telomere over-elongation on *PIF1*. Strains of genotype *est2Δ* (YKF501) or *est2Δpif1Δ* (YKF503) were transformed with *URA3* plasmids

expressing WT *EST2* (lanes 1-3, 10) or the indicated *est2* allele. Cells were grown ~75 generations to allow telomere length to stabilize. Genomic DNA isolated from the indicated strains was digested with *Xho*I, Southern blotted, and probed with telomeric DNA. Telomeres containing a subtelomeric Y' element are shown. M=DNA size marker.

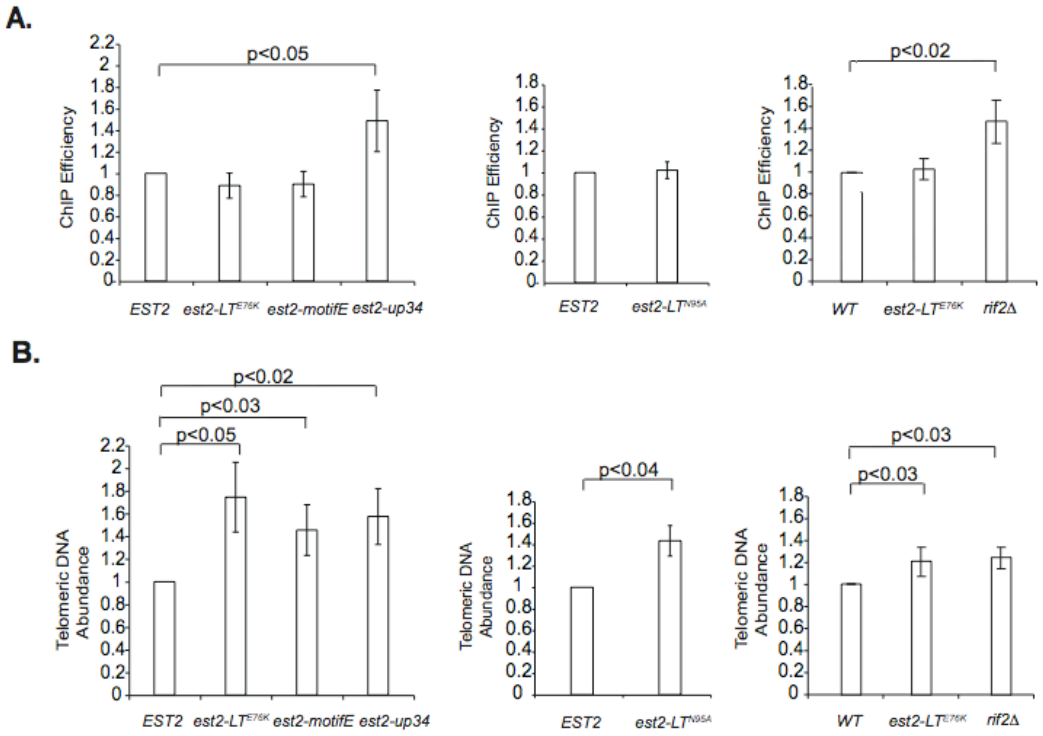

Figure 13. Association of Rap1p with WT and mutant telomeres correlates with telomeric silencing, but not with telomere length.

A. Association of Rap1p with WT and mutant telomeres. Chromatin immunoprecipitation was used to measure the association of Rap1p with telomeric DNA. Values represent the fraction of total telomeric DNA immunoprecipitated with anti-Rap1p antibody, normalized to WT in each independent experiment. Error bars represent standard deviation of at least three experiments. A paired T test was used to determine significance. P values are indicated (brackets) only for those samples that differ significantly from WT ($p<0.05$). (Left and center panels) Analysis of strains in the YKF501 (GA426 *est2Δ::TRP1*) background. The indicated *ProA-EST2* alleles (WT, *est2-LT^{E76K}*, *est2-motifE*, *est2-up34, and est2-LT^{N95A}*) were expressed from plasmid pKF410. Strains are identical to those utilized in Figure 1B and C. (Right panel) Analysis of strains in the GA426 background: GA426 (WT), YKF500 (GA426 with *est2-LT^{E76K}* integrated at the endogenous locus), and YKF502 (GA426 *rif2Δ::TRP1*).

B. Measurement of relative telomeric DNA abundance. Telomeric DNA abundance was quantified in input extracts from the identical samples shown in A. by measuring the ratio of signal generated with a telomeric DNA probe to that of a single-copy sequence (372-bp fragment of *ARO1*). Values were normalized to WT in each independent experiment. Error bars represent standard deviation of at least three experiments. A paired T test was used to determine significance. P values are indicated (brackets) for those samples that differ significantly from WT ($p<0.05$).

this possibility. To keep most telomeres intact, formaldehyde-crosslinked chromatin was sheared by sonication to 500-1000bp. Rap1p was immunoprecipitated and associated telomeric DNA was quantified by hybridization. To account for differences in telomere length, we expressed the amount of precipitated fragment as a percent of input telomeric DNA. Under these conditions, the efficiency of immunoprecipitation is proportional to the amount of Rap1p bound to each telomere. Values were normalized to those of a WT sample processed in parallel.

As predicted by the lack of increased telomeric silencing, the association of Rap1p with telomeres in *est2-LT*^{E76K}, *est2-LT*^{N95A}, and *est2-motifE* strains is indistinguishable from WT (Figure 13A). In contrast, expression of *est2-up34* significantly increases the efficiency of telomeric DNA immunoprecipitation by Rap1p (Figure 13A). To rule out the possibility that *est2-up34* abnormally increases Rap1p association, we monitored a control strain (*rif2Δ*) in which the extent of telomere over-elongation is similar to that observed in *est2-LT*^{E76K} and *est2-up34* (see below). As expected from Rif2p's role downstream of Rap1p [85], the elongated telomeres of a *rif2Δ* strain bind significantly more Rap1p than WT (Figure 13A).

To confirm that differences in Rap1p association cannot be attributed to differences in the extent of telomere over-elongation, we measured the ratio of hybridization of a telomere-specific probe to that of a single-copy control sequence (*ARO1*) in input samples from each strain. While the relative abundance of telomeric DNA was significantly increased over WT, the extent of telomere over-elongation in the different mutant strains was statistically indistinguishable (Figure 13B). The observation that the longer telomeres of *est2-LT*^{E76K}, *est2-LT*^{N95A} and *est2-motifE* strains bind no more

Rap1p than WT length telomeres is consistent with an overall reduction (per nucleotide) in the association of Rap1p within telomeres in these mutant strains. This result led us to address the role of Rap1p in generation of the long-telomere phenotype.

Generation of the long-telomere phenotype in **est2-LT** *strains requires the association of Rap1p with telomeric DNA*

Since telomere elongation is inhibited in a manner proportional to the amount of bound Rap1p, a reduction in the frequency of Rap1p association with telomeres should cause telomere over-elongation (as previously observed for certain mutations in the telomerase template;[162]. An equilibrium length is reached when telomeres bind, on average, an amount of Rap1p equivalent to that normally associated with WT telomeres. The observation that transcriptional silencing and total Rap1p association at the elongated telomeres of *est2-LT* and *est2-motifE* strains is equivalent to WT fits this prediction and suggests that telomere over-lengthening is a response to reduced binding by Rap1p. If true, telomere over-elongation in *est2-LT* strains should be Rap1p-dependent.

We initially set out to eliminate Rap1p function by deleting its binding partners, Rif1p and Rif2p. Unfortunately, the extreme length and heterogeneity of telomeres in this background made it impossible to determine if the *est2* alleles cause additional elongation (data not shown). To circumvent this difficulty, we took advantage of a strain in which the yeast RNA template is replaced with that of the human telomerase RNA, dictating synthesis of the hexanucleotide sequence (5'-TTAGGG) normally found at human telomeres [155]. This "humanized" sequence does not bind Rap1p, but telomeres are short and stable due to an alternate, Tbf1p-dependent mechanism [104, 163, 164]. An *est2Δ* strain expressing the humanized *TLC1* variant *(tlc1-human*) from its endogenous locus was

grown for approximately 50 generations in the absence of telomerase to allow telomere shortening. This strain was subsequently transformed with plasmids expressing WT or mutant *est2*, and telomerase was allowed to synthesize telomeres in the presence of the humanized RNA. Although the internal telomeric sequences in these strains retain wild-type sequence and are capable of binding Rap1p, any additional DNA synthesized by the mutant enzymes is derived from the humanized template. As one would predict for mutations dependent on Rap1p, neither *est2-LT*^{N95A} nor *est2-LT*^{E76K} increase telomere length compared to WT when utilizing the humanized RNA (Figure 14A and B). In contrast, *est2-up34* retains the ability to cause telomere over-lengthening in this background, consistent with a Rap1p-independent mode of action (Figure 14C). Surprisingly, *est2-motifE* also over-elongates telomeres in this background (Figure 14A, lanes 12-15). Telomeres cloned from the *est2-LT*^{E76K} and *est2-motifE* strains contain perfect six-nucleotide repeats at the chromosome terminus (data not shown), confirming that Rap1p binding is eliminated within the newly synthesized sequences. The failure of *est2-LT*^{E76K} and *est2-LT*^{N95A} to lengthen telomeres in the humanized background suggests that telomere lengthening occurs in response to the reduced frequency of telomeric Rap1p association *in vivo,* although we cannot eliminate the possibility that altering the template sequence has other unanticipated effects on the *est2-LT* phenotype. We also conclude that *est2-motifE* affects telomere length in a manner that is at least partially Rap1p-independent.

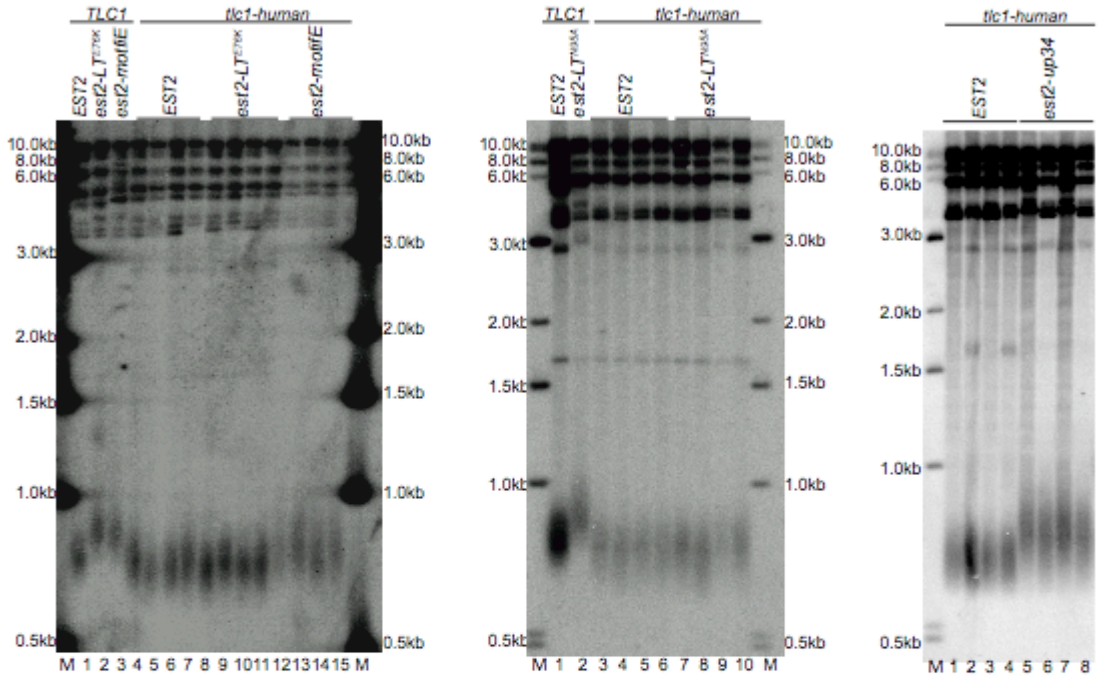

Figure 14. Telomere over-lengthening by the *est2-LT* alleles is suppressed in a background of "humanized" *TLC1*.

A. *est2Δ* strains expressing WT *TLC1* (lanes 1-3) or a *tlc1-human* variant (lanes 4-15) were transformed with plasmids bearing *EST2*, *est2-LT*^{E76K}, or *est2-motifE* as indicated. DNA was cleaved with *Pst*I, separated in a 1.5% agarose gel, Southern blotted, and probed with a mixture of two DNA fragments [*S. cerevisiae* telomere DNA and "humanized" $(TTAGGG)_n$ sequence]. M=DNA size marker.

B. *est2Δ* strains expressing WT *TLC1* (lanes 1 and 2) or a *tlc1-human* variant (lanes 3-10) were transformed with plasmids bearing *EST2* or *est2-LT*^{N95A} as indicated. Samples were treated as described in A.

C. *est2Δ* strains expressing a *tlc1-human* variant were transformed with plasmids bearing *EST2* or *est2-up34* as indicated. Samples were treated as described in A.

***Telomere over-elongation is associated with altered telomere sequences* in vivo**

We sought to understand the mechanism through which the frequency of Rap1p association is decreased at *est2-LT* telomeres. Given that Rap1p associates directly with telomeric DNA, altering the sequence of the telomeric repeat could have this effect. To examine this possibility, telomere sequences were obtained in two ways that allowed unambiguous identification of repeats synthesized by the mutant enzyme. In a multi-cell cycle analysis, telomeres were allowed to shorten for ~50 generations in the absence of *EST2*. WT or mutant *EST2* was introduced, telomere length was recovered for ~75 generations, and multiple clonal isolates of a single telomere were sequenced [14]. Because yeast telomerase generates irregular sequences, repeats synthesized after introduction of the complementing plasmid were identified by their divergence from the identical, internal repeats. In a second approach (Single Telomere Extension assay, or STEX), telomere repeats generated during a single S phase were analyzed [86]. *est2Δ* recipient cells with shortened telomeres were mated with donor cells expressing *EST2* or *est2-LT*^{E76K} at the endogenous locus. After zygotes proceeded through the first post-zygotic S phase, marked telomeres originating in the recipient strain were cloned and sequenced. Again, newly synthesized repeats were identified as those sequences that did not align between different telomeres. The frequency and extent of telomere elongation by *est2-LT*^{E76K} telomerase during a single S phase were not statistically different from WT, with a marked preference for elongation of the shortest telomeres, as previously reported (Figure 15; ref. [86]).

Detailed inspection of *est2-LT*^{E76K} telomeres did indeed reveal a change in telomere sequence. As previously described, approximately 90% of repeats in WT

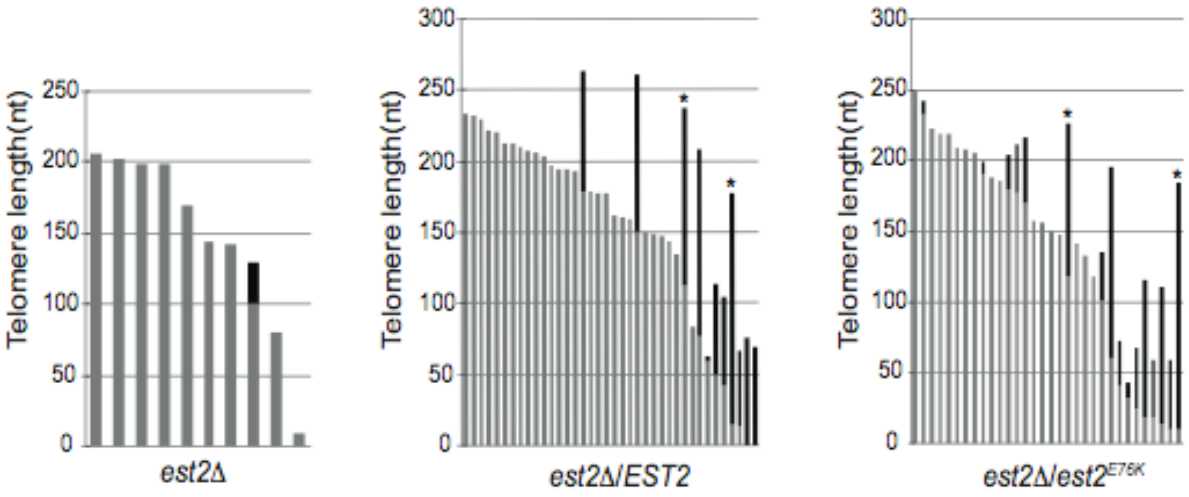

Figure 15. Analysis of telomere addition in a single cell cycle.
An *est2*Δ recipient strain was mated with strains expressing either wild-type *EST2* (center) or *est2-LT*^{E76K} (right). Telomeres were cloned and sequenced after completion of the first post-zygotic S phase. Lengths of individual telomeres are plotted. For each telomere, identical $TG_{1\text{-}3}$ sequences resulting from semi-conservative DNA replication (gray) and divergent sequences representing new telomere addition (black) are shown. Based on the low frequency of telomere addition in the absence of mating (left) and on observed significant differences in telomere sequence following mating to *EST2* or *est2-LT*^{E76K} donors (Table 4), we infer that most divergent sequences result from telomere extension by telomerase. The average amount of new telomere addition is 82 nt (*EST2*) and 58 nt (*est2-LT*^{E76K}). These differences are not statistically significant (p=0.084; nonparametric Kruskal-Wallis test). Likewise, the frequency of telomere addition is statistically indistinguishable between the two strains (p=0.09, Fisher's exact test). Telomeres utilized for experiments shown in Figures 17 and 18 are indicated (*).

Table 2. Comparison of telomere sequences added by WT and mutant telomerase.

	Percent of GG dinucleotide incorporation (values)[a]				
	Wild Type	*est2-LT^{E76K}*	*est2-LT^{N95A}*	*est2-motifE*	*est2-up34*
Multi-cell cycle	52.5 (31/59)	67.1 (53/79)	63.6 (35/55)	64.9 (37/57)	65.1% (56/86)
Single cell cycle	56.6 (43/76)	77.3 (51/66)[b]			
Telomere healing	63.5% (54/85)	66.2% (43/65)			

[a] Calculated as the percent of total core sequences that are followed by GG dinucleotide (see Chapter IV).
[b] The difference between WT and *est2-LT^{E76K}* telomeres is significant using a Fisher's Exact Test (p=0.012).

	Percent of overlapping core sequences (values)[c]				
	Wild Type	*est2-LT^{E76K}*	*est2-LT^{N95A}*	*est2-motifE*	*est2-up34*
Multi-cell cycle	29.2 (14/48)	17.5 (11/63)	20.5 (9/44)	14.5 (8/55)	15.6 (12/77)
Single cell cycle	27.7 (18/65)	12.7 (7/55)[d]			
Telomere healing	22.1 (18/81)	19.4 (12/62)			

[c] Calculated as the percent of overlapping core sequence event (Chapter IV).
[d] Fisher's Exact Test was used to compare the difference between WT and *est2-LT^{E76K}* telomeres (p=0.07).

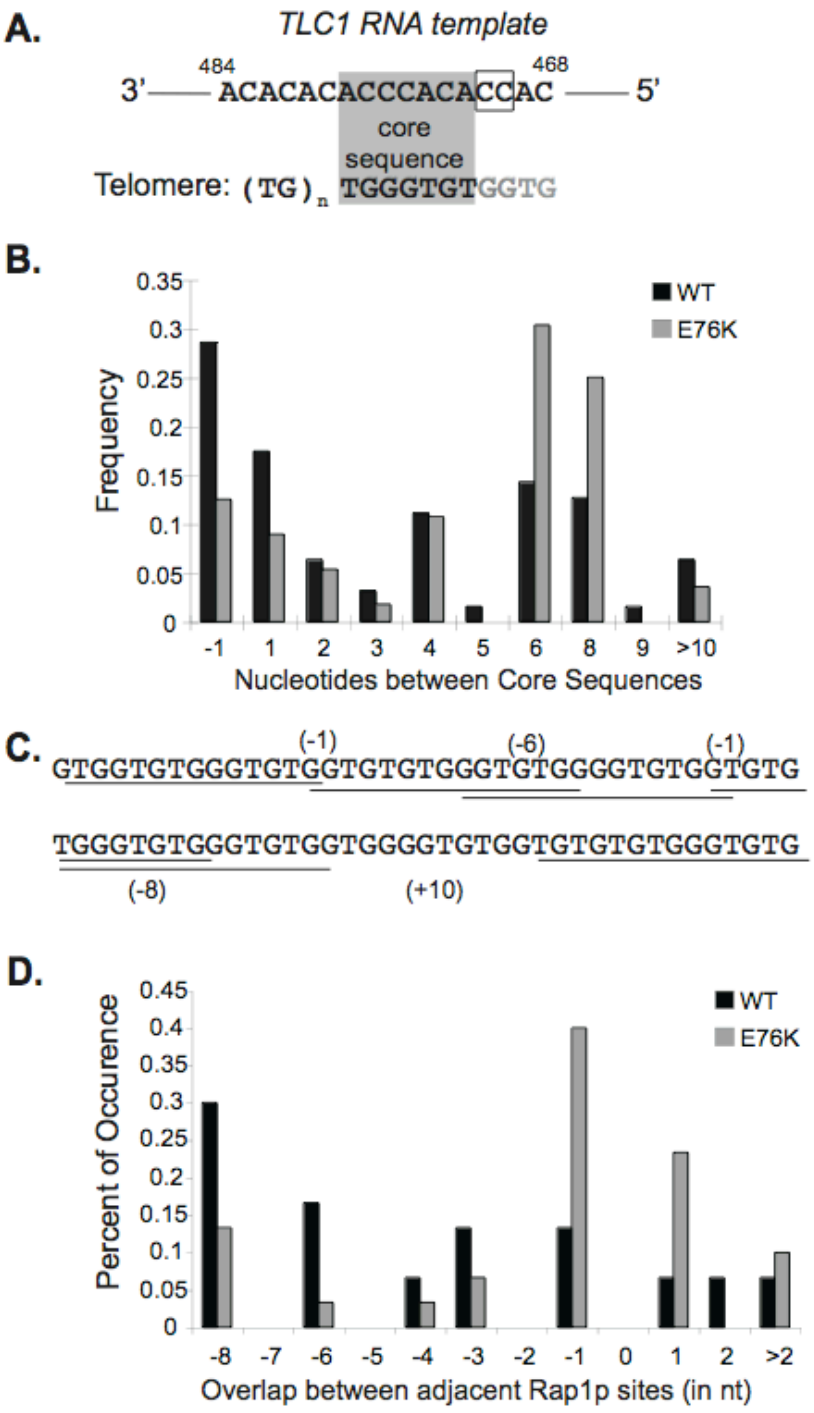

Figure 16. The pattern of telomere-repeat addition is altered in *est2-LT^{E76K}* strains.

A. Model of yeast telomere-repeat heterogeneity [14]. Processive reverse transcription (RT) of a central portion of the telomerase template RNA (gray) incorporates the 5'-TGGGTGT "core sequence" in ~90% of repeats. Heterogeneity is proposed to arise from a combination of poor processivity (gray nucleotides) and multiple registers of alignment and abortive RT at the 3' end of the template. The GG-dinucleotide is produced by RT of ^{470}CC^{471} (box).

B. The number of nucleotides between core sequences is significantly altered in *est2-LT^{E76K}* telomeres. The number of nucleotides between core sequences (5'-TGGGTGT) was graphed from WT and *est2-LT^{E76K}* telomeres synthesized during a single cell cycle. "-1" spacing occurs when the 3' T of one core sequence is identical to the 5' T of the next. Data derive from 65 WT repeats and 55 mutant repeats. Distributions of absolute values are statistically different ($p<0.02$) by the Chi-square contingency test.
C. The majority of predicted Rap1p binding sites overlap. Rap1p sites predicted within a representative WT sequence (see Chapter IV) are underlined. Overlap is indicated by negative values (parentheses).
D. Predicted Rap1p binding sites are more dispersed in *est2-LT^{E76K}* telomeres than in WT telomeres. The amount of overlap between 31 predicted Rap1p binding sites in WT telomeres and 31 sites in *est2-LT^{E76K}* telomeres was determined using the method illustrated in C and the frequency of each class was plotted. Distances of greater than 2 nucleotides were grouped. Distributions of absolute values are statistically different ($p=0.042$) by the Chi-square contingency test.

telomeres contain a 7-nucleotide "core sequence" (5'-TGGGTGT; Figure 16A), half of which are followed by two consecutive Gs (as templated by *TLC1*; ref. [14]). *est2-LT^{E76K}* telomeres contain this GG dinucleotide at increased frequency (67-77%; Table 2). A combined probability test examining the magnitude of the effect in telomeres generated by both experimental regimes indicates statistical significance (p=0.025; ref. [165]).

While the majority of core sequences in WT telomeres are separated by 2 or more nucleotides, nearly 30% overlap to generate the sequence 5'-TGGGTGTGGGTGT (a spacing of "-1"). Telomeres synthesized in a single cell cycle by Est2-LT^{E76K}p show a greater than 50% reduction in the "-1" spacer class (Table 2) and an overall shift in the distribution of spacer lengths (Figure 16B; p=0.03). This is the first reported example of a mutation within the yeast catalytic subunit that affects the patterning of telomere repeats *in vivo*.

To address potential impact on Rap1p binding, a computer algorithm (MatInspector) was used to identify putative Rap1p sites in WT and mutant sequences [166]. As previously described, nearly all predicted Rap1p binding sites fall into three classes corresponding to 13/13, 12/13, and 11/13 matches to the consensus sequence [153]. *est2-LT^{E76K}* telomeres shift the distribution among these classes, with a relative paucity of the 5'-TGGGTGTGGGTGTG sequence (11/13 match) reflecting the reduction in overlapping core sequences (Table 3). In addition, the extent of overlap between adjacent predicted Rap1p sites is reduced in *est2-LT^{E76K}* telomeres (Figure 16C and D; p=0.042). This effect is small and does not decrease the total number of predicted sites over the length of a telomere. However, we speculated that changing the relative spacing of adjacent sites might disproportionately affect Rap1p occupancy.

Table 3. Predicted Rap1p binding sites in wild type, *est2-LT^{E76K}* and *est2-LT^{N95A}* telomeres.

Rap1p sites	Matrix similarity	Match to 13bp consensus	Percent occurrence (values)[a]		
			Wild Type	*est2-LT^{E76K}*	*est2-LT^{N95A}*(b)
GGTGTGTGGGTGTG	0.902	13	40.0 (14/35)	47.2 (17/36)	31.7 (13/41)
TGTGTGTGGGTGTG	0.901	12	17.1 (6/35)	36.1 (13/36)	26.8 (11/41)
TGGGTGTGGGTGTG	0.806	11	25.7 (9/35)	11.1 (4/36)	17.0 (7/41)
GTGGTGTGGGTGTG	0.795	11	17.1(6/35)	5.6 (2/36)	21.9 (9/41)

[a] Rounded to one decimal place. The percentages do not sum to 100% in some cases due to rounding.
[b] *est2-LT^{N95A}* has one site with the sequence of TGTGTGTGGGTGG (11/13 match, matrix similarity 0.858) that is rarely present *in vivo*.
Note: Wild-type and *est2-LT^{E76K}* telomeric sequences are from single cell cycle experiments and *est2-LT^{N95A}* sequences are from multi-cell cycle experiments.

We reasoned that if the sequence alterations observed in *est2-LT^{E76K}* telomeres directly account for the reduced frequency of Rap1p binding (Fig. 13A), similar changes should be observed in other strains that exhibit this phenotype (*est2-LT^{N95A}* and *est2-motifE*). Indeed, sequencing of telomeres generated in both strains over multiple generations reveals sequence changes reminiscent of those observed in *est2-LT^{E76K}* (Table 2), with similar changes in the distribution of predicted Rap1p binding sites (data not shown). As a control, we examined telomere sequences from the *est2-up34* strain. Since Rap1p binding is increased at *est2-up34* telomeres *in vivo* (Figure 13A), we predicted no change in telomere sequence. Contrary to our expectation, *est2-up34* telomeres also display increased GG-dinucleotide frequency and reduced core sequence overlap compared with WT. Indeed, the telomere sequence changes among the four mutant strains are statistically indistinguishable (Table 2; p=0.98 and 0.87) when comparing GG incorporation and overlapping core sequences, respectively, in a 2x4 Chi-square contingency test). Given that changes in telomere sequence do not correlate with the extent of Rap1p binding *in vivo*, we conclude that altered telomere patterning is a consequence, rather than a cause, of telomere over-elongation in these mechanistically distinct *est2* strains.

***Rap1p association at WT and* est2-LT^{E76K} *telomeres is indistinguishable* in vitro**

Although telomere sequence alterations do not appear directly responsible for reduced Rap1p binding *in vivo*, we wanted to determine the consequence of the predicted changes in Rap1p binding sites observed at *est2-LT^{E76K}* telomeres. To address whether these altered sequences reduce Rap1p association, we assayed binding of recombinant Rap1p

to cloned WT and mutant telomeres *in vitro*. Matched WT and mutant clones containing approximately the same amount of telomeric DNA (~230bp or ~180bp) were chosen from the STEX experiment (Figure 15, telomeres marked with asterisk). In the mutant telomeres, 91% (E184) or 48% (E229) of the total TG_{1-3} sequence was synthesized by *est2-LT*^{E76K} telomerase. In general, sequences on these telomeres are representative of the overall trend of increased GG-dinucleotide incorporation and decreased core sequence overlap observed among all *est2-LT*^{E76K} telomeres (Figure 17A). The variability in GG-dinucleotide rate observed in the WT telomere sequences reflects stochastic variation given the small number of repeats in each clone. Consistent with the relatively small change in overlap between predicted Rap1p binding sites that we observe among all mutant telomeres (Figure 16C and D), the total number of predicted Rap1p binding sites is similar between size-matched WT and *est2-LT*^{E76K} telomere clones (Figure 17A).

To address the occupancy of predicted Rap1p sites, we monitored binding of full-length, recombinant Rap1p to WT and *est2-LT*^{E76K}-derived sequences by DNaseI footprinting. In all four telomeres, regions of protection correspond well with prediction (Figure 17B). Strong protection observed on *est2-LT*^{E76K} telomeres suggests that the majority of substrates are bound, arguing against a substantial decrease in binding efficiency.

To quantify Rap1p association more carefully, we measured the ability of the size-matched WT and *est2-LT*^{E76K} telomeres to compete for Rap1p binding to a short double-stranded substrate by gel shift. Unlabeled telomeric competitor DNA quantitatively reduces the association of Rap1p with the radiolabeled substrate (Figure 18A). Because each unlabeled DNA contains 14-17 potential Rap1p binding sites (Figure

A.

	Percent of GG dinucleotide (values)	Percent of overlapping core sequences(values)	Predicted Rap1p sites
W239	45 (9/20)	26.3 (5/19)	16
E229	63.2 (12/19)	16.7(3/18)	17
W178	64.3 (9/14)	30.8 (4/13)	14
E184	83.3 (10/12)	10 (1/10)	14

B.

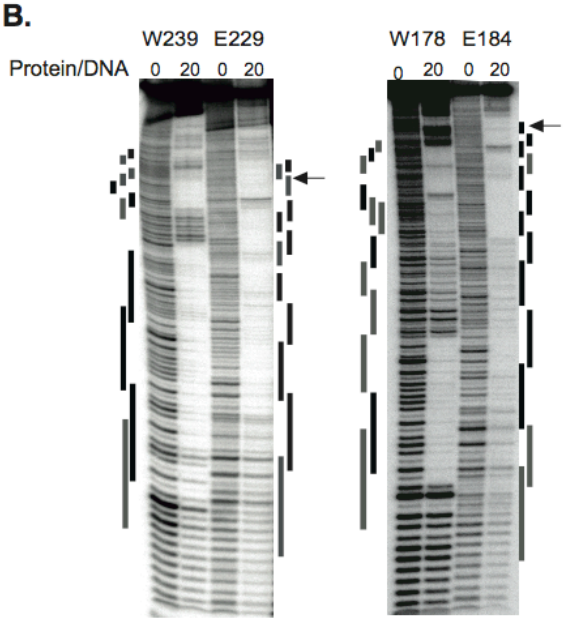

Figure 17. *est2-LT*^{E76K} telomeres bind Rap1p at predicted sites *in vitro*.

A. The characteristics of four cloned telomere fragments utilized in Figure 17B and Figure 18 are shown. Two WT telomeres (W239 and W178) and two *est2-LT*^{E76K} telomeres (E229 and E184) were generated by telomere addition in a single cell cycle. Numbers indicate the length of $TG_{1\text{-}3}$ repeat. In *est2-LT*^{E76K} telomeres, only a portion of this sequence is generated by the mutant enzyme (91% for E184 and 48% for E229). The percent of core sequences followed by "GG", percent of overlapping core sequences, and number of predicted Rap1p binding sites (see Chapter IV) are determined for the entire $TG_{1\text{-}3}$ sequence. Each DNA fragment also contains ~100bp of identical sub-telomeric and vector-derived sequences.

B. DNaseI footprinting analysis of Rap1p bound to telomeric substrates. Rap1p (20 fold molar excess) was bound to 100 fmoles of ^{32}P-end labeled telomeric DNA (W239, W178, E229, or E184 as indicated) prior to DNase I treatment. Control reactions (0) were incubated in the absence of Rap1p. A black bar indicates a 13/13 or 12/13 match to the Rap1p consensus sequence and a gray bar indicates an 11/13 match (see Chapter IV and Table 3). Not all Rap1p sites are shown due to poor resolution near the top of the gel. For E229 and E184, the transition between sequences synthesized by *est2-LT*^{E76K} telomerase (at the labeled end of the DNA molecule) and WT telomerase is indicated (arrow).

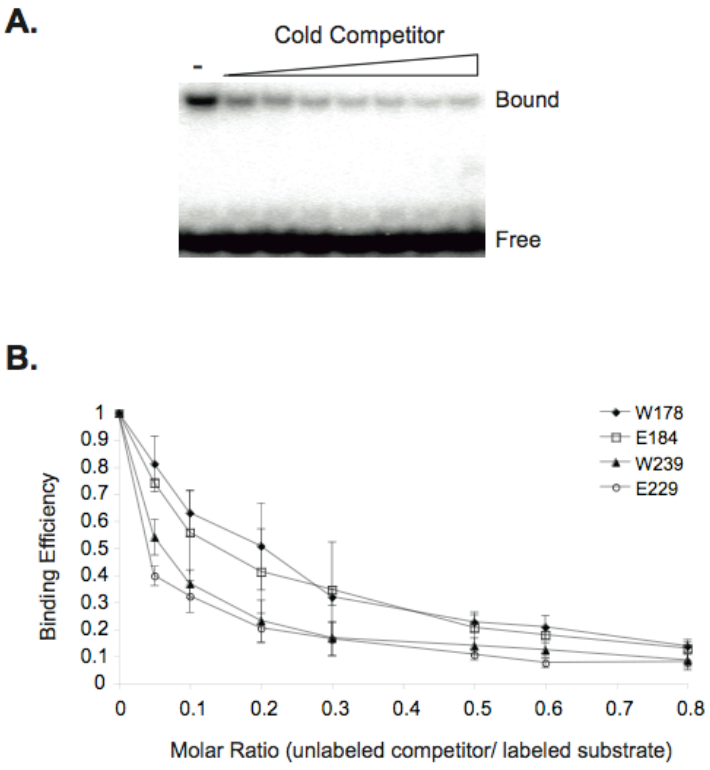

Figure 18. Association of Rap1p with *est2-LT*^{E76K} telomeres is not reduced *in vitro*.

A. Increasing amounts (0, 5, 10, 20, 30, 50, 60, 80 fmoles) of WT (W239) unlabeled telomeric DNA were mixed with 100 fmoles of an 18bp ^{32}P-labeled double-stranded DNA and 400 fmoles of recombinant Rap1p. Binding reactions were separated by polyacrylamide gel electrophoresis and visualized by phosphorimager.

B. Quantification of multiple experiments performed as in (A) using WT (W239 and W178) or mutant (E229 and E184) competitor DNAs. "% competition" was calculated by normalizing the fraction of oligonucleotide bound to Rap1p in each sample to the value observed in the absence of competitor. Error bars represent standard deviation from three independent experiments.

17A), effective competition occurs at low molar ratios. This assay is quite sensitive, as we could distinguish two WT telomere sequences differing by less than 30% in length (239bp versus 178bp; Figure 18B). The ability of the longer sequence to compete nearly half of the binding to the short oligonucleotide at a 1/20 molar ratio is consistent with the 16 predicted Rap1p sites on this fragment. *est2-LT*^{E76K} telomeres compete at least as well for Rap1p binding as their size-matched controls. For example, at the 1/20 molar ratio, *est2-LT*^{E76K} and WT telomeres of ~180bp reduce the shifted product by 25.5 +/- 1.5% and 18.9 +/- 10.2%, respectively. The longer *est2-LT*^{E76K} telomere (E229) competes even better than its WT counterpart, perhaps reflecting the additional Rap1p site predicted within this sequence (Figure 17A). We conclude that changes in telomere sequence cannot account for the reduced frequency with which Rap1p associates with *est-2LT* telomeres *in vivo*.

A mutation in the N-terminus of Sp*Trt1p causes telomere overelongation and alters telomere sequences* in vivo.

To determine whether the *est2-LT* region plays a similar role in another organism that has heterogeneous telomere sequences, several mutations were made in the N-terminal region of *S. pombe* TERT based on sequence homology (Figure 19A). A strain lacking endogenous *trt1*$^{+}$ was transformed with plasmids bearing either wild-type or mutant *trt1*, strains were restreaked three times, and telomere length was measured by Southern blot. While mutations of glutamic acid 101 (E101) to lysine and asparagine 124 (N124) to alanine had no consistent effect on telomere length (Figure 19B), multiple independent transformants expressing the *trt1*^{E98K} allele (glutamic acid 98 to lysine) displayed longer than normal telomeres (Figure 19B).

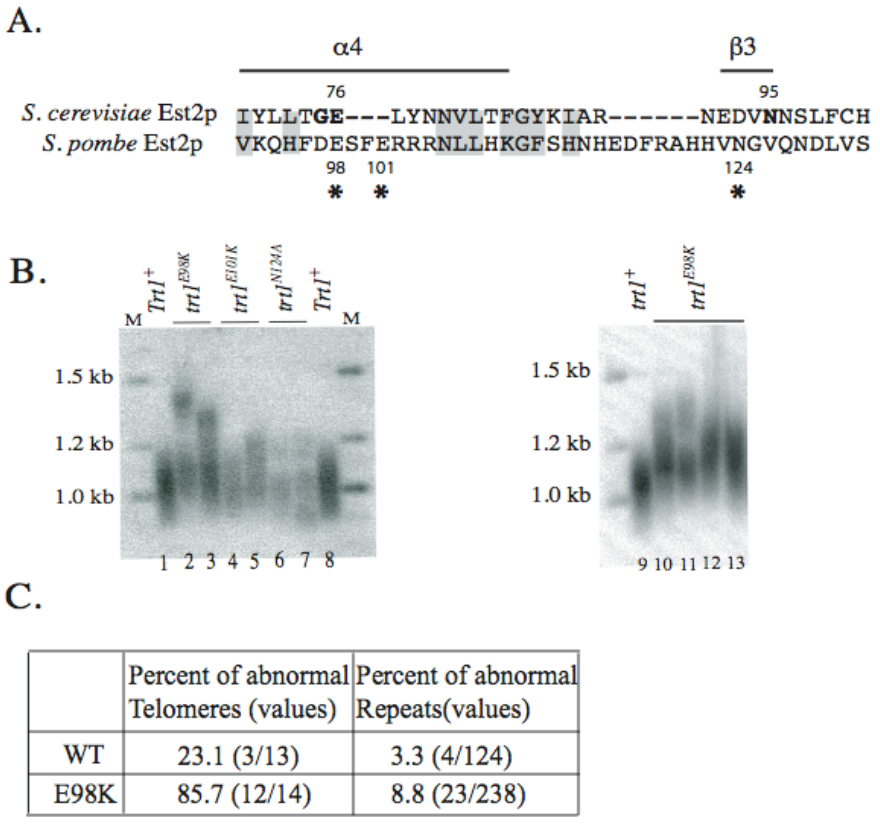

C.

	Percent of abnormal Telomeres (values)	Percent of abnormal Repeats(values)
WT	23.1 (3/13)	3.3 (4/124)
E98K	85.7 (12/14)	8.8 (23/238)

Figure 19. A mutation in the N-terminal domain of *S. pombe Trt1* causes telomere lengthening and alters telomere sequences.

A. Alignment of a portion of the TEN domain is shown for *S. cerevisiae* Est2p and *S. pombe* Trt1p (based on [161]). Positions showing amino acid similarity are highlighted in gray. Three residues of *S. pombe* Trt1p that align with *S. cerevisiae* residues E76 and N95 are indicated (*; Est2p E76 can be arbitrarily aligned with E98 or E101 of Trt1p). Secondary folds predicted by the crystal structure of *Tetrahymena thermophila* TERT are indicated.

B. Mutations at each of the three residues indicated in Figure 19A (E98K, lanes 2, 3,10, 11,12, 13; E101K, lanes 4 and 5; and N124A, lanes 6 and 7) were created on a plasmid bearing the kan*MX4* marker and introduced into a *trt1*$^{-}$*::his3*$^{+}$ strain bearing a *trt1*$^{+}$ complementing plasmid with an *HSV1-tk* marker gene (CF797; Table 4). A plasmid expressing wild-type *trt1*$^{+}$ was transformed as a control (lanes 1, 8, and 9). Transformants were selected on plates containing geneticin and subsequently streaked on plates containing 5-fluoro-2' deoxyuridine (5FUdR) to select for loss of the complementing plasmid (see Chapter IV). A single transformant was restreaked twice on plates containing geneticin, DNA was isolated from two colonies (For E98K, 6 colonies are picked), and telomeres were examined by Southern blot after cleavage with *Eco*RI. The sizes of radiolabeled molecular weight markers are indicated (M).

C. Mutation of *trt1* residue G98 to lysine alters telomere sequences *in vivo*. Telomeres in a *trt1*$^{-}$ strain were allowed to shorten before reintroduction of *trt1*$^{+}$ or *trt1*^{E98K} on a plasmid. Newly synthesized telomere sequences were obtained as described in Chapter IV. *S. pombe* telomeres consist of a 5'-GGTTAC core sequence followed by

a variable spacer. The occurrence of abnormal core sequences (_GTTAC or GG_TAC) was determined. “Percent of abnormal telomeres” is calculated as the percent of total sequenced telomeres that contain at least one abnormal core sequence. The differences are statistically significant by Fisher’s exact test ($p<0.002$ for the percent of abnormal telomeres and $p<0.03$ for the percent of abnormal telomeric repeats).

To assess whether telomere lengthening might occur through a similar mechanism to that observed in *S. cerevisiae*, we sequenced telomeres of the $trt1^{+}$ and $trt1^{E98K}$ strains. *S. pombe* telomere repeats contain a 5'-GGTTAC core sequence followed in most cases by either no spacer, a single A residue, or an A with a variable number of Gs. By multiple criteria (overall length, sequence distribution, and number of consecutive G residues), the spacer sequences are unaffected by the mutation. In contrast, a significantly higher fraction of the core sequences are abnormal [_GTTAC or GG_TAC (Figure 19C, $p<0.03$)] in the $trt1^{E98K}$ mutant. Most strikingly, nearly every $trt1^{E98K}$ telomere has at least one abnormal repeat (86%) compared with only 23% of WT telomeres ($p<0.002$). The occurrence of abnormal _GTTAC core sequences is probably underestimated because it is impossible to distinguish whether a preceding G residue derives from spacer or core sequences. These data demonstrate that residue E98 of $trt1^{+}$ influences how *S. pombe* telomeric repeats are generated, maybe through a similar mechanism as residue E76 in *S. cerevisiae.*

Discussion

We provide evidence that telomerase negatively influences telomere length through three distinct mechanisms corresponding to the three classes of *est2* mutations that over-elongate telomeres. Unexpectedly, a subset of these mutants decreases the frequency of Rap1p association with telomeric chromatin *in vivo*. While over-elongation is accompanied by changes in telomere sequence, such alterations are not restricted to strains in which Rap1p binding is reduced and do not decrease the binding of Rap1p to telomeric DNA *in vitro*. These data provide evidence that the catalytic subunit of

telomerase directly or indirectly influences the association of Rap1p with telomeric DNA in a manner independent of telomere sequence, suggesting that telomerase plays roles upstream and downstream of Rap1p in the regulation of telomere length.

Mechanisms of telomere over-elongation by **est2** *alleles*

Previous studies identified telomere over-elongating mutations in three regions of *EST2*. The "up" mutations in the finger subdomain alter interaction of Est2p with Pif1p [90], a helicase that disrupts the association of telomerase with its DNA substrate [89]. In contrast to the *est2-up* mutations, both *est2-LT* alleles tested here cause additional telomere lengthening in the absence of *PIF1*, indicating that these mutant proteins preserve normal interaction with Pif1p. Differential effects of *est2-up34* and the *est2-LT* mutations on Rap1p association with telomeric DNA *in vivo* underscore this distinction.

The mechanism of telomere over-elongation by the *est2-motifE* allele is more complex. This mutation mimics the viral consensus sequence within motif E of the RT domain and increases nucleotide-addition processivity *in vitro* [148], a phenotype not shared by *est2-LT*^{E76K} or *est2-LT*^{N95A} [160]. Despite this difference, *est2-motifE* decreases Rap1p association with telomeres *in vivo* in a manner indistinguishable from *est2-LT*^{E76K}. Persistence of the *est2-motifE* long-telomere phenotype in the absence of Rap1p association, however, suggests that altered enzymatic activity may contribute to telomere over-elongation.

Generation of abnormal sequences in long-telomere strains

Properties of yeast telomerase that influence telomere sequence *in vivo* are poorly understood. A previous study revealed normal sequences in strains with short but stable telomeres (*tel1Δ* and *ku70Δ*; ref. [153]). For the first time, we report a consistent change in telomere sequence in *est2* strains with long telomeres. The ubiquity of this effect suggests that telomerase activity may be altered under conditions of over-elongation. Alternatively, each *est2* mutation may similarly affect telomerase catalysis *in vivo*, despite increasing telomere length through genetically distinct pathways. The *est2-LT^{E76K}* mutation increases repeat-addition processivity of telomerase on certain primers *in vitro* [37]. However, our observation that the number of nucleotides added per telomere-lengthening event is not increased in this mutant (average 82 nt in WT versus 58 nt in *est2-LT^{E76K}*, p=0.084; Figure 15) suggests that this effect does not contribute to telomere over-elongation *in vivo*.

The most obvious explanation for increased GG-dinucleotide incorporation is an increased propensity of telomerase to reach the end of the template before dissociating or translocating. We addressed this possibility using an RNA template mutant containing a U at position 469 (Figure 16A; ref. [14]). WT and *est2-LT^{E76K}* strains incorporate the complementary A at indistinguishable rates (10.6% and 9.9% of total repeats, respectively). Therefore, any change in nucleotide addition processivity is restricted to template residue C^{470}. This interpretation assumes that excess GG dinucleotides are templated by residues ^{471}CC^{470}, as previously demonstrated for WT [14]. Indeed, a mutation that eliminates the templating CC dinucleotide (^{472}CAC^{471} to ACA) abolishes GG dinucleotides in *est2-LT^{E76K}* telomeres (data not shown). Combined, these observations

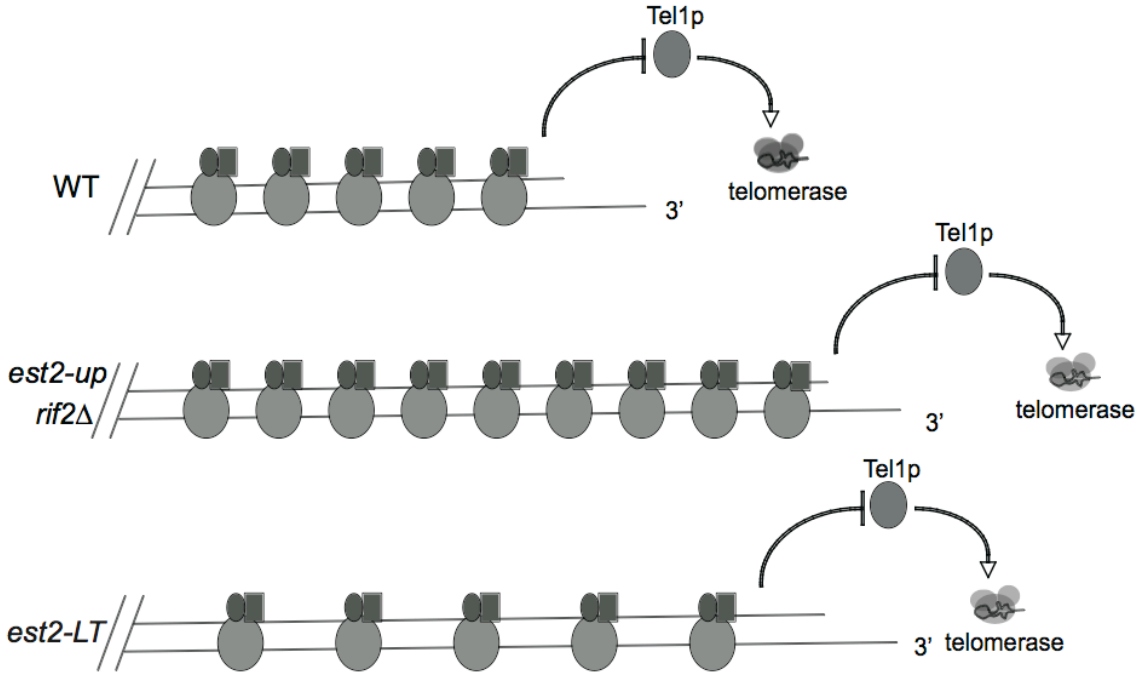

Figure 20. Model that explains how reduced Rap1p binding with telomeres causes telomere lengthening.

Telomere length is regulated by Rap1p's counting via its interaction with Rif1p and Rif2p. Tel1p is the downstream target of this counting pathway. Altered telomeric sequences by *est2-LT* mutants result in reduced Rap1p binding per telomere length unit (Figure 13), which in turn forces the lengthening of telomeres in order for certain amount of Rap1p to bind and reach an equilibrium of telomere length. The dependence of Rap1p and Tel1p support this model (Figure14; ref. [160]). For *rif2Δ* and *est2-up34*, Rap1p association with telomeres per unit remains the same as wildtype and total amount of Rap1p associated with telomeres is increased (Figure 13).

are inconsistent with large changes in nucleotide-addition processivity. We propose that the spectrum of permitted primer/template alignments is altered under conditions in which the normal negative regulation of telomere length is compromised.

Association of Rap1p with telomeres in vivo

We were surprised to discover that *est2-LT* and *est2-motifE* strains do not increase Rap1p association with telomeres *in vivo*, despite increasing telomere length by ~30%. Failure to detect this increase is not an experimental limitation, since *est2-up34* and *rif2Δ* strains similarly over-lengthen telomeres, but significantly increase the immunoprecipitation of telomeric DNA with Rap1p. We hypothesize that telomere over-elongation in an *est2-LT^{E76K}* strain is a response to reduced Rap1p association, since lengthening is not observed when Rap1p's regulatory function is bypassed in the "humanized" strain (Figure 20). We cannot exclude the possibility that increased processivity of Est2-LT^{E76K}p contributes to telomere over-elongation (and is suppressed by the humanized *TLC1* template). However, a model in which reduced Rap1p association causes telomere lengthening is consistent with our previous observation that expression of the *est2-LT^{E76K}* phenotype requires Tel1p, a downstream effector of the Rap1p pathway [160]. Furthermore, this model also explains the lack of significant change in the frequency or extent of telomere addition by *est2-LT^{E76K}* telomerase in a single cell cycle (Figure 15), since the telomeric substrates undergoing elongation have not previously encountered the mutant enzyme and are expected to bind Rap1p normally.

What accounts for the reduced association of Rap1p with *est2-LT* and *est2-motifE* telomeres *in vivo*? Our original hypothesis that Rap1p binding is reduced by changes in

telomere sequence is inconsistent with the observation that *est2-up34* telomerase generates similarly altered telomere sequences, but increases overall Rap1p association *in vivo*. Furthermore, sequences generated by *est2-LT*^{E76K} telomerase bind recombinant Rap1p at least as well as WT *in vitro*. Conflict between our observations can be reconciled if a mechanism independent of DNA sequence influences Rap1p association with telomeres *in vivo*. One possibility is that telomerase, either directly or indirectly, promotes the loading of Rap1p onto newly synthesized terminal sequences. Upon the reduction of this activity in *est2-LT* strains, telomeres continue to elongate until Rap1p binds at a level equivalent to that found at normal length telomeres. In this light, it is interesting to note that several subunits of the INO80 chromatin-remodeling complex have been recently shown to negatively regulate telomere length, perhaps through physical interaction with the telomerase complex [167]. Therefore, telomerase may participate in the normal formation of telomeric chromatin. Identification of other long-telomere strains that fail to increase Rap1p association will address these intriguing possibilities.

CHAPTER IV

MATERIALS AND METHODS

Saccharomyces cerevisiae strains and plasmids

Strains utilized are summarized in Table 4. The *est2-LT*^{E76K} mutation and an overlapping *Hin*dIII restriction site were generated by PCR utilizing primers *Hin*dIIIR (5'GTACGTTGTTGTAAAG**C**T**T**GCCCGTCAACAGG) and *Hin*dIIIF (5'CCTGTTGACGGGC**A**A**G**CTTACAACAACGTAC). Residues introducing the E76K mutation are bold and the *Hin*dIII restriction site is underlined. pKF409-TVL268 [*ProA-EST2 URA3*; ref. [50]] was template. The mutagenized PCR product was cleaved with *Afl*II and *Nhe*I and ligated to the corresponding sites of pKF409-TVL268. pKF408-E76K was created by cloning the *Afl*II-*Nhe*I fragment of pKF409-E76K into pKF408 [untagged *EST2 URA3*; ref. [134]]. The entire cloned fragment was sequenced.

PKF408-N95A *Aat*II was created as described above using mutagenic primers 5'CTGAAATGAAGACGTC**GC**A**A**ATAGTCTTTTTTGC and 5'GCAAAAAAGACTATT**TGC**GACGTCTTCATTTCTAGC (nucleotides introducing the N95A mutation are bold; the *Aat*II restriction site is underlined). The resulting PCR product was cleaved with *PflM*I and *Afl*II and ligated into the corresponding sites of pKF408 (*EST2 URA3*). The cloned fragment was fully sequenced.

A strain containing the *est2-LT*^{E76K} allele integrated at the endogenous locus was created by cleaving pKF408-E76K with *Cla*I and transforming strain YKF201 (see Table 1) by two-step gene replacement [168] to create strain YKF201-E76K.

Table 4. Strains used in this thesis.

Strain	Genotype	Source
TVL268	*MATa ura3-52 ade2-101 lys2-801 leu2- Δ1 trp1- Δ1 his3- Δ2̃CF⁺TRP1 SUP11*	V. Lundblad
YKF120-404	TVL268 *est2Δ*::*HIS3/ pKF404 (EST2 URA3 CEN)*	This thesis
YKF120-410	TVL268 *est2Δ*::*HIS3/ pKF410 (ProA-EST2 URA3 CEN)*	This thesis
YKF120-410^{LT}	TVL268 *est2Δ*::*HIS3/ pKF410-est2-LT (ProA-est2-LT URA3 CEN)*[a]	This thesis
YKF114-404	TVL268 *est2Δ*::*HIS3 rad52*::*LEU2/pKF404*	This thesis
YKF114-410	TVL268 *est2Δ*::*HIS3 rad52*::*LEU2 /pKF410*	This thesis
YKF114-E76K	TVL268 *est2Δ*::*HIS3 rad52*::*LEU2 /pKF410-E76K (ProA-est2-LT^{E76K} URA3 CEN)*	This thesis
YKF201[b]	*MATa trp1 leu2 ura3 his7*	[95]
YKF201-a	*MATa trp1 leu2 ura3 his7*	This thesis
YKF201-E76K	YKF201 *est2-LT^{E76K}*	This thesis
YKF202	YKF201 *tel1Δ*::*KAN^{R}*	This thesis
YKF202-E76K	YKF202 *est2-LT^{E76K}*	This thesis
YKF203	YKF201 *yku70Δ*::*KAN^{R}*	This thesis
YKF203-E76K	YKF203 *est2-LT^{E76K}*	This thesis
YKF204	YKF201 *rif1Δ*::*KAN^{R}*	This thesis
YKF204-E76K	YKF204 *est2-LT^{E76K}*	This thesis
YKF205	YKF201 *rif2Δ*::*KAN^{R}*	This thesis
YKF205-E76K	YKF204 *est2-LT^{E76K}*	This thesis
DKF206	*MATa/MATa trp1/trp1 leu2/leu2 ura3/ura3 his7/his7*	This thesis
DKF207	*MATa/MATa trp1/trp1 leu2/leu2 ura3/ura3 his7/his7 est2-LT^{E76K}/est2-LT^{E76K}*	This thesis
DKF208	*MATa/MATa trp1/trp1 leu2/leu2 ura3/ura3 his7/his7 EST2/est2-LT^{E76K}*	This thesis
BY4705a	*MATa ade2*::*hisG his3D200 leu2D0 lys2D0 met15D0 trp1D63 ura3D0 hdf1*::*LEU2*	R. Wellinger
GA426	*MAT**a** ade2*::*hisG ura3-52 his3-11 leu2 trp1 can1*::*hisG VR*::*ADE2-TEL*	[14]
YKF500	GA426 *est2-LT^{E76K}*	This thesis
YKF501	GA426 *est2*Δ::*TRP1*	This thesis
YKF502	GA426 *rif2*Δ::*TRP1*	This thesis
YKF503	YKF501 *pif1Δ*::*Kan^{R}*	This thesis
YKF504	YKF501 *tlc1-human* pKF417	This thesis
YKF505	GA426 *rad52Δ*::*LEU2*	This thesis
YKF506	YKF500 *rad52Δ*::*LEU2*	This thesis
YKF507	YKF505 *tlc1 Δ*::*Kan^{R}*	This thesis
YKF508	YKF506 *tlc1 Δ*::*Kan^{R}*	This thesis

Table 4, continued

YKF209	*MAT*α *trp1 leu2 ura3 his7 rif2Δ*::*TRP1*	This thesis
YKF210	YKF201 *pif1*Δ::*Kan*^{R}	This thesis
FYBL1-23D	*MAT*α *ura3*Δ*851 his3*Δ*200 trp1*Δ*63*	[86]
YKF510	FYBL1-23D *est2-LT*^{E76K}	This thesis
UCC5706	*MAT***a**-*inc ura3-52 lys2-801 ade2-101* ochre *trp1-63 his3-200 leu2-1*::*GAL1-HO-LEU2 TELVIIL*::*ADE2-TG*$_{1\text{-}3}$-Hosite-*LYS2 rad52*::*HISG*	[91]
YKF610	UCC5706 *est2-LT*^{E76K}	This thesis
CF797	h-, *leu1-32 ade6-M210 ura4-D18 his3-D1 trt1-*::*his3*+ [pNR210-trt1+ (*HSV1-tk, ade6*+*, trt1*+)]	P. Bauman

[a] pKF410-*est2-LT* are variants of plasmid pKF410 expressing mutant *est2-LT* alleles (*est2-LT*^{G75A}, *est2-LT*^{E76K}, *est2-LT*^{N95A}, *est2-LT*^{N95D}, *est2-motifE*) as indicated in the text.
[b] This strain was previously named 4053-5-2.

Complete gene disruptions of *TEL1, YKU70, RIF1,* and *RIF2* were obtained by amplifying the KAN^R gene and flanking DNA from the appropriate strain [Open Biosystems, Huntsville, AL; ref. [169]]. After transformation of the PCR product into YKF201and YKF201-E76K, transformants were selected on YPD media containing 200μg/mL geneticin. Successful knockout was confirmed by PCR and/or Southern blot.

Homozygous diploid strains were obtained by transforming YKF201 and YKF201-E76K with pHO, a plasmid expressing the HO endonuclease [170]. Transformants were restreaked twice, plated on 5-FOA to select for plasmid loss, and tested for diploidy. The heterozygous diploid strain (*EST2/est2-*LT^{E76K}) was obtained by mating YKF201-E76K with YKF201α (obtained by sporulation of the *EST2/EST2*diploid described above).

est2-LT^{E76K} was integrated into GA426, FYBL1-23D and UCC5706 by two-step gene replacement to create YKF500 and YKF510 and YKF610, respectively. *EST2* was replaced with *TRP1* in GA426 by transforming a *Sac*I-*Sph*I fragment from pKF404-HX*TRP*a (*TRP1* from pRS314 cloned into the *Hind*III and *Xba*I sites of pKF404; [50] to create YKF501. *RIF1* was replaced with Kan^R in GA426 to create strain YKF502 [160]. *RIF2* was replaced in YKF201-α and GA426 by *TRP1* using pFA6a-*TRP1* [171] as template to create strains YKF209 and YKF503, respectively. A heterozygous diploid (*EST2*/*est2-*LT^{E76K} *RIF1*/*rif1Δ RIF2*/*rif2Δ*) was generated by mating YKF204-E76K (YKF201 *est2-*LT^{E76K} *rif1Δ*::Kan^R) and YKF209.

The *RAD52* gene in GA426 and YKF500 was replaced with *LEU2* by transforming a *BamH*I fragment from plasmid pSM20[134] to create strain YKF505 and

YKF506. *TLC1* gene in these strains was disrupted with *Kan*^{R} using PCR product generated by primes: 5'-ACCTTCTTTGTAGCTTTTAGTGTGAA TTTTCTGGTTTGAGCGGATCCCCGGGTTAATTAA-3' and 5'-TATATTCTAAAA AGAAGAAGCCATTTGGTGGGCTTTATTAGAATTCGAGCTCGTTTAAAC-3' to create strains YKF507 and YKF508.

PIF1 gene disruption was accomplished in YFK201 by transforming a PCR fragment [primers: 5'-GTAGTTTTGTGATGCTGTTCAG-3' and 5'-GTGAGTTA GTCTCCTTTGGC-3'; template: genomic DNA from *pif1Δ*::*Kan*^{R} strain (Open Biosystems, Huntsville, AL)] to generate YKF210. *TLC1* was replaced with *tlc1-human* as described [155] in strain YKF501 [containing pKF417 (*EST2 CEN LEU2*)] to create YKF504. Following transformation with pKF410 (*ProA-EST2 CEN URA3*; ref. [160] or its mutant derivatives, colonies were screened for loss of pKF417.

Schizosaccharomyces pombe strains and plasmids

Genotype of the *S. pombe* strain utilized in this study (CF797) is listed in Table 4. Plasmid pKAN-trt1^{+} [172] contains the wild type *trt1*$^{+}$ gene and a *KanMX4* selectable marker. To facilitate mutagenesis, a *Kpn*I-*Sal*I fragment containing the majority of the *trt1*$^{+}$ open reading frame was subcloned into pUC19 to create pUC19-trt1^{+}. Standard PCR-mediated site-directed mutagenesis was used to separately introduce mutations of glutamic acid 98 to lysine, glutamic acid 101 to lysine, and asparagine 124 to alanine by amplification of a portion of *trt1*$^{+}$ between unique *Xba*I and *Bgl*II restriction sites. The mutant PCR products were cleaved with *Xba*I and *Bgl*II and ligated to pUC19-trt1^{+} vector cleaved with the same restriction enzymes. To facilitate cloning of the

mutagenized *Sal*I-*Kpn*I fragment back into pKAN-trt1$^+$, a *Kpn*I site within the polylinker of pKAN-trt1$^+$ was destroyed by partial digestion with *Kpn*I, treatment with T4 DNA polymerase, and religation to create pKAN-trt1$^+$ -Kpn. A completely sequenced *Sal*I-*Kpn*I fragment of each pUC19-trt1 mutant was transferred back into pKAN-trt1$^+$–Kpn by ligation between a unique *Sal*I site and the remaining *Kpn*I site. Each of the resulting plasmids bearing mutant or wild-type *trt1* were transformed into a *trt1$^-$::his3$^+$* strain bearing a *trt1$^+$* complementing plasmid with an *HSV1-tk* marker gene (CF797; Table 4). Transformants were selected on YES (yeast extract supplements) plates containing 100 μg/ml geneticin and subsequently streaked on YES plates containing 5-fluoro-2' deoxyuridine (5FUdR; 50μM) to select for loss of the complementing plasmid. After two restreaks on plates containing geneticin, DNA was isolated by glass bead lysis, cleaved with *Eco*RI, Southern blotted, and probed with a telomeric fragment.

Screen for long-telomere mutants

Construction of pKF410-*est2-LT^{N95A}, est2-LT^{G75A},* and *est2-LT^{N95D}* has been described [50]. Additional alleles of *est2-LT* were created by a gap repair approach utilizing unique *Afl*II and *Pfl*MI restriction sites located at amino acids 59 and 119 of Est2p, respectively. Primers JW75 (5'-GTTTCGCACTACCAAATTCAAG) and JW95 (5'-CTGCCCATTAAATTGAATTACTG) were used to amplify a 305 base pair fragment by error prone PCR as described [173]. The resulting PCR product and pKF410 FS vector (linearized with *Afl*II and *Pfl*MI) were cotransformed into strain YKF120 (Table 1; following loss of complementing plasmid on 5-FOA). pKF410 FS was created by ligating an *Nhe*I-*Afl*II fragment of pKF408-N95A *Aat*II (see above) into the *Nhe*I-*Afl*II

sites of pKF410. The resulting plasmid was cleaved with *Aat*II, treated with T4 DNA polymerase, and religated.

Ura$^+$ transformants obtained by gap repair were restreaked several times to eliminate mutants that inactivated *EST2*. DNA was isolated from transformants showing robust growth after the third restreak using either the DNA-Pure Yeast Genomic kit (CPG Inc.) or bead lysis [174] and telomere length was analyzed by Southern blot as previously described [50] following cleavage with *Pst*I or *Xho*I as indicated in the figure legends. Genomic DNA from strains showing longer-than-normal telomeres by Southern blot was used to transform *E. coli* by electroporation and rescued plasmids were retested for effects on telomere length.

In-gel hybridization procedure

In-gel hybridization was done as described with some modifications [[175], A. Bertuch, personal communication]. A 22mer (5'CCCACCACACACACCCACACCC) was gel purified and labeled by incubation at 37°C for 45 min with γ^{32}P-ATP and T4 polynucleotide kinase (Roche). Yeast genomic DNA was isolated using bead lysis [174] and equivalent amounts of DNA were digested by *Xho*I in a 100 μl reaction volume. Reactions were terminated by precipitation with 20μL 3M NaOAc and 660μL 100% EtOH. Pellets were resuspended in 12μL binding buffer (10 mM Tris-HCl, 50 mM NaCl, 10 mM $MgCl_2$, 1 mM dithiothreitol, pH 7.9 at 25°C) and 1μL probe (100,000cpm) was added to each sample and incubated for 10min at 37°C, followed by incubation for one hour on ice. Samples were loaded on Sephadex G50 columns to eliminate unbound probe. DNA samples were separated in a 0.7% agarose gel by electrophoresis for 16hr at

~2V/cm in the cold room. Gels were dried at 23˚C (using a SGD5040 Slab Gel Dryer; Savant) for 24-28min until the gel was very thin and even, and the gel was exposed to Phosphorimager screen.

To denature the chromosomal DNA, the gel was washed in denaturing solution (0.15M NaCl, 0.5M NaOH) for 25min at RT, followed by a 25-min wash in neutralizing solution (0.15M NaCl, 0.5M Tris HCl, pH 8.0). The gel was briefly prehybridized with 25ml hybridization solution [78] and 18μl of the probe described above was added. The gel was incubated at 36°C overnight. The gel was washed in 0.25xSSC at RT overnight and exposed to phosphorimager screen.

Primer competition assay

Extract preparation and immunoprecipitation of Protein A tagged Est2p was performed as described[134] except that beads were washed two times with TMG (10 mM Tris-Cl at pH 8, 1 mM $MgCl_2$, 10% glycerol, 0.1 mM DTT) plus 200 mM NaCl and 0.5% Tween-20, twice with TMG [plus 2μl/ml RNasin (Promega)], and resuspended in 20 μl of TMG (plus 2 μl/ml RNasin, 0.5 mM DTT). Prior to immunoprecipitation, extract concentrations were adjusted to 20 mg/ml. Packed beads (5 μl) from the immunoprecipitation were mixed with 0.5 μl of water or 0.5 μl of 1 mg/ml RNase A and incubated 10 min. at 30˚C. 5.5 μl of a 2X reaction mixture consisting of 80 mM Tris-Cl at pH 8, 100 mM NaCl, 10% glycerol, 5 mM $MgCl_2$, 1 mM spermidine, 1 mM DTT, 5 μM initial substrate oligonucleotide (see below), 200 μM each dTTP, dATP, and dCTP, and 1.5 μl [α^{32}P]dGTP (800 Ci/mM; 10 μCi/μl) was added per sample on ice and the reaction was initiated by incubation at 30˚C. After 7 minutes, 1.4 μl of 20 μM challenge oligonucleotide (or 1.5 μl buffer) was added and the incubation was continued for an

additional 23 minutes. The reaction was stopped by addition of 1.5 μl of stop buffer (250 mM Tris at pH 8, 250 mM EDTA at pH 8, 2% SDS) and 1.75 μl of proteinase K (20 mg/ml) for 30 minutes at 60˚C. Reaction products were phenol extracted, precipitated, and separated in a 12% acrylamide/8M urea sequencing gel. Product was quantitated after exposure to phosphorimager. Oligonucleotide +1 marker was made by treating the appropriate oligonucleotide with terminal transferase (GE Healthcare) in the presence of [^{33}P]ddTTP. Substrate (and challenge) oligonucleotides were as described [36]: 14 (5' GTGTGGTGTGTGGG); 5'NT (5' GACCGCGGTGTGTGGG); and 29 (5' GGGTGTGGTGTGTGGGTGTGGTGTGTGGG).

Nucleotide-addition processivity

Extract preparation and immunoprecipitation were as described above. To visualize differences in processivity between wild-type and *est2-motifE* strains, the conditions of the telomerase assay were modified as described [148]. Reactions were incubated at room temperature for 1 hour, then processed as described above. Reaction products were quantified by determining the intensity of each band (+1 to +7) by phosphorimager analysis. Processivity^{+3} was calculated as the sum of signal in bands +4 to +7 divided by the total amount of signal in bands +1 to +7. Signal was corrected for specific activity by dividing the intensity of each position by the number of G residues expected to be incorporated into product at that position (+2, +3 = 1; +4 = 2; +5, +6 = 3; +7 = 4).

Analysis of primer binding

Extract preparation, immunoprecipitation, and telomerase assay were done essentially as described above for the primer competition assay with the following adjustments. All dNTPs were omitted and [α^{32}P] dTTP (800 Ci/mM; 10 μCi/μl) was substituted for dGTP. Primer was added to immunopurified telomerase at 5X decreasing final concentrations of 2.5 μM, 0.50 μM, 0.10 μM, 0.02 μM, 0.004 μM, and 0.0008 μM for 10 minutes on ice. Reactions were initiated by the addition of telomerase reaction mix containing dTTP and allowed to proceed for seven minutes at 30˚C before being terminated by the addition of STOP buffer and proteinase K as described above. Equal amount of an end-labeled 29-mer oligonucleotide was added to each sample prior to phenol extraction and precipitation to serve as a loading control. Reaction products were quantified by phosphorimager. The intensity of each +1 product band (corrected for background) was divided by the intensity of the loading control to correct for variations in yield during sample processing. The corrected value for the +1 product was then normalized to that of the highest primer concentration to correct for variations between experiments in specific activity of the loading control.

Western blotting

Protein extraction and immunoprecipitation with IgG Sepharose beads (GE Healthcare) were performed as previously described [134]. Samples were loaded on a NuPAGE™ 10% Bis-Tris Gel (Invitrogen). Protein was transferred to Hybond-P membrane (GE Healthcare). Primary antibody was mouse monoclonal anti-Protein A (Sigma). Secondary was peroxidase-conjugated goat anti-mouse antibody (Chemicon International).

Cloning and sequencing of *S. cerevisiae* telomeres

Multi-cell cycle analysis. YKF501 bearing plasmid pKF410 was restreaked on plates containing 5-fluoroorotic acid (5-FOA) and restreaked once to allow telomere shortening. After reintroduction of pKF410 bearing WT or mutant *est2-LT,* transformants were restreaked three times (~75 generations). Genomic DNA was extracted by glass bead lysis [174] and telomere PCR was performed [86]. After gel purification (Qiagen), products were ligated into pGEM T-easy (Promega) according to manufacturer's instructions. Inserts were sequenced by FASTERIS (Plan les Quates, Switzerland) using primer M13F.

Isolation of telomeres extended in a single cell cycle. A fresh GA426 *est2Δ*::*TRP1* colony ("recipient") was grown overnight in 5 ml SD-Trp medium. $1X10^8$ telomerase-deficient recipient cells were mixed with $1X10^9$ cells of strains FYBL1-23D or YKF510 (donor) as described [86] and incubated at 30°C for 4 hours on YPD plates. Mating efficiency [monitored by comparing growth on SD-Trp (recipients and diploids) with growth on SD-Leu-Trp (diploids only)] was nearly 100% (data not shown). Telomere PCR was performed as above.

Isolation of telomeres added to a newly-formed telomeric end. UCC5706 and UCC5706-E76K strains were pregrown in SD-Lys (2% glucose) overnight, diluted into YEP-2.5% raffinose for three or four generations before being arrested with 10mg/ml nocodazole (in DMSO, final concentration of 10ug/ml) for 4 hours. Cells were centrifuged and resuspended in YEP-3% galactose and grown overnight. Genomic DNA was extracted and telomere PCR was performed as above, with primers 5'-GCCAAGATATCAAAC

TGTAAAT-3' and 5'-CGGGATCCG$_{18}$-3'.

Cloning and Sequencing of *Schizosaccharomyces pombe* telomeres

CF797 was streaked on YES plates containing 5-fluoro-2' deoxyuridine (5FUdR; 50μM) to select for loss of the complementing plasmid. Plasmids pKAN-*trt1*$^{+}$-Kpn and pKAN-*trt1*^{E98K}-Kpn were transformed and selected on YES (yeast extract supplements) plates containing 100 μg/ml geneticin. After two restreaks on plates containing geneticin, DNA was isolated by glass bead lysis, and telomeric sequences were amplified as previously described and sequenced as described above.

Chromatin immunoprecipitation and dot blot

ChIP was performed as described, with some modifications [176]. Yeast strains were grown to OD_{600}= ~0.5 (50ml in YPD). Crosslinking was initiated with 1.4mL 37% formaldehyde and terminated after 5 minutes by addition of 2.5mL 2.5M glycine. Cells were pelleted and washed sequentially with HBS (50mM HEPES pH 7.5, 140mM NaCl) and ChIP lysis buffer with PMSF (50mM HEPES pH 7.5, 140mM NaCl, 1mM EDTA pH 8.0, 1% IGEPAL CA-630, 1% sodium deoxycholate and 1mM PMSF). Pellets were resuspended in 400μl ChIP lysis buffer (plus one Roche Complete Mini-Protease Inhibitor tablet per 10ml) and disrupted by glass bead lysis. Lysate was obtained by centrifugation and DNA was sonicated to fragments of 500-1000bp. Sonicated lysate was cleared twice by centrifugation at 7000K for 2 minutes and input samples (25μl of 400μl) were obtained. Remaining lysate was incubated on ice with 20μl anti-Rap1p antibody (Santa Cruz Biotechnology). Samples were immunoprecipitated with 80μl Protein G Dynabeads

(Invitrogen). Crosslinking was reversed by overnight incubation at 65°C and DNA was detected by dot blot. Probe was random-primed *S. cerevisiae* telomeric DNA or a random primed fragment from the *ARO1* gene (primers 5′-TGACTGGTACTACCGTAACGGTT C-3′ and 5′-GAATACCATCTGGTAATTCTGTAGTTTTGAC-3′). Data analysis has been described [177].

Analysis of telomere sequence data

Data analysis utilized newly synthesized sequences identified by alignment of identical internal repeats. The frequency of GG-dinucleotide incorporation was calculated as the number of 5'-TGGGTGT sequences followed by GG divided by total 5'-TGGGTGT sequences. When a core sequence overlapped with an adjacent repeat (5'-TGGGTGTGGGTGT), the 5' core (underlined) was considered to lack the GG. Such overlapping core sequences generate a spacer with a value of -1. The frequency of "overlapping core sequences" is defined as the number of spacers in the -1 class divided by total spacers. Predicted Rap1p binding sites were identified as described [153] with MatInspector (www.genomatix.de) using a 14 bp similarity matrix to assign confidence scores [178].

Rap1 protein expression, purification, and binding assays

Protein expression from pET28a (+)-Rap1p (*Xho*I-*EcoR*I) [179] was induced overnight in BL21 *E. coli* with 1 mM IPTG (isopropyl-β-D-thiogalactopyranoside) at 16˚C. Recombinant His_6-tagged full-length Rap1p was purified on NTA-agarose beads (Qiagen) by manufacturer's instructions and purified by ion-exchange chromatography.

Eluted protein was dialyzed in 20mM Tris-HCl (pH7.5), 50mM NaCl, 20mM KCl, 6% glycerol. Protein concentration was estimated by comparison with BSA standards.

For the gel shift assay, oligonucleotides (5'-ATAT**ACACCCATACATT**GA-3' and 5'-GTC**AATGTATGGGTGT**ATA-3'; [179] were annealed to create a single Rap1p binding site (bold) and labeled with Klenow polymerase (Roche) in the presence of α-^{32}PdCTP. 100 fmoles of ^{32}P-labeled DNA was mixed with increasing amounts of unlabeled telomeric DNA (0-80 fmoles). 400 fmoles of recombinant Rap1p was added in 20μl binding buffer [20 mM Tris-HCl (pH 7.5), 70mM KCl, 1mM dithiothreitol, 6% vol/vol glycerol, 25μg/ml bovine serum albumin, 2.5μg/ml poly(dG-dC), 0.1 mM EDTA] and reactions were incubated on ice for 10 minutes followed by 20 minutes at RT. Samples were separated by 6% polyacrylamide Tris/borate-EDTA gels, dried, and quantified by phosphorimager.

For DNaseI footprinting, ^{32}P-end labeled telomeric sequences (100 fmoles) and 20 fold excess recombinant Rap1p were mixed in 20μl binding buffer, incubated on ice for 10 minutes, and one hour at RT. Samples were incubated with 0.5 unit DNase I (Promega) for 1 minute, followed by addition of 45μl stop solution (supplied by manufacturer). DNA was phenol/chloroform extracted and ethanol precipitated. Samples were resuspended in 5μl formaldehyde loading buffer, separated on 10% polyacrylamide gels, and analyzed by phosphorimager.

CHAPTER V

GENERAL DISCUSSION AND FUTURE DIRECTIONS

General Summary

In this dissertation, I have explored the role of *S. cerevisiae* Est2p in regulating telomere length. As the catalytic subunit of telomerase, Est2p positively regulates telomere length. Interestingly, we identified several mutations clustered in the N-terminus of Est2p (named *est2-LT*) that cause telomere lengthening, suggesting that Est2p may contribute to negative regulation as well. These mutations do not cause detectable changes in catalytic nucleotide addition *in vitro* or alter the affinity of mutant Est2p for its DNA substrate. Genetic epistasis analysis suggests that the over-extension of telomeres in *est2-LT* strains is dependent upon Tel1p and acts through the Rap1p counting mechanism. Indeed, the association of Rap1p (per nucleotide) with endogenous telomeres is reduced in *est2-LT* strains. As a result, telomeres lengthen until enough Rap1p is bound to reach a new equilibrium length (Figure 20). Associated with the long-telomere phenotype, there are certain telomere sequence changes in *est2-LT* strains. Similar changes are observed in other long telomere mutants (*est2-up34* and *est2-motifE*), suggesting that sequences changes in *est2-LT* are a consequence, not the cause, of telomere over-extension. The basis of these changes is under investigation. Although the sequence changes modestly affect predicted Rap1p binding sites, Rap1p binds to mutant telomeric sequences equally well as to wild-type telomeric sequences *in vitro*, suggesting

a possible role of Est2p in regulating Rap1p binding to telomeres *in vivo*. Experiments to explore the mechanism of this effect are described below.

Future Directions

Why is Rap1p's association with telomeres in est2-LT *strains decreased?*

The observation that Rap1p association is reduced at *est2-LT* and *est2-motifE* telomeres but not *est2-up34* telomeres (described in Chapter III) suggests that the effect on Rap1p association is less likely a general effect of over-lengthened telomeres. However, it is unclear how general this phenomenon might be. We will measure Rap1p's association with telomeres in other mutants that have over-lengthened telomeres (for example, *dna2-1*). If less Rap1p association only occurs in *est2-LT* mutants, it will suggests that Est2p has a direct role in influencing Rap1p association with telomeres. If some of the long telomere mutants in lagging strand replication machinery have reduced Rap1p association, this may suggest that these mutants cause telomere lengthening through a similar or related mechanism as *est2-LT*.

Est2p might influence Rap1p's association in two ways, indirectly and/or directly. Mutations in Est2p might affect chromatin assembly and consequently change Rap1p's association. There is precedence for a link between replication and chromatin assembly in the CAF-1 complex that assembles nucleosomes on newly replicated DNA in a manner linked to the replication fork through PCNA[180-182]. It is possible that telomere replication must be linked to appropriate nucleosome deposition or even specifically to Rap1p deposition. Chromatin remodeling is mediated by two distinct classes of molecular processes that are highly intertwined. The first class remodels chromatin by post-

translational modification of histones, such as acetylation, methylation, phosphorylation, ubiquitylation, and sumoylation. The second class is ATP-dependent and is catalyzed by chromatin remodeling complexes. By changing DNA-histone interactions, ATPases can slide, eject, insert or restructure histone octamers. One of these complexes is the INO80 complex, several subunits of which are preferentially associated with telomeric DNA, consistent with a direct role of this complex at telomeres[167]. Deletion of INO80 subunits (for example, Ies3p) causes telomere lengthening. Ies3p has been shown to interact with Est1p, however, the significance of this interaction remains unclear. Whether any component of INO80 complex interacts with Est2p is unknown.

To test whether *est2-LT* mutants influence Rap1p association through the INO80 complex resulting in telomere overlengthening, double mutants between *ies3Δ* and *est2-LT^{E76K}* will be generated and telomere length will be assayed by Southern blotting. If there is no additional lengthening in the double mutant compared with *est2-LT^{E76K}*, we can conclude that *ies3Δ* and *est2-LT^{E76K}* act through the same genetic pathway in telomere regulation and that Est2p influences Rap1p association in an indirect way, likely through the INO80 complex. If additional telomere lengthening is observed in the double mutant, then Est2p may play a more direct role in dictating Rap1p association with telomeres, possibly via a protein-protein interaction. CoIP or yeast two-hybrid experiments will be performed to address this possibility.

Reduced Rap1p association in *est2-LT* and *est2-motifE* with telomeres might change the chromatin structure, although these changes might not affect the silencing of genes localized at telomeres (Figure 12 in Chapter III). Micrococcal nuclease and DNase I analysis of yeast chromatin show that the subtelomeric X and Y' elements are

assembled in nucleosomes while the entire terminal tracts of TG_{1-3} repeats are assembled in a non-nucleosome structure termed the telosome[183]. The telosome is separated from adjacent nucleosome by a region of DNA that is highly accessible to enzymes and it can be cleaved from chromosome ends with nuclease and solubilized as protein-DNA complexes. Since Rap1p is a component of this telosome complex, reduced Rap1p association might disrupt the telosome structure and increase the sensitivity of telomeric chromatin to nucleases. To address this possibility, MNase and Dnase I digestion will be used to examine whether the telosome structure is affected in *est2-LT* mutants.

What is the basis of the altered sequences in* est2-LT *strains?

Telomerase uses *TLC1* RNA as a template to add nucleotides consecutively onto chromosome ends, a process termed nucleotide addition processivity. After one repeat is added, telomerase translocates and initiates another round of nucleotide addition (repeat addition processivity). Yeast telomerase has low nucleotide and repeat addition processivity, which causes heterogeneity of the yeast telomere sequence. This heterogeneity is proposed to arise from a combination of incomplete Reverse Transcription (RT) and multiple registers of alignment between telomeres and template RNA[14]. The central region of *TLC1* RNA is incorporated in ~90% of all telomeric repeats, which is named the "core sequence" (Figure 16 in Chapter III). In WT cells, telomerase has only ~50% chance of copying past template residues $^{471}CC^{470}$ to generate a GG dinucleotide and rarely extends to the end of the template. When telomerase translocates, there are multiple registers in which it can align with the template, resulting in different numbers of TGs between "core sequences" (termed the spacer). The rate of

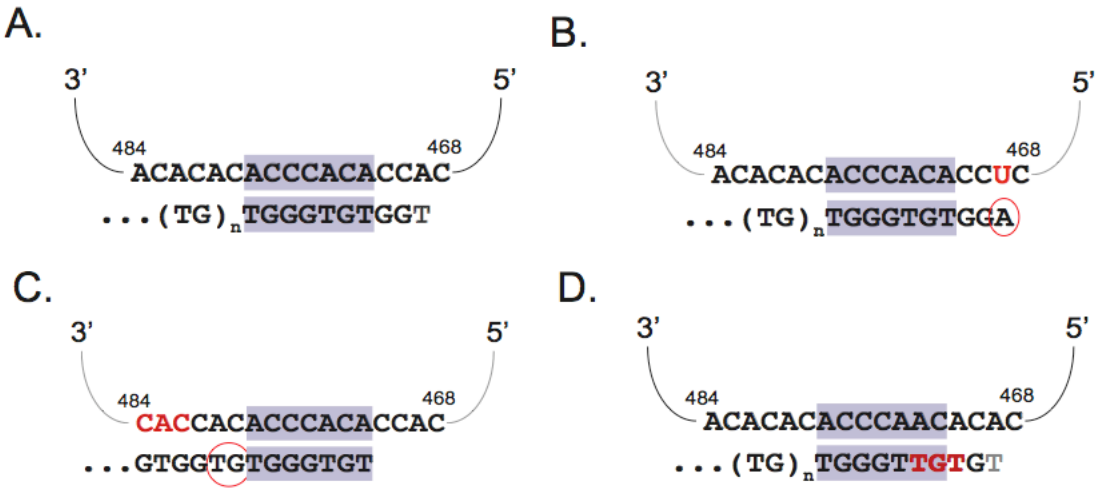

Figure 21. Proposed RNA template mutants and predicted effects on telomere sequence. TLC1 RNA is shown above and chromosome sequence below. Purple: core sequence.

A. *TLC1*
B. *tlc1*U^{469}->A
C. *tlc1*$^{484}CAC^{482}$->ACA
D. *tlc1*$^{473}CAC^{471}$->ACA

incorporation of the GG-dinucleotide and average spacer length can be used to the behavior of telomerase *in vivo*. In *est2-LT* strains, there is a higher rate of GG-dinucleotide incorporation and significantly longer spacer regions. Although the increased incorporation of the GG dinucleotide is most easily explained as an increase in nucleotide addition porcessivity, the lack of increased incorporation of position 469 suggests that increased Type I processivity cannot explain the alterations in telomeric sequences (Figure 21B; Chapter III).

The presence of extremely long spacers (>10nt) in WT strains suggests that the spacer can be generated by the slippage of telomerase. So the increased spacer length can't be fully accounted for by increased processsivity. At least some heterogeneity in TG repeats must arise from multiple alignment registers in the 3' end of the template. Expression of *tlc1* ^{484}ACA^{482} to CAC increases the number of base pairs formed between a GG dinucleotide-containing 3' terminus and the RNA template (Figure 21C). In WT cells, this increased pairing "locks" the alignment register such that all GG sequences are followed by a single TG dinucleotide. If, in this mutant, spacers are reduced to 1 TG, it will suggest that the longer spacers in *est2-LT*^{E76K} arise in part from preferential alignment of the mutant enzyme at the extreme 3' end of the RNA template. Southern Blotting will be used to determine whether telomere lengthening is suppressed. If the long spacers still exist, it will imply that this mutant enzyme is extremely prone to slippage or abortive RT.

In the process of analyzing telomeric sequences resulting from different RNA template mutant in wild-type or E76K background, I made several interesting observations. First, in presence of the U^{469}->A mutant (Figure 21B), the frequency of GG incorporation and overlapping core sequences are greatly changed (Table 5). Secondly, in the *tlc1*^{473}CAC^{471} to

Table 5. Sequence changes in *tlc1*U^{469} to A template mutant.

	GG incorporation (Percent)	
	WT	E76K
WT template	52.5	67.10
U^{469} to A	68.2	32.6

	Overlapping core sequences (Percent)	
	WT	E76K
WT template	29.2	17.5
U^{469} to A	36.8	63.3

ACA mutant where GG incorporation is disrupted (Figure 21D), in presence of WT telomerase there is always a spacer between two core sequences (TGGGTTG). In contrast, in presence of E76K telomerase there are 25% neighboring core sequences (TGGGTTGTGGGTTG, significantly different from WT, p=0.0015) that are most likely generated the same way as the overlapping core sequences. Although these changes are striking and interesting, we are unable to come up with a model of telomerase synthesis that could explain these data. More RNA template mutants will be utilized to distinguish the behavior of WT and mutant telomerase.

The conventional processivity assay described in Chapter II utilized a canonical DNA primer with maximal base-pairing with RNA template and low dGTP concentrations (~0.2μm) and in this assay yeast telomerase does not exhibit Type II processivity. However, recently Lue and colleagues modified this assay with a mutated DNA primer that has two mis-pairing with the RNA template and high dGTP concentration (3.2μm), and observed telomerase Type II processivity[184]. Under these conditions, Est2-LT^{E76K} telomerase shows a weak increase in Type II processivity[37]. Although it is not consistent with the reduced average telomere addition *in vivo* (Figure 15 in Chapter III), this observation may reflect alterations in the enzymatic properties of Est2-LT^{E76K} telomerase such as anchor-sites interaction. Primers with different sequences and length will be used in the processivity assay to test this possibility.

WT telomerase has low type II processivity *in vivo* based on the observation of closely interspersed repeat types in strains simultaneously expressing two different template alleles[36]. In a single cell cycle experiment monitoring sequences added by either wild-type telomerase or *est2-LT^{E76K}* telomerase were analyzed, preliminarily I found an increase in frequency of telomere addition although it is not statistically significant (p=0.09, Fisher's exact test). More telomeres will be obtained and analyzed to get statistically significant results. I also found that the

frequency of telomere addition to the *de novo* telomeric end in *rif2*Δ and *est2-LT*^{E76K} strains are both increased compared with WT strain (Figure 22A and 22B), consistent with the result from the single cell-cycle experiments (Figure 15; ref. [86]). This increase in frequency of telomere addition might result form decreased Type II processivity *in vivo*. A two-template single-telomere extension assay (2T-STEX) was used to determine the Type II processivity in WT strain[185]. In this experiment, two clearly distinct RNA templates are co-expressed so that telomere addition by two telomerase can be easily distinguished. Telomere sequences are sequenced and Type II processivity can be calculated as the average number of WT or mutant repeats added per telomere addition event. A similar experiment will be performed co-expressing *TLC1* and a *tlc1* ^{473}CAC^{471} to ACA mutant in *est2-LT*^{E76K} strain (Figure 21D). While this mutant does not significantly affect telomere length, it will incorporate a clearly distinguishable GGGTT(GT)$_n$ repeat. If WT and mutant RNAs are expressed at the same level (will be determined by RT-RCR), we would expect repeat-type heterogeneity on every replicated telomere. If *est2-LT*^{E76K} increases Type II processivity, we would see telomeric repeats on one telomere are mostly WT or mutant.

Are there two modes of telomerase synthesis?

I found that telomeric sequences added by WT telomerase to a newly formed telomeric "seed" have a pattern that more closely resemble that of the long-telomere mutants than WT (Table 2 in Chapter III and Table 6). To eliminate the trivial possibility that this difference is due to the strain background, Robin Bairley has sequenced telomeres present at natural chromosome ends in this strain. She found that these natural telomere repeats are similar to those found in

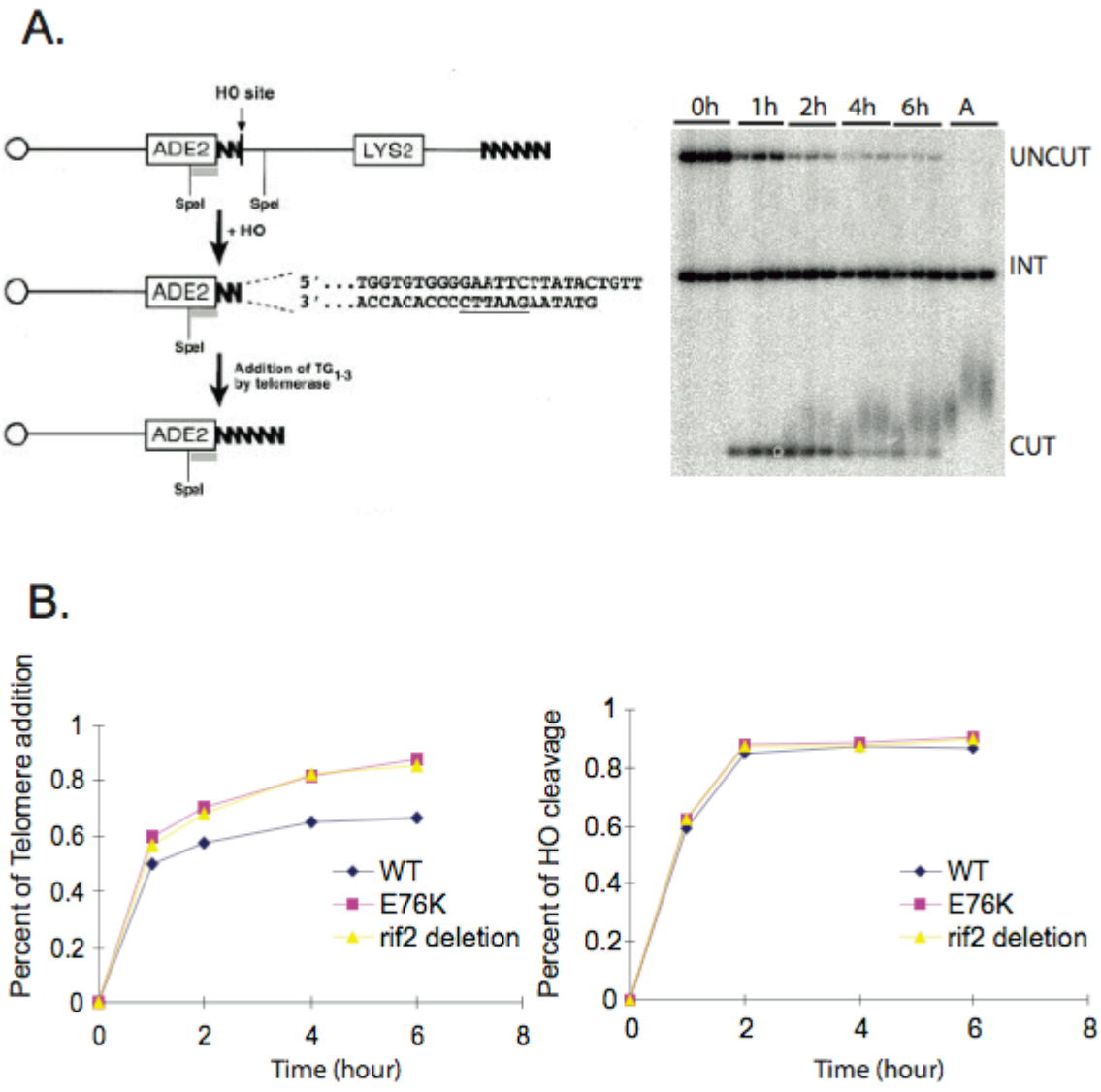

Figure 22. Increased kinetics of sequence addition onto the TG1–3/HO end in *rif2*Δ and *est2-LT*^{E76K} strains.

A. WT, *est2-LT*^{E76K} and *rif2*Δ cells were arrested using nocodazole for 4 hours at 30°C. Galactose was added to induce HO expression. Cells were harvested at 0h, 1h, 2h, 4h, 6h times point in nocodazole block after HO induction or grew without nocodazole block overnight. DNA was isolated, digested by *Spe*I, subject to Southern blotting and probed with the ADE2 probe (Grey bar). INT is an internal control fragment result from *Spe*I digestion. This assay is modified from[91].

B. Graphical representation of sequence addition onto the TG1–3/HO end. The percent of addition is calculated as the reduction of the cut signal over the total cut signal.

C. HO cleavage efficiency in strains indicated in A. It is calculated as cut signal at each time point/original uncut (0h time point) signal.

Table 6. Sequence comparison of telomeres added to a natural chromosome end and an HO-cleaved end.

	GG incorporation (Percent)	
	WT	E76K
Multiple cell cycle	52.5	67.10
Telomeres added to XVL	53.8(70/130)	
Telomeres added to HO-cleaved end	63.5	
	Overlapping core sequences (Percent)	
	WT	E76K
Multiple cell cycle	29.2	17.5
Telomeres added to XVL	28.6 (36/130)	
Telomeres added to HO-cleaved end	22.1	

other WT strains (Table 6). Based on these results, we hypothesize that telomerase may behave differently during *de novo* synthesis than during conventional synthesis. Based on this idea, we would postulate that the *est2-LT* mutations alter the properties or regulation of telomerase so that mutant telomerase works in this second mode at chromosome ends. If this is true, comparing the behavior of telomerase at chromosome ends and DSB will unmask the mechanism of *est2-LT* affecting telomere length regulation. Although many labs use the HO cleavage assay to study the recruitment/regulation of telomerase, there is evidence suggesting that telomerase behaves differently at a DSB and at chromosome ends. For example, the *de novo* end is lengthened efficiently in G2/M phase, while a native telomere is not elongated at all. The *MRE11/RAD50/XRS2* genes are absolutely required for telomerase-mediated addition in the *de novo* assay, and in the absence of Rad50, the association of the single-stranded $TG_{1\text{-}3}$ DNA binding protein Cdc13p is abolished[186]. In contrast, on a natural telomere, the association of Cdc13p with yeast telomeres occurs efficiently in the absence of Tel1p, Mre11p, Rad50p, or Xrs2p, and the MRX complex is not absolutely required for telomere elongation[71].

As mentioned earlier, I have found a RNA mutant (*tlc1* ^{473}CAC^{471} to ACA) in which the WT and mutant telomerase behave significantly different ($p=0.0015$). While the basis of this phenomenon is unclear, this mutant can be used in the HO cleavage experiment to compare telomere synthesis by WT and E76K telomerase to obtain statistically significant results with a small set of data.

Does the LT region have a conserved role in telomere length regulation?

The crystal structure of the TEN domain in *Tetrahymena* TERT has been solved. Due to low identity (20%) between *S. cerevisiae* Est2p and *T. thermophila* TERT, preliminary model

building began with six different sequence alignments. Ten models were generated to each alignment and the top-scoring model for each alignment was visualized using Chimera software. Among these ten models, the model that has all the expected secondary structure in *Tetrahymena* TERT was chosen as our working model of *S. cerevisiae* Est2p (Figure 23A).

In our working model, G75 and E76 are localized at α4 and N95A is localized within a loop between α4 and α5. These residues appear to lie on a potential functional surface that could interact with protein or DNA. E76 to R and E76 to A mutations are being constructed to explore the role of charge in generating the long telomere phenotype. Several additional residues will be mutated to test aspects of this model. For example, N79 located on the putative surface will be mutated to alanine, lysine and arginine. Since helices 4 and 6 appear important for the structural integrity of this region and are predicted to interact, mutations will be made at the helical interface (V128, L131, L73 and L77). We predict that such mutations will compromise Est2p structure. Indeed, a mutation of V81 (located along the interface at the end of helix 4) to alanine supports normal growth and telomere length, while mutation to trytophan causes telomere shortening and senescence (data not shown), consistent with the position of this residue in the interface. One interpretation of this result is that a bulky residue cannot be tolerated where the two helices pack tightly in the structure. Given the locations of F127 and L73 in the model, we are testing whether swapping the position of these two residues is compatible with protein function. Elliott Kim is constructing both single mutations and the double mutation. Our model will be further supported if the double mutation retains more function than either single mutant.

It is attempting to speculate that polymorphisms in *EST2* could contribute to differences in telomere length. It is interesting that the yeast *Saccharomyces paradoxus* (a very close relative of *S. cerevisiae*) has longer telomeres than *Saccharomyces cerevisiae*. QTL analysis revealed

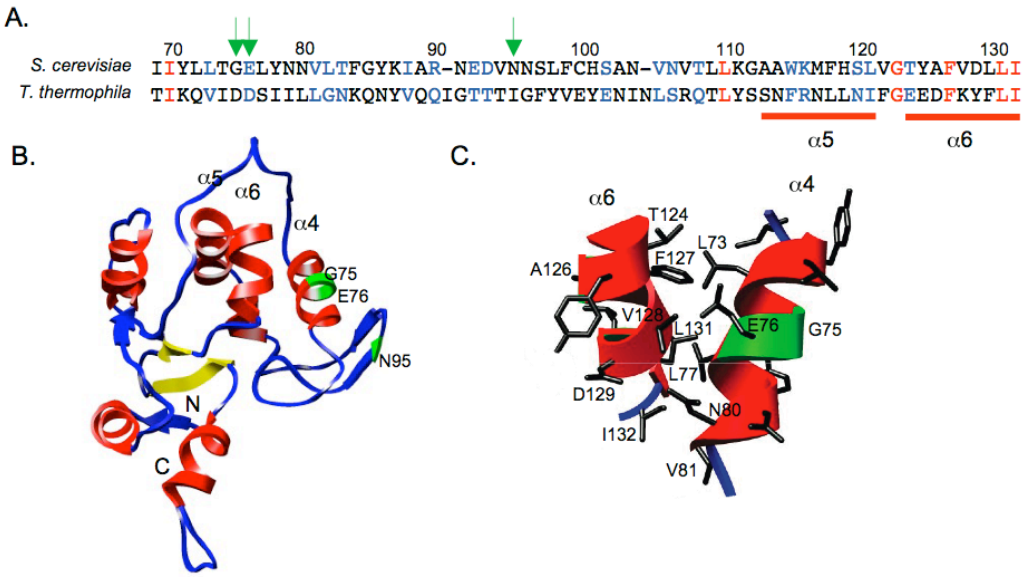

Figure 23. Representative model of the TEN domain of *S. cerevisiae* Est2p

A. Sequence alignment of *S. cerevisiae* and *T. thermophila* TERT used to generate the model shown in B. Only the portion encompassing helices 4 and 6 is shown. Red: identical residues. Blue: conserved. Residues mutated to produce over-lengthened telomeres are indicated by green arrows.

B. Model of *S. cerevisiae* TEN domain.

C. Helices 4 and 6 are magnified and amino acid side chains are shown. Green indicates long-telomere mutations. Figures generated with Chimera.

that Est2p plays an important role in generating this telomere length (Ed Louis, personal communication). Sequence alignment shows that *Sp*Est2p has an E76G polymorphism and Bethany Cartwright is working on determining the extent of the contribution of this residue to the telomere length.

In Chapter III, I also describe a mutation in the N-terminus of *S. pombe* Trt1p (E98K) that causes telomere overelongation companied by sequence changes *in vivo*. Less is known about the RNA template in *S. pombe*, making it difficult to determine the basis of these sequence changes. Lack of more mutations that cause telomere lengthening makes it hard to conclude that this is a conserved region in the N-terminus of Trt1p that regulates telomere length. A PCR-based mutagenesis method can be utilized to screen for additional mutations that result in longer than normal telomeres.

Telomerase activity is up-regulated in many tumor cells, making telomerase a target for cancer treatment. Telomerase defects also contribute to inherited degenerative diseases and premature aging syndromes. Studies of a mice model lacking telomerase suggest that short telomere length rather than telomerase level determines the renewal capacity of stem cells. An understanding of telomere length regulation by telomerase and other regulators will be critical to create a novel method to maintain normal telomere length in cells with short telomeres. My study identified a novel role of Est2p N-terminal region in negatively regulating telomere length through Rap1p. In the process of understanding the underlying mechanism, I discovered several surprising phenotypes associated with mutations in this region that cause telomere over-elongation. These observations reveal interesting aspects of telomerase function and further study will contribute to our better understanding of telomere length regulation and drug discovery.

APPENDIX

TESTING THE INTERACTION BETWEEN Est2p AND LAGGING-STRAND REPLICATION COMPONENTS

Introduction

DNA replication is one of the most important events in living cells. According to the current model of DNA replication, an initiator protein complex (ORC) is bound to an origin of replication. ORC recruits other proteins such as MCMs, Cdc6 and Cdc7/Dbf4, leading to the formation of an initiation complex. Following these events, DNA structure is altered locally by helicase activity, the single stranded DNA is protected and stabilized by Replication Protein A (RPA), and polymerase α/primase and helicase are recruited to initiate polymerization. After limited DNA synthesis by polα/primase, PCNA and RFC facilitate the switch to polδ. polα/primase also initiates Okazaki fragment synthesis of the lagging strand by extending an RNA primer, followed by replacement by polδ. Synthesis of the leading strand and lagging strand are likely coordinated by dimerzation of polδ holoenzymes. The RNA primer and the short region of DNA synthesized by polα/primase is removed by Dna2p and Fen1p and two adjacent Okazaki fragments are ligated by DNA ligase I. Topological constrains are released by Topoisomerase I.

This highly coordinated process encounters difficulties at the extreme end of the chromosome, potentially causing cumulative sequence loss. This telomere loss is counteracted by the activity of telomerase to add telomeric sequences *de novo*, followed by lagging strand synthesis. This order of events suggests that telomere synthesis by telomerase is likely to be coordinated with synthesis of the opposite C-strand. Such coordination may prevent telomerase

from generating excessively long single-stranded tails, which may be deleterious to chromosome stability.

Many components of DNA replication influence telomere length. For example, in *S. cerevisiae*, Polα, Polδ and DNA primase are required for telomerase-mediated telomere addition to a *de novo* telomere[91]. CoIP experiments in *S. pombe* showed that Polα interacts with TERT, suggesting that these proteins physically coexist in a complex *in vivo*[187]. In a *polα* mutant that exhibited abnormal telomere lengthening and slightly reduced telomere position effect, the cellular level of the Trt1 (TERT in *S. pombe*) protein was significantly reduced and coimmunoprecipitation of Trt1 and Polα was severely compromised compared to wild-type *Polα* cells. These data suggest that the replication complex is in close association with Trt1p. In support of this model, telomerase and polymerase α-primase from *Euplotes crassus* are physically associated[94].

Dna2p is a multifunctional protein that was first identified in budding yeast in a screen for temperature-sensitive mutants defective in DNA replication in a cell permeabilized assay[188]. It contains two essential domains (Figure 24), an endonuclease domain and a helicase domain. The endonuclease domain is essential for cell viability and is proposed to be responsible for cleavage of the displaced 5' RNA–DNA flap during Okazaki fragment maturation[189]. The helicase domain may play a role in unwinding duplex DNA at or near the site of endonuclease cleavage[190].

Dna2p also plays a role in telomere length regulation and virtually all *dna2* mutants have a slight telomere lengthening phenotype[95]. Dna2p is a component of telomeric chromatin and its localization to telomeres is dynamic, suggesting that it might have a role in telomere replication and telomere capping[191]. Both chromatin immunoprecipitation (ChIP) and

immuofluorescence experiments show that Dna2p is preferentially associated with telomeric DNA in G1 phase. Because there is no telomere replication at this point in the cell cycle, it has been proposed that Dna2p plays a role in capping the chromosome end. Consistent with its role in Okazaki fragment replication, Dna2p is redistributed in S phase from the telomeres to sites throughout the replicating chromosomes. In late S phase Dna2p returns to telomeres and remains there until the following S phase. Furthermore, Dna2p has been shown by *de novo* telomere addition assay to be required for telomerase-dependent telomere replication. Using this assay, there is no telomerase-mediated telomere addition in a *dna2-2* mutant at restrictive temperature. *dna2-2 est2Δ* or *dna2-2 est1Δ* strains have an accelerated senescence phenotype compared with either single mutant, suggesting that Dna2p and telomerase may cooperate in telomere maintenance or stability through different pathways. Taken together, these results suggest that the completion of lagging-strand replication involving Dna2p at telomeres may require tight coordination of the lagging-strand replication with telomerase activity.

This appendix describes experiments to explore generic and physical interactions between the lagging strand replication machinery and telomerase Est2p. While suggestive genetic interactions are observed, no physical interactions have been detected.

Results

Genetic Interactions between EST2 *and* DNA2

Considering the slight telomere lengthening effects of *dna2* alleles, we reasoned that if *est2-LT* mutants partially affect the same pathway, combining the two mutations might produce a synergistic phenotype. We first created strains that are *dna2-1* (a ts mutation in the endonuclease

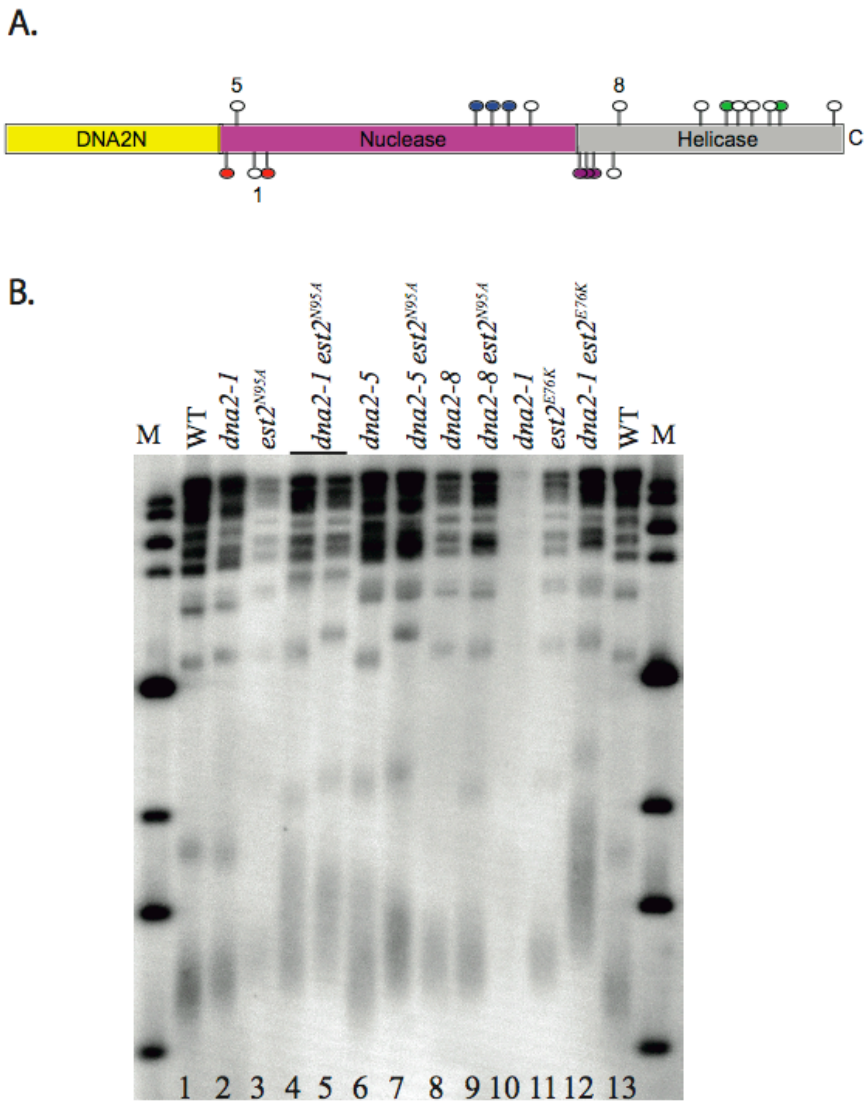

Figure 24. *DNA2* affects telomere length and interacts with *EST2*.

A. Schematic structure of Dna2p (modified from[95]). All mutations marked have longer than normal telomeres.

B. Allele-specific interaction between *dna2* alleles and *est2-LT* ^{N95A} or *est2-LT* ^{E76K}. Genomic DNA from wild type (lanes 1, 13) or the indicated mutant strains were digested with *Xho*I and separated on a 1.2% agarose gel. A ^{32}P labeled telomeric probe was used to detect the telomeres. Color indicates multiple mutations in the same allele. Not all alleles have been completely sequenced [95].

Note: This experiment was performed by Geoff Todd.

Table 7. Genetic interaction between *dna2* and *est2-LT*.

Strains	Average Telomere length (bp)	Change compared with WT (bp)
WT	300	
est2-LT^{N95A}	347	47
dna2-1	369	69
est2-LT^{N95A} dna2-1	585	285
est2-LT^{N95A} dna2-1	579	279
dna2-5	441	141
est2-LT^{N95A} dna2-5	456	156
dna2-8	416	116
est2-LT^{N95A} dna2-8	425	125
dna2-1	369	69
est2-LT^{E76K}	395	95
est2-LT^{E76K} dna2-1	741	441

Telomere length calculation from the gel shown in Figure 24. A standard curve was generated from the molecule mobilities. The median of the telomere smear of each sample was estimated by eye and the size in base pair was calculated using the standard curve.

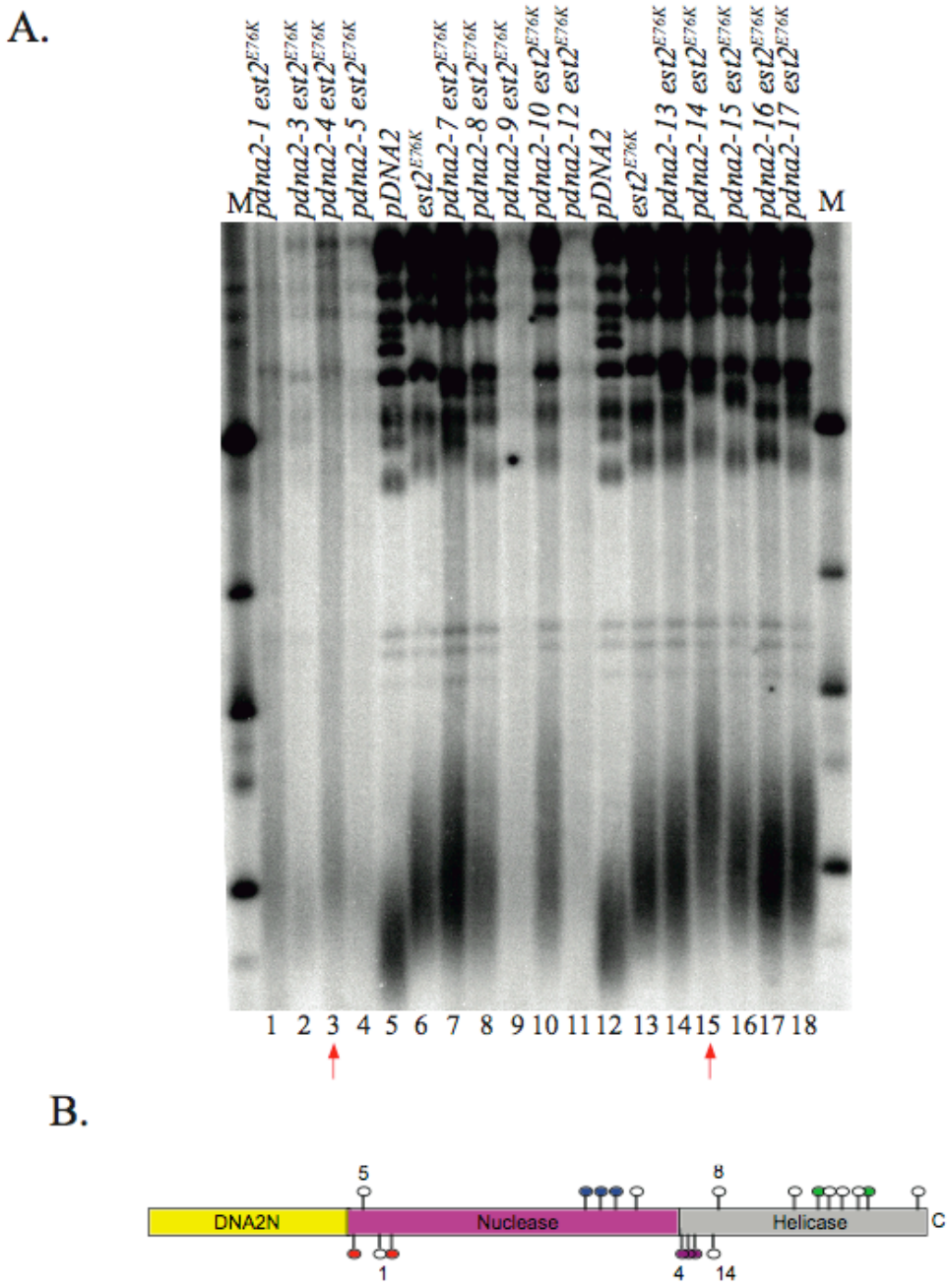

Figure 25. Allele-specific interactions between plasmid-borne *dna2* and *est2-LT^{E76K}*

A. Genomic DNA from the indicated strains was digested with *Xho*I and separated on a 1.2% agarose gel. A ^{32}P-labeled telomeric probe was used to detect the telomeres. Note: This experiment was performed by Stan Sonu.

B. Summary of genetic interactions between *DNA2* and *est2-LT^{E76K}*. A schematic of *DNA2* functional domains is shown. Mutations below the line cause a synergistic phenotype in combination with *est2-LT^{E76K}*. Color indicates multiple mutations in the same allele. Not all alleles have been completely sequenced [95].

domain of *DNA2*) *est2-LT*^{N95A} or *dna2-1 est2-LT*^{E76K}. *est2-LT*^{N95A} causes telomere over-extension by ~50bp, and *dna2-1* cause telomere over-extension by ~70bp, so if the effect is additive, we would expect a telomere lengthening of ~120bp in the double mutant. Strikingly, the telomere length of the double mutant is ~280bp longer than that of wild-type (Figure 24B, Table 7), suggesting a synergistic effect. This phenotype is even more pronounced in *dna2-1 est2-LT*^{E76K}, which has ~440bp over-extension effect instead of the ~170bp predicted by additivity. For two other temperature sensitive mutations in *DNA2*, *dna2-5* and *dna2-8*, the length of the double mutants is only slightly longer than either single mutant (Figure 24B, compare lane 5 with 6, lane 7 with 8), suggesting that the interaction between *EST2* and *DNA2* is allele-specific.

To test the extent of this allele-specificity, a genetic system was set up to create double mutants by sporulation and dissection. An *est2-LT*^{E76K}/*est2-LT*^{E76K} *DNA2*/*DNA2* diploid was created by transient expression of HO endonuclease in a *MATa est2-LT*^{E76K} strain. Because *DNA2* is essential for cell viability, one copy of *DNA2* was replaced by the *KanMX* gene in this diploid by one-step gene replacement. Individual plasmids containing 17 sequenced *dna2* alleles (gift of T. Formosa) were transformed into the *est2-LT*^{E76K}/*est2-LT*^{E76K} *DNA2/dna2*::*Kan*^{R} strain. The resulting diploids were sporulated and dissected to obtain haploid *est2-LT*^{E76K} *dna2*::*Kan*^{R} strains expressing a *dna2* allele on a *LEU2* plasmid. The *dna2* single mutants was generated in a similar manner by creating an *EST2/EST2 DNA2/dna2*::*Kan*^{R} diploid and transforming with *dna2* alleles as described above. These experiments were conducted separately because of the difficulty in screening rapidly for presence of the *est2-LT*^{E76K} mutation in the haploid spores. Telomere length of the double mutants was assayed by Southern Blot and compared with that of either single mutant. The *est2-LT*^{E76K} *dna2*::*Kan*^{R} p*dna2-1* strain show less telomere lengthening than *est2-LT*^{E76K} *dna2-1* (compare lane 12 in Figure 24B with lane 1 in Figure 25A) in which the

mutation is integrated into the chromosomal *DNA2* locus. This result likely reflects suppression of the *dna2-1* defect due to maintenance of more than one copy of plasmid in one cell. Preliminarily we found that *dna2-4, dna2-14* show possible synergistic interactions with *est2-LT^{E76K}*. To confirm this result, these mutations will be integrated into the genome.

Genetic interaction between* est2-LT *and other lagging stand mutants

Many strains containing mutations in components of the lagging strand replication machinery have longer than normal telomeres, the mechanism of which is unclear. It is hypothesized that these mutants are defective in lagging strand synthesis, which disrupts Rap1p's association with telomeres and results in telomere lengthening, suggesting a general mechanism in all such mutants. Given the allele-specific interaction between *DNA2* and *EST2*, I set out to examine whether other mutations in the lagging strand replication machinery interact geneticall with *est2-LT^{E76K}*.

An *EST2*/*est2-LT^{E76K} CDC17*/*cdc17-2* diploid was created and sporulated. Telomere length of WT, *est2-LT^{E76K}*, *cdc17-2* and *est2-LT^{E76K} cdc17-2* strains was assayed by Southern Blotting. As shown in Figure 26A, there is additive telomere lengthening in the double mutant compared with each single mutant, suggesting that *est2-LT^{E76K}* and *cdc17-2* cause telomere over-extension through distinct mechanisms. Furthermore, *cdc17-2* is not *TEL1* dependent (Figure 26B), supporting that it causes telomere lengthening by a different mechanism than *est2-LT^{E76K}*. This result also suggests that the telomere overlengthening in *cdc17-2* is not dependent on Rap1p counting. Preliminary data suggests that other long telomere mutants in lagging strand replication machinery (*rad27Δ*, *pol12-216*) do not interact with *est2-LT^{E76K}* either (data not shown).

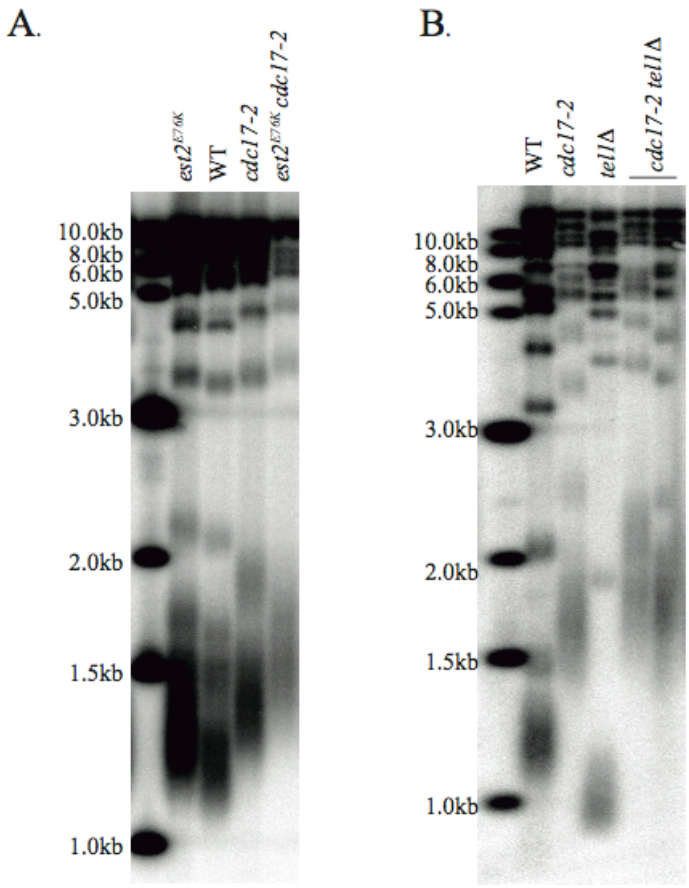

Figure 26. Genetic interaction between *CDC17* and *EST2*.

A. *cdc17-2* is genetically independent of *est2-LT*^{E76K}.
Genomic DNA from indicated strains were digested with *Xho*I and separated on a 1.2% agarose gel. A ^{32}P labeled telomeric probe was used to detect the telomeres

B. Telomere lengthening phenotype of *cdc17-2* is Tel1p-independent. Southern Blotting was performed as described in A.
The length difference between *cdc17-2* in A and B is possibly due to different strain background.

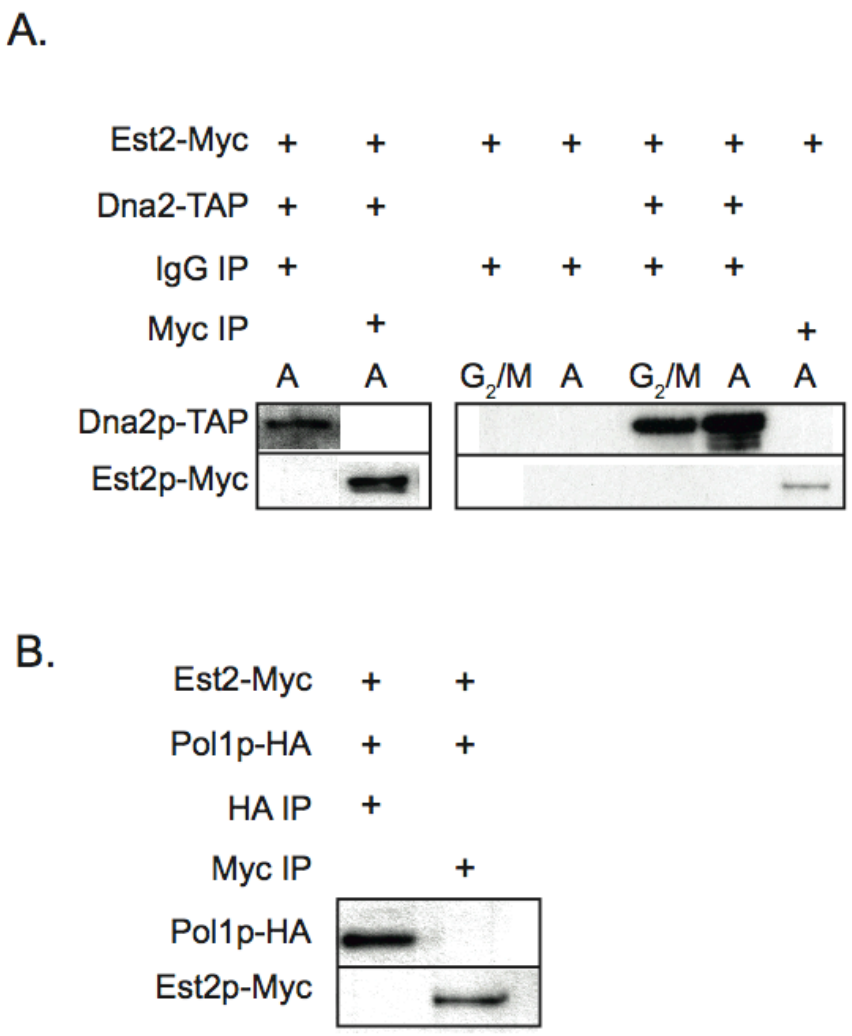

Figure 27. Physical interactions between Est2p and Dna2p or Pol1p.

A. There is no detectable interaction between Dna2p-TAP and Myc_9-Est2p in asynchronous or nocodazole-blocked cultures. Protein Extract was made from BY4741 Dna2-TAP Myc_9-Est2 grown asynchronously (A) or blocked in nocodazole (G2/M) and immunoprecipitation was performed using IgG beads or anti-Myc antibody as indicated.

B. There is no detectable interaction between Pol1p-HA_3 and Myc_9-Est2p in asynchronous culture. Protein extract was made from BY4741 Dna2-TAP Myc_9-Est2 grown asynchronously or blocked in nocodazole and immunoprecipitation was performed using anti-Myc or anti-HA antibody as indicated. All experiments have been repeated at least twice.

Physical interactions between Est2p and components in lagging strand replication

Physical Interactions between TERT and other lagging strand replication components such as Pol1p have been shown in ciliates and fission yeast. The allele-specific interaction between *DNA2* and *EST2* also suggests a possible physical interaction between Dna2p and Est2p.

In order to test whether there are such interactions in *S. cerevisiae*, coimmunoprecipitation between Est2p and Dna2p or Pol1p was performed. Dna2p-TAP was immunoprecipitated and probed for Myc_9-Est2p. Interactions between Myc_9-Est2p and Pol1p-HA_3 was tested in both directions. As shown in Figure 27, there are no detectable interactions between Est2p and Dna2p or Pol1p. The interaction between Est2p and Dna2p was examined in nocodazole-blocked cells when Dna2 is required for *de novo* telomere addition and there is no detectable interaction either (Figure 27B). It is possible that the interaction between Est2p and Dna2p or Pol1p is transient *in vivo*, so *in vivo* crosslinking by DSP was performed to stabilize any interaction. CoIP after DSP treatment did not detect any interaction between Est2p and Dna2p (data not shown). Northern blotting was used to examine if there is any interaction between telomerase TLC1 RNA and components in lagging strand replication including Dna2p, Pol1p and Pol12p. Strains expressing TAP-tagged alleles of each of these genes were obtained from a strain collection (Open Biosystems, AL). An Auxilin-like protein involved in vesicular transport (Swa2p) and a protein component of the H/ACA snoRNP pseudouridylase complex (Gar1p) were used as negative controls and Est2p-TAP was used as a positive control. As shown in Figure 28, because some residual association of TLC1 can be detected with Swa2p and Gar1p, it is unclear whether the weak association of TLC1 with Pol1p and Pol12p is significant. Binding

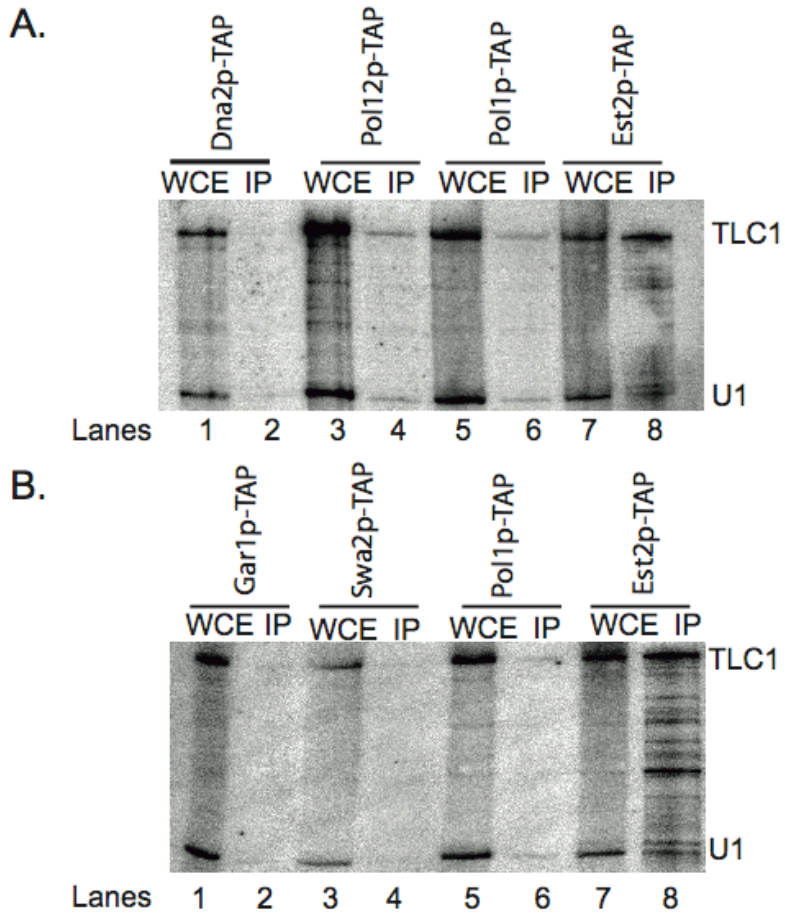

Figure 28. Pol1p, Pol12p and Dna2p do not reproducibly interact with *TLC1* RNA. Protein extracts were immunoprecipitated with IgG beads as previously described. RNA was isolated from 10ul protein extract or immunoprecipitation beads and detected by Northern Blotting as described. Hybridization was performed simultaneously with probes specific for random primed ^{32}p-*TLC1* RNA and ^{32}p-labeled *U1* snRNA.

to Dna2p was not detected. RT-PCR was also attempted but failed because of non-specific amplification in non-tagged strain (data not shown).

A corresponding mutation in *S. pombe trt1*^{E98K} causes telomere lengthening (as shown in Chapter III). Since the interaction between Pol1p and Trt1p was previously demonstrated, it provided an opportunity to explore whether this interaction might be disturbed by E98K mutation. Coimmunoprecipitation experiments were performed to detect the interaction between Pol1p-Flag and plasmid-born Trt1p-Myc or Trt1p^{E98K}-Myc. Consistent with previous publications Pol1p interacts with Trt1p *in vivo*. Because the results were complex and E98K and E101K mutations seem to alter the interaction in a similar manner that is not related to telomere lengthening, they have not been further pursued (data not shown).

Discussion

In this part of my thesis, I examined possible interactions between Est2p and proteins of the lagging strand replication machinery. Although we have detected allele-specific genetic interactions between *dna2* and *est2-LT*, I was unable to detect any physical interaction between Dna2p and Est2p. Therefore, the mechanism of this genetic interaction remains unclear.

Clustering of the mutations that act synergistically with *est2-LT*^{E76K} (Figure 22B) in the primary sequence of *DNA2* is intriguing and strongly suggests a functional interaction between these proteins. It is possible that these two proteins affect telomere length through the same pathway without direct protein-protein interaction. With a list of new phenotypes identified in *est2-LT* by telomere sequence analysis, ChIP, telomeric silencing, we can test

whether similar alterations in the *dna2* alleles that genetically interact with *est2-LT*^{E76K} can be observed.

Meanwhile, the specificity of the genetic interaction between *dna2* and *est2* can be tested in the *est2* direction (*est2-LT, est2-motifE* and *est2-up34*) discussed in previous chapters). Since all these long telomere mutants have similar sequence change, I proposed in Chapter III that the telomere sequence change in these mutants might be a consequence, rather than a cause of telomere lengthening. Elucidating the specificity of *est2-dna2* genetic interaction will further test this hypothesis.

Materials and Methods

Yeast strains used are listed in Table 8. One copy of the *DNA2* gene in diploid strains DKF206 and DKF207 (Table 4) was replaced with Kan^R by PCR product from primers: 5'-TTTGTGCAAGCAAACACTGACAATTGAAGAGATCGTCAGGCGGAT CCCCGGGTTAATTAA-3' and 5'-TAGCTTTCCTGTTATGGAGAAGCTCTTCTTATT CCCCCTGGAATTCGAGCTCGTTTAAAC-3' using pFA6a-KanMX6 to create Strain DKF209 and DKF210. pTF098 (*DNA2 LEU2 CEN*), pTF098-1 (*dna2-1 LEU2 CEN*), pTF098-3 to pTF098-17(*dna2-3 LEU2 CEN* to *dna2-17 LEU2 CEN*), pTF098-19 (*dna2-19 LEU2 CEN*), and pTF098-23 (*dna2-23 LEU2 CEN*) were transformed into DKF209 and DKF210 and the diploids were sporulated and dissected. *DNA2*:: Kan^R pTF098-X and *est2-*LT^{E76K} *DNA2*:: Kan^R pTF098-X were selected on YPD+Geneticin and SD-LEU plates.

Plasmids pTF098-1, pTF098-3 to pTF098-17, pTF098-19 and pTF098-23 were obtained from T. Formosa. pTF098-1 was made by ligating SacII-XmaI fragment from PCR product using genomic DNA from *dna2-1* strain as template into the SacII-XmaI vector fragment of pTF098.

Plasmid pRS304+Myc_9+*EST2* bearing a Myc_9 epitope tag at the N-terminus of *EST2* was digested with *Hpa*I and integrated into YKF250 (BY4741 Dna2-TAP) to create strain YKF251.

PCR product from Primers 5'-CTACGTTGATATGACTAGCATATTTGATTTC ATGCTAAATCGGATCCCCGGGTTAATTAA-3' and 5'-GAATATTCATGAGATCAC ACAACACATACAAAATACTTACGAATTTCGAGCTCGTTTAAAC-3' using pFA6a-3HA-KanMX6 as template was used to integrate an HA_3 epitope tag at the N-terminus of Pol1p (YKF252).

Southern Blotting and Western blotting were performed as previously described in Chapter IV. Northern Blotting was performed as described in[49]. Protein extracts were immunoprecipitated using IgG beads.

Table 8. Strains used in the Appendix.

Strain	Genotype	Source
DKF209	*MATa/MATa trp1/trp1 leu2/leu2 ura3/ura3 his7/his7 DNA2/dna2*Δ:: *Kan*^{R}	This thesis
DKF210	*MATa/MATa trp1/trp1 leu2/leu2 ura3/ura3 his7/his7 est2-LT*^{E76K}*/est2-LT*^{E76K} *dna2*Δ:: *Kan*^{R}	This thesis
DKF211	*MATa/MATa trp1/trp1 leu2/leu2 ura3/ura3 his7/his7 DNA2/dna2*Δ:: *Kan*^{R} pTF098	This thesis
DKF212	*MATa/MATa trp1/trp1 leu2/leu2 ura3/ura3 his7/his7 est2-LT*^{E76K}*/est2-LT*^{E76K} *dna2*Δ:: *Kan*^{R} pTF098	This thesis
YKF250	*BY4741; MATa his3 Δ1 leu2 Δ0 met15 Δ0 ura3 Δ0 DNA2-TAP*	Open Biosystems
YKF251	*MATa his3 Δ1 leu2 Δ0 met15 Δ0 ura3 Δ0 DNA2-TAP Myc*$_9$*-EST2*	This thesis
YKF305	*MATa leu2 trp1 ura3-52 prb1 prc1 pep4-3 Myc*$_9$*-EST2*	[49]
YKF252	*MATa leu2 trp1 ura3-52 prb1 prc1 pep4-3 Myc*$_9$*-EST2 HA*$_3$*-POL1*	This thesis

REFERENCES

1. de Lange, T., Blackburn, E. H. & Lundblad, V. (eds.) Telomeres (Cold Spring Harbor Laboratory Press, Cold Spring Harbor, NY, 2006).

2. Marcand, S., Brevet, V. & Gilson, E. Progressive *cis*-inhibition of telomerase upon telomere elongation. EMBO J. 18, 3509-3519 (1999).

3. Cooper, J. P., Nimmo, E. R., Allshire, R. C. & Cech, T. R. Regulation of telomere length and function by a Myb-domain protein in fission yeast. Nature 385, 744-7 (1997).

4. Ancelin, K. et al. Targeting assay to study the cis functions of human telomeric proteins: evidence for inhibition of telomerase by TRF1 and for activation of telomere degradation by TRF2. Mol Cell Biol 22, 3474-87 (2002).

5. Watson, J. D. Origin of concatemeric T7 DNA. Nat New Biol 239, 197-201 (1972).

6. Olovnikov, A. M. Principle of marginotomy in template synthesis of polynucleotides. Doklady Akademii Nauk SSSR 201, 1496-1499 (1971).

7. Ohki, R., Tsurimoto, T. & Ishikawa, F. In vitro reconstitution of the end replication problem. Mol Cell Biol 21, 5753-66 (2001).

8. Harley, C. B., Futcher, A. B. & Greider, C. W. Telomeres shorten during ageing of human fibroblasts. Nature 345, 458-460 (1990).

9. Greider, C. W. & Blackburn, E. H. Identification of a specific telomere terminal transferase activity in *Tetrahymena* extracts. Cell 43, 405-413 (1985).

10. Lingner, J., Cooper, J. P. & Cech, T. R. Telomerase and DNA end replication: No longer a lagging strand problem? Science 269, 1533-1534 (1995).

11. Biessmann, H., Walter, M. F. & Mason, J. M. Drosophila telomere elongation. Ciba Found Symp 211, 53-67; discussion 67-70 (1997).

12. Schaetzlein, S. & Rudolph, K. L. Telomere length regulation during cloning, embryogenesis and ageing. Reprod Fertil Dev 17, 85-96 (2005).

13. Cech, T. R. Telomere structure and function. Geron Telomerase and Cancer Symposium 0, 9 (1996).

14. Förstemann, K. & Lingner, J. Molecular basis for telomere repeat divergence in budding yeast. Mol. Cell. Biol. 21, 7277-7286 (2001).

15. Griffith, J. D. et al. Mammalian telomeres end in a large duplex loop. Cell 97, 419-422 (1999).

16. de Lange, T. Shelterin: the protein complex that shapes and safeguards human telomeres. Genes Dev 19, 2100-10 (2005).

17. Smogorzewska, A. & de Lange, T. Regulation of telomerase by telomeric proteins. Annual Review of Biochemistry 73, 177-208 (2004).

18. Stansel, R. M., de Lange, T. & Griffith, J. D. T-loop assembly in vitro involves binding of TRF2 near the 3' telomeric overhang. Embo J 20, 5532-40 (2001).

19. Li, B., Oestreich, S. & de Lange, T. Identification of human Rap1: implications for telomere evolution. Cell 101, 471-83 (2000).

20. Li, B. & de Lange, T. Rap1 affects the length and heterogeneity of human telomeres. Mol Biol Cell 14, 5060-8 (2003).

21. Wang, F. et al. The POT1-TPP1 telomere complex is a telomerase processivity factor. Nature 445, 506-10 (2007).

22. Wellinger, R. J., Wolf, A. J. & Zakian, V. A. *Saccharomyces* telomeres acquire single-strand TG1-3 tails late in S phase. Cell 72, 51-60 (1993).

23. Marcand, S., Brevet, V., Mann, C. & Gilson, E. Cell cycle restriction of telomere elongation. Curr. Biol. 10, 487-490 (2000).

24. Tham, W. H. & Zakian, V. A. Transcriptional silencing at Saccharomyces telomeres: implications for other organisms. Oncogene 21, 512-21 (2002).

25. Weinrich, S. L. et al. Reconstitution of human telomerase with the template RNA component hTR and the catalytic protein subunit hTRT. Nat. Genet. 17, 498--502 (1997).

26. Beattie, T. L., Zhou, W., Robinson, M. O. & Harrington, L. Reconstitution of human telomerase activity *in vitro*. Curr Biol 8, 177-80 (1998).

27. Lingner, J., Cech, T. R., Hughes, T. R. & Lundblad, V. Three Ever Shorter Telomere (*EST*) genes are dispensable for *in vitro* yeast telomerase activity. Proc. Natl. Acad. Sci. USA 94, 11190-11195 (1997).

28. Singer, M. S. & Gottschling, D. E. *TLC1*: Template RNA component of *Saccharomyces cerevisiae* telomerase. Science 266, 404-409 (1994).

29. Cech, T. R., Nakamura, T. M. & Lingner, J. Telomerase is a true reverse transcriptase. A review. Biochemistry (Mosc) 62, 1202-5 (1997).

30. Goldstein, N. I., Moore, M. A. S., Allen, C. & Tackney, C. A human fetal spleen cell line, immortalized with SV40 T-Antigen, will support the growth of CD34+ long-term culture-initiating cells. Mol.Cell.Diff. 1, 301-321 (1993).

31. Hammond, P. W., Lively, T. N. & Cech, T. R. The anchor site of telomerase from *Euplotes aediculatus* revealed by photo-cross-linking to single- and double-stranded DNA primers. Mol. Cell. Biol. 17, 296-308 (1997).

32. Armbruster, B. N., Banik, S. S., Guo, C., Smith, A. C. & Counter, C. M. N-terminal domains of the human telomerase catalytic subunit required for enzyme activity *in vivo*. Mol. Cell. Biol. 21, 7775-7786 (2001).

33. Lue, N. F. A physical and functional constituent of telomerase anchor site. J. Biol. Chem. 280, 26586-26591 (2005).

34. Moriarty, T. J., Ward, R. J., Taboski, M. A. & Autexier, C. An anchor site-type defect in human telomerase that disrupts telomere length maintenance and cellular immortalization. Mol Biol Cell 16, 3152-61 (2005).

35. Wyatt, H. D., Lobb, D. A. & Beattie, T. L. Characterization of physical and functional anchor site interactions in human telomerase. Mol Cell Biol 27, 3226-40 (2007).

36. Prescott, J. & Blackburn, E. H. Functionally interacting telomerase RNAs in the yeast telomerase complex. Genes Dev. 11, 2790-2800 (1997).

37. Lue, N. F. & Li, Z. Modeling and structure function analysis of the putative anchor site of yeast telomerase. Nucleic Acids Res 35, 5213-5222 (2007).

38. Beattie, T. L., Zhou, W., Robinson, M. O. & Harrington, L. Functional multimerization of the human telomerase reverse transcriptase. Mol Cell Biol 21, 6151-60 (2001).

39. Moriarty, T. J., Marie-Egyptienne, D. T. & Autexier, C. Functional organization of repeat addition processivity and DNA synthesis determinants in the human telomerase multimer. Mol. Cell. Biol. 24, 3720-3733 (2004).

40. Lin, J. & Blackburn, E. H. Nucleolar protein PinX1p regulates telomerase by sequestering its protein catalytic subunit in an inactive complex lacking telomerase RNA. Genes Dev. 18, 387-396 (2004).

41. Chen, J. L., Blasco, M. A. & Greider, C. W. Secondary structure of vertebrate telomerase RNA. Cell 100, 503-14 (2000).

42. Zappulla, D. C. & Cech, T. R. Yeast telomerase RNA: a flexible scaffold for protein subunits. Proc Natl Acad Sci U S A 101, 10024-9 (2004).

43. Zappulla, D. C., Goodrich, K. & Cech, T. R. A miniature yeast telomerase RNA functions in vivo and reconstitutes activity in vitro. Nat. Struct. Mol. Biol. 12, 1072-1077 (2005).

44. Vulliamy, T. et al. The RNA component of telomerase is mutated in autosomal dominant dyskeratosis congenita. Nature 413, 432-5 (2001).

45. Lendvay, T. S., Morris, D. K., Sah, J., Balasubramanian, B. & Lundblad, V. Senescence mutants of *Saccharomyces cerevisiae* with a defect in telomere replication identify three additional *EST* genes. Genetics 144, 1399-1412 (1996).

46. Seto, A. G., Livengood, A. J., Tzfati, Y., Blackburn, E. H. & Cech, T. R. A Bulged Stem Tethers Est1p to Telomerase RNA in Budding Yeast. Genes Dev. 16, 2800-2812 (2002).

47. Qi, H. & Zakian, V. A. The *Saccharomyces* telomere-binding protein Cdc13p interacts with both the catalytic subunit of DNA polymerase alpha and the telomerase-associated Est1 protein. Genes Dev. 14, 1777-1788. (2000).

48. Evans, S. K. & Lundblad, V. Est1 and Cdc13 as comediators of telomerase access. Science 286, 117-120. (1999).

49. Osterhage JL, T. J., Friedman KL. Proteasome-dependent dergradation of Est1p regulates the cell cycle restricted assembly of telomerase in *Saccharomyces cerevisiae*. Nat Struct Mol Biol (2006).

50. Friedman, K. L., Heit, J. J., Long, D. & Cech, T. R. N-terminal domain of yeast telomerase reverse transcriptase: recruitment of Est3p to the telomerase complex. Mol. Biol. Cell 14, 1-13 (2003).

51. Sharanov, Y. S., Smekalova, E. M., Zvereva, M. I. & Dontsova, O. A. Isolation of active yeast telomerase protein Est3p and investigation of its dimerization in vitro. Biochemistry (Mosc) 72, 702-6 (2007).

52. Sharanov, Y. S., Zvereva, M. I. & Dontsova, O. A. Saccharomyces cerevisiae telomerase subunit Est3p binds DNA and RNA and stimulates unwinding of RNA/DNA heteroduplexes. FEBS Lett 580, 4683-90 (2006).

53. Lin, J. et al. Characterization of a novel effect of hPinX1 on hTERT nucleolar localization. Biochem Biophys Res Commun 353, 946-52 (2007).

54. Seto, A. G., Zaug, A. J., Sabel, S. G., Wolin, S. L. & Cech, T. R. *Saccharomyces cerevisiae* telomerase is an Sm small nuclear ribonucleoprotein particle. Nature 401, 177-180 (1999).

55. Reichenbach, P. et al. A human homolog of yeast Est1 associates with telomerase and uncaps chromosome ends when overexpressed. Curr Biol 13, 568-74 (2003).

56. Snow, B. E. et al. Functional conservation of the telomerase protein Est1p in humans. Curr Biol 13, 698-704 (2003).

57. Forsythe, H. L., Jarvis, J. L., Turner, J. W., Elmore, L. W. & Holt, S. E. Stable association of hsp90 and p23, but Not hsp70, with active human telomerase. J Biol Chem 276, 15571-4 (2001).

58. Toogun, O. A., Zeiger, W. & Freeman, B. C. The p23 molecular chaperone promotes functional telomerase complexes through DNA dissociation. Proc Natl Acad Sci U S A 104, 5765-70 (2007).

59. Zakian, V. A. Telomere functions: Lessons from yeast. Trends Cell Biol. 6, 29-33 (1996).

60. Bodnar, A. G. et al. Extension of life-span by introduction of telomerase into normal human cells. Science 279, 349--52 (1998).

61. Vaziri, H. & Benchimol, S. Reconstitution of telomerase activity in normal human cells leads to elongation of telomeres and extended replicative life span. Curr. Biol. 8, 279--282 (1998).

62. Cristofari, G. & Lingner, J. Telomere length homeostasis requires that telomerase levels are limiting. Embo J 25, 565-74 (2006).

63. Hao, L. Y. et al. Short telomeres, even in the presence of telomerase, limit tissue renewal capacity. Cell 123, 1121-31 (2005).

64. Mozdy, A. D. & Cech, T. R. Low abundance of telomerase in yeast: implications for telomerase haploinsufficiency. Rna 12, 1721-37 (2006).

65. Lundblad, V. & Blackburn, E. H. An alternative pathway for yeast telomere maintenance rescues *est1*$^{-}$ senescence. Cell 73, 347-360 (1993).

66. Lundblad, V. & Szostak, J. W. A mutant with a defect in telomere elongation leads to senescence in yeast. Cell 57, 633-643 (1989).

67. Lin, C. Y. et al. Extrachromosomal telomeric circles contribute to Rad52-, Rad50-, and polymerase delta-mediated telomere-telomere recombination in Saccharomyces cerevisiae. Eukaryot Cell 4, 327-36 (2005).

68. Le, S., Moore, J. K., Haber, J. E. & Greider, C. W. RAD50 and RAD51 define two pathways that collaborate to maintain telomeres in the absence of telomerase. Genetics 152, 143-52 (1999).

69. Teng, S.-C. & Zakian, V. A. Telomere-telomere recombination is an efficient bypass pathway for telomere maintenance in *Saccharomyces cerevisiae*. Mol. Cell. Biol. 19, 8083-8093 (1999).

70. Chien, C.-T., Buck, S., Sternglanz, R. & Shore, D. Targeting of SIR1 protein establishes transcriptional silencing at HM loci and telomeres in yeast. Cell 75, 531-541 (1993).

71. Tsukamoto, Y., Taggart, A. K. P. & Zakian, V. A. The role of the Mre11-Rad50-Xrs2 complex in telomerase-mediated lengthening of *Saccharomyces cerevisiae* telomeres. Current Biology 11, 1328-1335 (2001).

72. Bryan, T. M., Englezou, A., Dalla-Pozza, L., Dunham, M. A. & Reddel, R. R. Evidence for an alternative telomere-lengthening mechanism in human tumours and tumour-derived cell lines. Nature Med. In Press, 0 (1997).

73. Harley, C. B. & Sherwood, S. W. Telomerase, checkpoints and cancer. Cancer Surv 29, 263-84 (1997).

74. Wright, W. E., Shay, J. W. & Piatyszek, M. A. Modifications of a telomeric repeat amplification protocol (TRAP) result in increased reliability, linearity and sensitivity. Nucleic Acids Res. 23, 3794-3795 (1995).

75. Martens, U. M., Chavez, E. A., Poon, S. S., Schmoor, C. & Lansdorp, P. M. Accumulation of short telomeres in human fibroblasts prior to replicative senescence. Exp Cell Res 256, 291-9 (2000).

76. de Lange, T. et al. Structure and variability of human chromosome ends. Mol.Cell.Biol. 10, 518-527 (1990).

77. Hastie, N. D. et al. Telomere reduction in human colorectal carcinoma and with ageing. Nature 346, 866-868 (1990).

78. Counter, C. M. et al. Telomere shortening associated with chromosome instability is arrested in immortal cells which express telomerase activity. EMBO J. 11, 1921-1929 (1992).

79. Murnane, J. P., Sabatier, L., Marder, B. A. & Morgan, W. F. Telomere dynamics in an immortal human cell line. EMBO J. 13, 4953-4962 (1994).

80. Bryan, T. M., Englezou, A., Gupta, J., Bacchetti, S. & Reddel, R. R. Telomere elongation in immortal human cells without detectable telomerase activity. EMBO J. 14, 4240-4248 (1995).

81. Opitz, O. G. et al. Cyclin D1 overexpression and p53 inactivation immortalize primary oral keratinocytes by a telomerase-independent mechanism. J Clin Invest 108, 725-32 (2001).

82. Grobelny, J. V., Kulp-McEliece, M. & Broccoli, D. Effects of reconstitution of telomerase activity on telomere maintenance by the alternative lengthening of telomeres (ALT) pathway. Hum Mol Genet 10, 1953-61 (2001).

83. Yeager, T. R. et al. Telomerase-negative immortalized human cells contain a novel type of promyelocytic leukemia (PML) body. Cancer Res 59, 4175-9 (1999).

84. Hardy, C. F. J., Sussel, L. & Shore, D. A *RAP1*-interacting protein involved in transcriptional silencing and telomere length regulation. Genes Dev. 6, 801-814 (1992).

85. Wotton, D. & Shore, D. A novel Rap1p-interacting factor, Rif2p, cooperates with Rif1p to regulate telomere length in *Saccharomyces cerevisiae*. Genes Dev. 11, 748-760 (1997).

86. Teixeira, M. T., M, A., P, S. & Lingner, J. Telomere length homeostasis is achieved via a switch between telomerase-extendible and -nonextendible states. Cell 117, 323-335 (2004).

87. Budd, M. E., Reis, C. C., Smith, S., Myung, K. & Campbell, J. L. Evidence suggesting that Pif1 helicase functions in DNA replication with the Dna2 helicase/nuclease and DNA polymerase delta. Mol Cell Biol 26, 2490-500 (2006).

88. Boule, J. B. & Zakian, V. A. The yeast Pif1p DNA helicase preferentially unwinds RNA DNA substrates. Nucleic Acids Res 35, 5809-18 (2007).

89. Boule, J. B., Vega, L. R. & Zakian, V. A. The yeast Pif1p helicase removes telomerase from telomeric DNA. Nature 438, 57-61 (2005).

90. Eugster, A. et al. The finger subdomain of yeast telomerase cooperates with Pif1p to limit telomere elongation. Nat. Struct. Mol. Biol. 13, 734-739 (2006).

91. Diede, S. J. & Gottschling, D. E. Telomerase-mediated telomere addition *in vivo* requires DNA primase and DNA polymerases alpha and delta. Cell 99, 723-733. (1999).

92. Dahlen, M., Sunnerhagen, P. & Wang, T. S. Replication proteins influence the maintenance of telomere length and telomerase protein stability. Mol Cell Biol 23, 3031-42 (2003).

93. Fan, X. & Price, C. M. Coordinate regulation of G- and C-strand length during new telomere synthesis. Mol. Biol. Cell 8, 2145-2155 (1997).

94. Ray, S., Karamysheva, Z., Wang, L., Shippen, D. E. & Price, C. M. Interactions between telomerase and primase physically link the telomere and chromosome replication machinery. Mol. Cell. Biol. 22, 5859-5868 (2002).

95. Formosa, T. & Nittis, T. Dna2 mutants reveal interactions with DNA polymerase alpha and Ctf4, a Pol alpha accessory factor, and show that full Dna2 helicase activity is not essential for growth. Genetics 151, 1459-1470 (1999).

96. Adams, A. & Holm, C. Specific DNA replication mutations affect telomere length in *Saccharomyces cerevisiae*. Mol. Cell. Biol. 16, 4614-4620 (1996).

97. Parenteau, J. & Wellinger, R. J. Accumulation of single-stranded DNA and destabilization of telomeric repeats in yeast mutant strains carrying a deletion of RAD27. Mol Cell Biol 19, 4143-52 (1999).

98. Smolikov, S., Mazor, Y. & Krauskopf, A. *ELG1*, a regulator of genome stability, has a role in telomere length regulation and in silencing. PNAS 101, 1656-1661 (2004).

99. Pennock, E., Buckley, K. & Lundblad, V. Cdc13 delivers separate complexes to the telomere for end protection and replication. Cell 104, 387-396. (2001).

100. Lin, J.-J. & Zakian, V. A. The *Saccharomyces CDC13* protein is a single-strand $TG_{1\text{-}3}$ telomeric DNA-binding protein *in vitro* that affects telomere behavior *in vivo*. Proc. Natl. Acad. Sci. USA 93, 13760--13765 (1996).

101. Chandra, A., Hughes, T. R., Nugent, C. I. & Lundblad, V. Cdc13 both positively and negatively regulates telomere replication. Genes Dev. 15, 404-414. (2001).

102. Ritchie, K. B. & Petes, T. D. The Mre11p/Rad50p/Xrs2p Complex and the Tel1p Function in a Single Pathway for Telomere Maintenance in Yeast. Genetics 155, 475-479 (2000).

103. Ray, A. & Runge, K. W. Varying the number of telomere-bound proteins does not alter telomere length in tel1 delta cells. PNAS 96, 15044-15049 (1999).

104. Brevet, V. et al. The number of vertebrate repeats can be regulated at yeast telomeres by Rap1-independent mechanisms. EMBO J. 22, 1697-1706 (2003).

105. Bertuch, A. A. & Lundblad, V. The Ku heterodimer performs separable activities at double-strand breaks and chromosome termini. Mol Cell Biol 23, 8202-15 (2003).

106. Porter, S., Greenwell, P., Ritchie, K. & Petes, T. The DNA-binding protein Hdf1p (a putative Ku homologue) is required for maintaining normal telomere length in *Saccharomyces cerevisiae*. Nucl. Acids Res. 24, 582-585 (1996).

107. Gravel, S., Larrivee, M., Labrecque, P. & Wellinger, R. J. Yeast Ku as a regulator of chromosomal DNA end structure. Science 280, 741-4 (1998).

108. Takata, H., Kanoh, Y., Gunge, N., Shirahige, K. & Matsuura, A. Reciprocal association of the budding yeast ATM-related proteins Tel1 and Mec1 with telomeres in vivo. Mol Cell 14, 515-22 (2004).

109. Zhang, X. & Paull, T. T. The Mre11/Rad50/Xrs2 complex and non-homologous end-joining of incompatible ends in S. cerevisiae. DNA Repair (Amst) 4, 1281-94 (2005).

110. Andrews, C. A. & Clarke, D. J. MRX (Mre11/Rad50/Xrs2) mutants reveal dual intra-S-phase checkpoint systems in budding yeast. Cell Cycle 4, 1073-7 (2005).

111. Chan, S. W. L., Chang, J., Prescott, J. & Blackburn, E. H. Altering telomere structure allows telomerase to act in yeast lacking ATM kinases. Current Biology 11, 1240-1250 (2001).

112. Goudsouzian, L. K., Tuzon, C. T. & Zakian, V. A. S. cerevisiae Tel1p and Mre11p are required for normal levels of Est1p and Est2p telomere association. Mol Cell 24, 603-10 (2006).

113. Askree, S. H. et al. A genome-wide screen for Saccharomyces cerevisiae deletion mutants that affect telomere length. Proc Natl Acad Sci U S A 101, 8658-63 (2004).

114. Moretti, P., Freeman, K., Coodly, L. & Shore, D. Evidence that a complex of SIR proteins interacts with the silencer and telomere-binding protein RAP1. Genes Dev. 8, 2257-2269 (1994).

115. Moretti, P. & Shore, D. Multiple interactions in Sir protein recruitment by Rap1p at silencers and telomeres in yeast. Mol. Cell. Biol. 21, 8082-8094 (2001).

116. Luo, K., Vega-Palas, M. A. & Grunstein, M. Rap1-Sir4 binding independent of other Sir, yKu, or histone interactions initiates the assembly of telomeric heterochromatin in yeast. Genes Dev 16, 1528-39 (2002).

117. Moazed, D., Rudner, A. D., Huang, J., Hoppe, G. J. & Tanny, J. C. A model for step-wise assembly of heterochromatin in yeast. Novartis Found Symp 259, 48-56; discussion 56-62, 163-9 (2004).

118. Palladino, F. et al. SIR3 and SIR4 proteins are required for the positioning and integrity of yeast telomeres. Cell 75, 543-555 (1993).

119. Kyrion, G., Liu, K., Liu, C. & Lustig, A. J. RAP1 and telomere structure regulate telomere position effects in Saccharomyces cerevisiae. Genes Dev. 7, 1146-1159 (1993).

120. Boulton, S. J. & Jackson, S. P. Components of the Ku-dependent non-homologous end-joining pathway are involved in telomeric length maintenance and telomeric silencing. Embo J 17, 1819-28 (1998).

121. Mishra, K. & Shore, D. Yeast Ku protein plays a direct role in telomeric silencing and counteracts inhibition by rif proteins. Curr Biol 9, 1123-6 (1999).

122. Jiang, X. R. et al. Telomerase expression in human somatic cells does not induce changes associated with a transformed phenotype. Nat Genet 21, 111-4 (1999).

123. Morales, C. P. et al. Absence of cancer-associated changes in human fibroblasts immortalized with telomerase. Nat Genet 21, 115-8 (1999).

124. Thomas, M. et al. Cooperation of hTERT, SV40 T antigen and oncogenic Ras in tumorigenesis: a cell transplantation model using bovine adrenocortical cells. Neoplasia 4, 493-500 (2002).

125. Wellinger, R. J. & Sen, D. The DNA structures at the ends of eukaryotic chromosomes. Eur. J. Cancer 33, 735-749 (1997).

126. Greider, C. W. & Blackburn, E. H. The telomere terminal transferase of *Tetrahymena* is a ribonucleoprotein enzyme with two kinds of primer specificity. Cell 51, 887-898 (1987).

127. Greider, C. W. & Blackburn, E. H. A telomeric sequence in the RNA of *Tetrahymena* telomerase required for telomere repeat synthesis. Nature 337, 331-337 (1989).

128. Lingner, J. et al. Reverse transcriptase motifs in the catalytic subunit of telomerase. Science 276, 561-567 (1997).

129. Nugent, C. I., Hughes, T. R., Lue, N. F. & Lundblad, V. Cdc13p: A single-strand telomeric DNA binding protein with a dual role in yeast telomere maintenance. Science 274, 249-252 (1996).

130. Malik, H. S., Burke, W. D. & Eickbush, T. H. Putative telomerase catalytic subunits from *Giardia lamblia* and *Caenorhabditis elegans*. Gene 251, 101-108. (2000).

131. Miller, M. C., Liu, J. K. & Collins, K. Template definition by *Tetrahymena* telomerase reverse transcriptase. Embo J. 19, 4412-4422. (2000).

132. Xia, J., Peng, Y., Mian, I. S. & Lue, N. F. Identification of functionally important domains in the N-terminal region of telomerase reverse transcriptase. Mol. Cell. Biol. 20, 5196-5207. (2000).

133. Moriarty, T. J., Huard, S., Dupuis, S. & Autexier, C. Functional multimerization of human telomerase requires an RNA interaction domain in the N terminus of the catalytic subunit. Mol. Cell. Biol. 22, 1253-1265 (2002).

134. Friedman, K. L. & Cech, T. R. Essential functions of N-terminal domains in the yeast telomerase catalytic subunit revealed by selection for viable mutants. Genes Dev. 13, 2863-2874 (1999).

135. Beattie, T. L., Zhou, W., Robinson, M. O. & Harrington, L. Polymerization defects within human telomerase are distinct from telomerase RNA and TEP1 binding. Mol. Biol. Cell 11, 3329-3340. (2000).

136. Bryan, T. M., Goodrich, K. J. & Cech, T. R. Telomerase RNA bound by protein motifs specific to telomerase reverse transcriptase. Mol. Cell 6, 493-499. (2000).

137. Lai, C. K., Mitchell, J. R. & Collins, K. RNA binding domain of telomerase reverse transcriptase. Mol. Cell. Biol. 21, 990-1000. (2001).

138. Armbruster, B. N., Etheridge, K. T., Broccoli, D. & Counter, C. M. Putative telomere-recruiting domain in the catalytic subunit of human telomerase. Mol. Cell. Biol. 23, 3237-3246 (2003).

139. Armbruster, B. N. et al. Rescue of an hTERT mutant defective in telomere elongation by fusion with hPot1. Mol. Cell. Biol. 24, 3552-3561 (2004).

140. Lee, S. R., Wong, J. M. Y. & Collins, K. Human telomerase reverse transcriptase motifs required for elongation of a telomeric substrate. J. Biol. Chem. 278, 52531-52536 (2003).

141. Collins, K. & Greider, C. W. *Tetrahymena* telomerase catalyzes nucleolytic cleavage and nonprocessive elongation. Genes Dev. 7, 1364-1376 (1993).

142. Lee, M. S. & Blackburn, E. H. Sequence-specific DNA primer effects on telomerase polymerization activity. Mol.Cell.Biol. 13, 6586-6599 (1993).

143. Kyrion, G., Boakye, K. A. & Lustig, A. J. C-terminal truncation of *RAP1* results in the deregulation of telomere size, stability and function in *Saccharomyces cerevisiae*. Mol. Cell. Biol. 12, 5159-5173 (1992).

144. Marcand, S., Gilson, E. & Shore, D. A protein-counting mechanism for telomere length regulation in yeast. Science 275, 986-990 (1997).

145. Levy, D. L. & Blackburn, E. H. Counting of Rif1p and Rif2p on *Saccharomyces cerevisiae* telomeres regulates telomere length. Mol. Cell. Biol. 24, 10857-10867 (2004).

146. Lustig, A. J. & Petes, T. D. Identification of yeast mutants with altered telomere structure. Proc.Natl.Acad.Sci.USA 83, 1398-1402 (1986).

147. Craven, R. J. & Petes, T. D. Dependence of the regulation of telomere length on the type of subtelomeric repeat in the yeast *Saccharomyces cerevisiae*. Genetics 152, 1531-1541 (1999).

148. Peng, Y., Mian, I. S. & Lue, N. F. Analysis of telomerase processivity: mechanistic similarity to HIV-1 reverse transcriptase and role in telomere maintenance. Mol. Cell 7, 1201-1211 (2001).

149. Seto, A. G. et al. A template-proximal RNA paired element contributes to *Saccharomyces cerevisiae* telomerase activity. RNA 9, 1323-1332 (2003).

150. Teixeira, M. T., Foerstemann, K., Gasser, S. M. & Lingner, J. Intracellular trafficking of yeast telomerase components. EMBO rep. 3, 652-659 (2002).

151. Grossi, S., Puglisi, A., Dmitriev, P. V., Lopes, M. & Shore, D. Pol12, the B subunit of DNA polymerase alpha, functions in both telomere capping and length regulation. Genes Dev. 18, 992-1006 (2004).

152. Hiraoka, Y. Meiotic telomeres: a matchmaker for homologous chromosomes. Genes Cells 3, 405-13 (1998).

153. Ray, A. & Runge, K. W. Yeast telomerase appears to frequently copy the entire template *in vivo*. Nucleic Acids Res. 29, 2382-2394 (2001).

154. Putnam, C. D., Pennaneach, V. & Kolodner, R. D. Chromosome healing through terminal deletions generated by *de novo* telomere additions in *Saccharomyces cerevisiae*. Proc. Natl. Acad. Sci. USA 101, 13262-13267 (2004).

155. Henning, K. A., Moskowitz, N., Ashlock, M. A. & Liu, P. P. Humanizing the yeast telomerase template. Proc. Natl. Acad. Sci. USA 95, 5667-5671 (1998).

156. Zakian, V. A. Telomeres: Beginning to understand the end. Science 270, 1601-1607 (1995).

157. Gilson, E., Laroche, T. & Gasser, S. M. Telomeres and the functional architecture of the nucleus. Trends Cell Biol. 3, 128-134 (1993).

158. Pardo, B. & Marcand, S. Rap1 prevents telomere fusions by nonhomologous end joining. EMBO J. 24, 3117-3127 (2005).

159. Negrini, S., Ribaud, V., Bianchi, A. & Shore, D. DNA breaks are masked by multiple Rap1 binding in yeast: implications for telomere capping and telomerase regulation. Genes Dev. 21, 292-302 (2007).

160. Ji, H., Platts, M. H., Dharamsi, L. M. & Friedman, K. L. Regulation of telomere length by an N-terminal region of the yeast telomerase reverse transcriptase. Mol. Cell. Biol. 25, 9103-9114 (2005).

161. Jacobs, S. A., Podell, E. R. & Cech, T. R. Crystal structure of the essential N-terminal domain of telomerase reverse transcriptase. Nat. Struct. Mol. Biol. 13, 218-225 (2006).

162. Prescott, J. C. & Blackburn, E. H. Telomerase RNA template mutations reveal sequence-specific requirements for the activation and repression of telomerase action at telomeres. Mol. Cell. Biol. 20, 2941-2948. (2000).

163. Alexander, M. K. & Zakian, V. A. Rap1p telomere association is not required for mitotic stability of a C(3)TA(2) telomere in yeast. EMBO J. 22, 1688-1696 (2003).

164. Berthiau, A. S. et al. Subtelomeric proteins negatively regulate telomere elongation in budding yeast. EMBO J. 25, 846-856 (2006).

165. Sokal, R. R. & Rohlf, F. J. Biometry (Freeman and Co. , NY, 1995).

166. Cartharius, K. et al. MatInspector and beyond: promoter analysis based on transcription factor binding sites. Bioinformatics 21, 2933-2942 (2005).

167. Yu, E. Y. et al. Regulation of telomere structure and functions by subunits of the INO80 chromatin remodeling complex. Mol Cell Biol 27, 5639-49 (2007).

168. Scherer, S. & David, R. W. Replacement of chromosome segments with altered DNA sequences constructed *in vitro*. Proc. Natl. Acad. Sci. USA 76, 4951-4955 (1979).

169. Giaever, G. et al. Functional profiling of the *Saccharomyces cerevisiae* genome. Nature 418, 387-391 (2002).

170. Graham, T., Seeger, M., Payne, G., MacKay, V. & Emr, S. Clathrin-dependent localization of alpha 1,3 mannosyltransferase to the Golgi complex of *Saccharomyces cerevisiae*. J. Cell Biol. 127, 667-678 (1994).

171. Longtine M.S., M. I. A., Demarini D.J., Shah N.G., Wach A., Brachat A., Philippsen P., Pringle J.R. Additional modules for versatile and economical PCR-based gene deletion and modification in *Saccharomyces cerevisiae*. Yeast 14, 953-961 (1998).

172. Haering, C. H., Nakamura, T. M., Baumann, P. & Cech, T. R. Analysis of telomerase catalytic subunit mutants *in vivo* and *in vitro* in *Schizosaccharomyces pombe*. Proc. Natl. Acad. Sci. U S A 97, 6367-6372. (2000).

173. Fromant, M., Blanquet, S. & Plateau, P. Direct random mutagenesis of gene-sized DNA fragments using polymerase chain reaction. Anal. Biochem. 224, 347-353 (1995).

174. Rose, M. D., Winston, F. & Hieter, P. Methods in Yeast Genetics: A Laboratory Course Manual (Cold Spring Harbor Laboratory Press, Cold Spring Harbor, NY, 1990).

175. Dionne, I. & Wellinger, R. J. Cell cycle-regulated generation of single-stranded G-rich DNA in the absence of telomerase. Proc.Natl.Acad.Sci.USA 93, 13902-13907 (1996).

176. Taggart, A. K. P., Teng, S.-C. & Zakian, V. A. Est1p as a cell cycle-regulated activator of telomere-bound telomerase. Science 297, 1023-1026 (2002).

177. Smith, C. D., Smith, D. L., DeRisi, J. L. & Blackburn, E. H. Telomeric protein distributions and remodeling through the cell cycle in *Saccharomyces cerevisiae*. Mol. Biol. Cell 14, 556-570 (2003).

178. Lascaris, R. F., Mager, W. H. & Planta, R. J. DNA-binding requirements of the yeast protein Rap1p as selected *in silico* from ribosomal protein gene promoter sequences. Bioinformatics 15, 267-277 (1999).

179. Garbett, K. A., Tripathi, M. K., Cencki, B., Layer, J. H. & Weil, P. A. Yeast TFIID serves as a coactivator for Rap1p by direct protein-protein interaction. Mol. Cell. Biol. 27, 297-311 (2007).

180. Enomoto, S., McCune-Zierath, P. D., Gerami-Nejad, M., Sanders, M. A. & Berman, J. RLF2, a subunit of yeast chromatin assembly factor-I, is required for telomeric chromatin function in vivo. Genes Dev 11, 358-70 (1997).

181. Zhang, Z., Shibahara, K. & Stillman, B. PCNA connects DNA replication to epigenetic inheritance in yeast. Nature 408, 221-5 (2000).

182. Krude, T. & Keller, C. Chromatin assembly during S phase: contributions from histone deposition, DNA replication and the cell division cycle. Cell Mol Life Sci 58, 665-72 (2001).

183. Wright, J. H., Gottschling, D. E. & Zakian, V. A. Saccharomyces telomeres assume a non-nucleosomal chromatin structure. Genes Dev 6, 197-210 (1992).

184. Bosoy, D. & Lue, N. F. Yeast telomerase is capable of limited repeat addition processivity. Nucleic Acids Res 32, 93-101 (2004).

185. Chang, M., Arneric, M. & Lingner, J. Telomerase repeat addition processivity is increased at critically short telomeres in a Tel1-dependent manner in Saccharomyces cerevisiae. Genes Dev 21, 2485-94 (2007).

186. Diede, S. J. & Gottschling, D. E. Exonuclease activity is required for sequence addition and Cdc13p loading at a de novo telomere. Curr Biol 11, 1336-40 (2001).

187. Dahlen, M., Sunnderhagen, P. & Wang, T. S.-F. Replication proteins influence the maintenance of telomere length and telomerase protein stability. Mol. Cell. Biol. 23, 3031-3042 (2003).

188. Budd, M. E. & Campbell, J. L. A yeast gene required for DNA replication encodes a protein with homology to DNA helicases. Proc Natl Acad Sci U S A 92, 7642-6 (1995).

189. Bae, S. H. et al. Dna2 of Saccharomyces cerevisiae possesses a single-stranded DNA-specific endonuclease activity that is able to act on double-stranded DNA in the presence of ATP. J Biol Chem 273, 26880-90 (1998).

190. Bae, S. H. et al. Coupling of DNA helicase and endonuclease activities of yeast Dna2 facilitates Okazaki fragment processing. J Biol Chem 277, 26632-41 (2002).

191. Choe, W., Budd, M., Imamura, O., Hoopes, L. & Campbell, J. L. Dynamic localization of an okazaki fragment processing protein suggests a novel role in telomere replication. Mol. Cell. Biol. 22, 4202-4217 (2002).